Anti-apoptotic and Pro-inflammatory Signaling in Cancer Cells: Status and Modulation by Chemotherapeutic Drugs

DISSERTATION

Zur Erlangung des akademischen Grades eines
Doktors der Naturwissenschaften (Dr. rer. nat.)
des Fachbereiches für Biologie
an der
Universität Konstanz

vorgelegt von

Gabriele Imre

Tag der mündlichen Prüfung: 26. Februar 2007
Referent: Prof. Dr. Klaus Schäfer
Referent: Prof. Dr. Albrecht Wendel

Die vorliegende Arbeit wurde in der Abteilung Pharmakologie-Onkologie (Leiter Dr. Volker Gekeler, ALTANA Pharma AG, Konstanz) unter der maßgeblichen Betreuung durch Dr. Markus Boehm durchgeführt. Herrn Dr. Gekeler möchte ich für seine Förderung und wissenschaftliche Unterstützung, sowie die kritische Durchsicht der Dissertationsschrift danken. Ganz besonderer Dank gilt Herrn Dr. Markus Boehm für die intensive Betreuung, seine konstruktive Kritik und Anregungen, sowie die vielen Stunden fruchtbarer Diskussionen, die zum Gelingen dieser Arbeit beigetragen haben. Er hat eine Atmosphäre in der Arbeitsgruppe geschaffen, die Forschung zu einer spannenden Tätigkeit macht.

Besonderer Dank gilt Herrn Dr. Karl Sanders für die Förderung und Unterstützung meiner Dissertation. Dank gilt auch Herrn Dr. Thomas Beckers, der die Anregung gab mit Histondeacetylase Inhibitoren zu arbeiten. Herrn Dr. Hans-Peter Hofmann möchte ich für eine sehr gute Zusammenarbeit sowie Frau Dr. Astrid Leja für die Unterstützung danken.

Besonderer Dank gilt Prof. Dr. Klaus Schäfer sowie Prof. Dr. Albrecht Wendel für die Bereitschaft, als Gutachter diese Dissertation zu beurteilen.

Vielen Dank an alle MitarbeiterInnen der Onkologie (Abteilungen RPR/P3 und RPR/B4) für die freundliche Aufnahme und angenehme Atmosphäre. Im Besonderen möchte ich meinen beiden Laborkolleginnen Josi Innig und Karin Burger für die sehr gute Zusammenarbeit danken, ohne die eine so reibungslose Durchführung dieser Arbeit nicht möglich gewesen wäre. Ein herzliches Dankeschön an Daniela Drache, Christina Engesser, Susanne Fischer, Carola Grebe, Tanja Greif, Heiko Julius, Donja Reiner, Annegret Sprinkart, Claudia Weller sowie Sabine Winderl für die freundschaftliche Atmosphäre auch über die Arbeit hinaus.

Ein riesengroßes Dankeschön gilt meinem Ehemann Bernd sowie meinen Eltern für ihre fortwährende persönliche Unterstützung.

17-AAG	17-allylamino 17-demethoxygeldanamycin
ABC	ATP binding cassette
AMC	7-amino-4-methylcoumarin
AMV	avian myeloblastosis virus
ANOVA	analysis of variance
AT	ataxia telangiectasia
ATM	ataxia telangiectasia mutated
β-TrCP	beta-transducin repeat containing protein
BCA	bicinchoninic acid
BCL-x_L	Bcl2-like 1; Bcl2 related protein (long isoform)
BSA	bovine serum albumin
CBP	CREB binding protein
CD40L	CD40 ligand
CDKN1A	p21; cyclin-dependent kinase inhibitor 1A
c-FLIP	CFLAR; CASP8 and FADD-like apoptosis regulator
CRM1	exportin 1; chromosome region maintenance 1 protein
C-terminal	carboxyterminal
DLBCL	diffuse large B-cell lymphoma
DMSO	dimethylsulfoxide
DTT	dithiothreitol
EC_{50}	half maximal effective concentration
EDTA	ethylenediaminetetraacetic acid
ELISA	enzyme linked immunosorbent assay
EMSA	electrophoretic mobility shift assay
ER-α	estrogen receptor alpha
FACS	fluorescence activated cell sorting
FADD	FAS-associated via death domain
FAS	CD95; tumor necrosis factor receptor superfamily member 6
FCS	fetal calf serum
GAPDH	glyceraldehyde-3-phosphate dehydrogenase
GATA-1	globin transcription factor 1
GNAT	glycine-N-acyltransferase like 1
HAT	histone acetyltransferase
HDA1	histone deacetylase 1 (yeast)
HDAC	histone deacetylase
HDI	histone deacetylase inhibitor
HEPES	4-(2-hydroxyethyl)-1-piperazineethanesulfonic acid
HIV-1 LTR	human immunodeficiency virus-1 long terminal repeat
HRP	horseradish peroxidase
Hsp90	heat shock protein 90
ICAM1	CD54; intercellular adhesion molecule 1
IFN	interferon
IKK	inhibitor of NFκB kinase
IL	interleukin
IκB	inhibitor of NFκB
κB	kappa-B
kDa	kilo-Dalton
LMB	leptomycin B
LPS	lipopolysaccharide
LT	lymphotoxin

MAP3K	MEKK; mitogen-activated protein kinase kinase kinase
MDR1	multidrug resistance protein 1
MRE11	meiotic recombination 11
NAD+	nicotinamide adenine dinucleotide
NAK	NFκB activating kinase
NBS1	nibrin; nijmegen breakage syndrome
NDA	new drug application
NEMO	NFκB essential modulator
NFκB	nuclear factor kappa-B
NIK	NFκB inducing kinase
NLS	nuclear localization signal
NSCLC	non-small cell lung cancer
N-terminal	aminoterminal
PBS	phosphate buffered saline
PKA	protein kinase A; cAMP-dependent protein kinase
PMA	phorbol myristate acetate
PVDF	polyvinylidenedifluoride
Rel	reticuloendotheliosis
REV-A	reticuloendotheliosis virus (strain A)
RHD	rel homology domain
RIP	receptor interacting protein
RLT buffer	RNeasy Lysis buffer
RPD3	reduced potassium dependency 3 (yeast)
RT	room temperature
SAEC	small airway epithelial cells
SAHA	suberoylanilide hydroxamic acid
SCLC	small cell lung cancer
SDS	sodiumdodecylsulfate
SIR2	silent information regulator 2 (yeast)
siRNA	short interfering RNA
Sp1	specificity protein 1
STAT	signal transducer and activator of transcription
TAK1	transforming growth factor-β-activated kinase 1
TEMED	N,N,N,N-tetramethylethylendiamin
TNF	tumor necrosis factor
TNF-R	TNF receptor
TPA	12-O-tetradecanoylphorbol-13-acetate
TRADD	TNF-R1 associated death domain protein
TRAF2	TNF receptor associated factor 2
TRAIL	TNF-related apoptosis-inducing ligand
TRAIL-R	TRAIL receptor
TSA	trichostatin A
VEGF	vascular endothelial growth factor
VPA	valproic acid
Wt	wildtype
XIAP	x-linked mammalian inhibitor of apoptosis protein

1 INTRODUCTION

1.1 Cancer

Cancer, besides heart disease and stroke, is the leading cause for death in the Western world. Approximately one-third of the population dies of cancer, amounting to seven million a year[1]. According to statistics the primary organs most frequently affected are lung, breast, prostate, colon, and rectum. At a later stage in tumor progression, cancer cells spread through the blood or lymphoid system to other organs such as liver, bones, or lung giving rise to secondary tumors (metastases). The likelihood of developing cancer increases with age. Besides age, major causes for cancer are carcinogens such as tobacco, ionising radiation, or asbestos as well as virus infections and genetic predisposition[2,3].

The development of a tumor is a multi-step process involving the activation of oncogenes and the inactivation of tumor suppressor genes[4-6]. Each event confers specific malignant features such as self-sufficiency in growth signals, insensitivity to antigrowth signals, evasion of apoptosis, unlimited replicative potential, induction of angiogenesis, and tissue invasion and metastasis[7].

1.1.1 Drug discovery

Over the last decades, the development of new cancer treatments has made significant advances in a number of tumor entities, leading to marked increases in the overall survival rate of patients. Modern molecular diagnostic tools and biomedical research is beginning to reveal the molecular mechanisms underlying the formation and progression of tumors. More detailed knowledge may allow the shift in development from broad-spectrum cytotoxic substances to target-specific and even patient-individualised drugs. Drugs customized for the patient and targeted to the specific tumor will be combined for the best treatment outcome. Different approaches to treat cancer can be applied:

1. Inhibition of tumor growth by cytotoxic drugs, which interfere with general cellular mechanisms such as mitosis, DNA, or protein synthesis. These conventional drugs target not only tumor cells; they also affect normal cells that have a high proliferation rate, such as the bone marrow cells and hair follicles[8,9].
2. Hormone deprivation therapy to treat hormone-dependent tumors such as prostate and breast cancer[10-12].
3. Target-specific approaches aiming at molecular mechanisms of cell growth or apoptosis. The good tolerability of this treatment is likely due to the high selectivity for cancer cells[13-15].
4. Suppression of angiogenesis, i.e. the feeding of cancer cells by building new blood vessels[16,17].
5. Inhibition of invasive growth[18,19].
6. Immunostimulating agents as supportive medication[20-22].

1.1.2 Drug resistance

In spite of the significant advances in drug development over the past decades, a cure for cancer is still not within reach for most tumor entities. One of the key reasons for this is drug resistance. A tumor is very heterogeneous, consisting of cells with different mutations and dysfunctions. Chemotherapeutic drugs kill tumor cells that are sensitive to the administered drug. However, a small number of cells usually survives because of several reasons, such as expression of apoptosis repressors or other resistance factors. By the time the treatment is completed, the tumor regrows and chemotherapy fails because the remaining cells are now resistant to the drug.

Tumor cells become resistant by activating different genes and pathways (figure 1.1). A major gene involved in drug resistance is the multidrug resistance protein 1 (MDR1). Drug resistant cells produce large amounts of the MDR1 protein, a membrane-spanning ABC-transporter[23], which pumps drugs out of the cell[24,25]. Other resistance mechanisms are reduced influx of the drug administered[26,27], or activation of detoxifying enzymes[28-30]. Mutations in various pro-apoptotic proteins and cell cycle regulators may allow the cells to survive despite DNA damage, as well as alterations in apoptotic pathways during drug exposure[31,32]. Finally, the activation of repair enzymes may allow the survival of impaired cells. A key factor for drug resistance is

nuclear factor kappa-B (NFκB), which is activated by a number of chemotherapeutic drugs and acts predominantly anti-apoptotic.

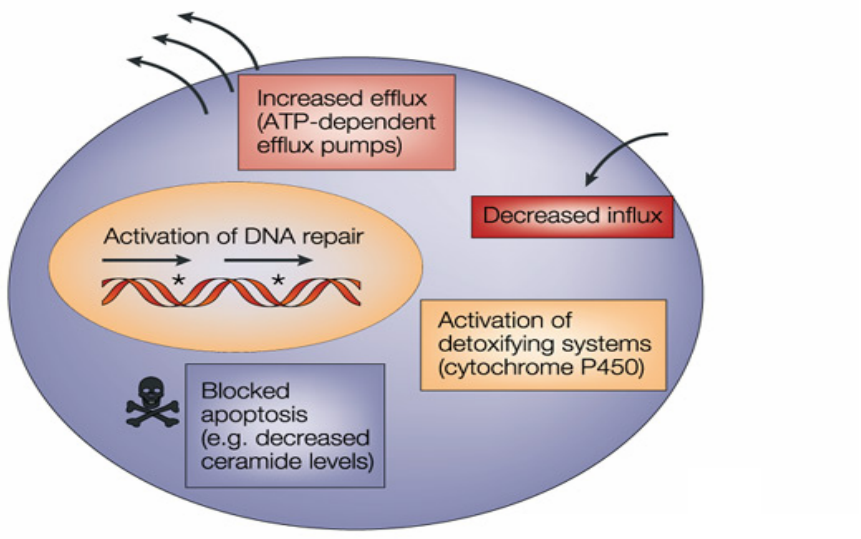

Figure 1.1: Mechanisms of tumor cells to evade apoptosis.
Tumor cells may evade apoptosis and become resistant to antitumor drugs by activation of efflux pumps, decrease of drug influx, activation of detoxifying enzymes, acquisition of mutations in pro- or anti-apoptotic proteins, and activation of DNA repair genes (taken from Gottesman et al., Nat. Rev. Cancer, Vol. 2, 2002).

1.2 NFκB activation and cancer

Early evidence for the implication of NFκB in cancerogenesis was the discovery of the v-Rel oncogene, a member of the NFκB family. It arose from a recombination event between the envelope sequence of the reticuloendotheliosis virus (REV-A) and c-Rel sequences of the turkey[33]. Infection with v-Rel causes rapid and fatal B-cell lymphoma in young birds within ten days[34]. It has also been shown that v-Rel alone is sufficient to transform lymphoid cells[35]. Further research on NFκB family members supported the oncogenic potential of the transcription factor family. Numerous studies show that NFκB is constitutively active in many tumor cell lines, whereas in normal cells aberrant NFκB levels are only found rarely.

The progression of breast cancer tumors from an estrogen receptor-dependent, antiestrogen-sensitive to an estrogen receptor-independent, antiestrogen-resistant phenotype with metastatic potential is associated with the induction of NFκB[36]. Many other human cell lines and tissues derived from patients, e.g. prostate carcinoma cells[37], pancreatic adenocarcinoma cells[38], colorectal carcinomas[39], multiple myeloma[40], and Hodgkin's lymphoma[41] exhibit increased NFκB activity.

Chromosomal aberrations in human c-Rel, p65, NFκB1, and NFκB2 genes are found in hematopoietic and solid tumors[42]. Studies on diffuse large cell lymphoma patients reveal amplification of c-Rel in 23 % of cases[43]. Rearrangements of NFκB2 are present in B-cell non-Hodgkin's lymphomas, chronic lymphocytic leukemia, cutaneous T-cell lymphomas, and multiple myelomas[44-47], whereas chromosomal aberrations in the p65 gene are rarely found in cancer. Inactivating mutations of the inhibitor IκB-α are often observed in Hodgkin's lymphoma[41,48].

Moreover, in some tumor entities, the constant secretion of proinflammatory cytokines, e.g. tumor necrosis factor alpha (TNF-α), or interleukin 1 (IL-1), persistently stimulates inhibitor of NFκB kinase (IKK) activity, causing constitutive NFκB activation. Examples are Hodgkin's lymphoma, colon, renal cell, pancreatic, or prostate cancer[49-51]. Studies on NFκB activation in childhood acute lymphoblastic

leukemia patients reveal that 93 % of cases exhibit constitutive NFκB activation, due to activation of upstream kinases[52].

Besides cytokines, chemotherapeutic drugs and ionizing radiation may activate NFκB. Activation of NFκB is part of the early response to ionizing radiation. Studies demonstrate that radiation induces NFκB nuclear binding activity and target gene expression within one hour of treatment in vitro and in vivo[53-55]. Many common chemotherapeutic drugs result in both NFκB nuclear translocation and DNA binding[56], nevertheless, a great diversity of NFκB responses is observed.

1.2.1 The transcription factor "Nuclear Factor kappa-B" (NFκB)

Nuclear factor kappa-B (NFκB) was originally discovered by Sen and Baltimore in 1986[57] in the nucleus of B cells. Since then, researchers have spent tremendous attention on signaling and activation pathways, and biological responses of this mammalian transcription factor. NFκB regulates a wide variety of genes, including those involved in cell growth[58], immune response[59], and apoptosis[60]. There are five known members of the mammalian NFκB/Rel family forming various homo- and heterodimers: p65 (Rel-A), c-Rel, Rel-B, NFκB1 (p105/p50), and NFκB2 (p100/p52). Cells synthesize p65, c-Rel, and Rel-B in mature forms, whereas both p105 and p100 are proteolytically processed by the proteasome producing the active subunits p50 and p52, respectively[61]. Common to all five members is the Rel-homology domain (RHD) for dimerization, nuclear localisation (containing the nuclear localisation signal), and DNA binding[62]. In unstimulated cells, NFκB dimers are sequestered in the cytoplasm through interaction with inhibitor of NFκB (IκB) proteins. The IκB family includes IκB-α, IκB-β, IκB-γ, IκB-ε, Bcl-3, and the NFκB precursors p100 and p105. Common to all IκBs are six to seven ankyrin-repeats mediating the binding to the RHD masking the nuclear localisation signal (NLS) of NFκB[63,64]. Interestingly, p105 and p100 can function both as reservoir for the mature p50 and p52 subunits and as IκBs, trapping Rel proteins in the cytoplasm. The most abundant form of NFκB is the heterodimer of p65 and p50, retained in the cytoplasm by IκB-α (figure 1.2).

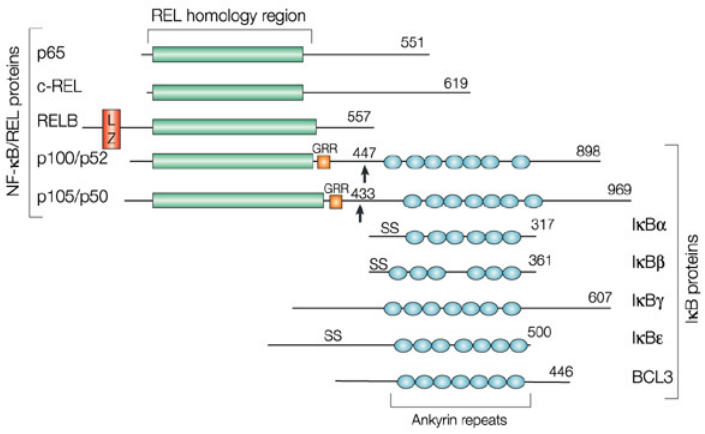

Figure 1.2: NFκB and IκB proteins.
Mammals express five NFκB proteins: p65, c-Rel, Rel-B, p100/p52, and p105/p50. They form various dimers and are characterized by their RHD. NFκB is retained in the cytoplasm by IκB proteins. IκB proteins include IκB-α, IκB-β, IKK-γ, IκB-ε, Bcl-3, and the NFκB precursors p100 (p52) and p105 (p50). All IκBs have a domain containing 6 – 7 ankyrin repeats, mediating their binding to the RHD (taken from Karin et al., Nat. Rev. Drug Discov., Vol. 3, 2004).

1.2.2 Classical versus alternative NFκB activation pathways

The canonical or classical pathway of NFκB activation is triggered in response to viral and microbial infections or various proinflammatory cytokines, e.g. TNF-α or IL-1. In unstimulated cells, NFκB dimers are kept inactive in the cytoplasm by IκB-α proteins. Above-named stimuli activate the inhibitor of NFκB kinase (IKK) complex consisting of the kinase catalytic subunits IKK-α and IKK-β and the regulatory subunit IKK-γ (NEMO)[65-67]. IKK activation depends on phosphorylation of IKK-β at serines 177/181 and of IKK-α at serines 176/180 causing a conformational change resulting in kinase activation[68]. Activated IKK phosphorylates the inhibitor IκB-α at serines 32/36 leading to its dissociation from NFκB[69]. Phosphorylated IκB-α generates a high affinity binding site for the ubiquitin ligase beta transducin repeat containing protein (β-TrCP), causing its subsequent ubiquitination and proteasomal degradation[70,71]. Degradation of IκB-α allows a rapid and transient translocation of the NFκB transcription factor into the nucleus. Once in the nucleus, NFκB binds to κB-sequences within promoter regions thereby activating gene transcription of a wide variety of genes[72,73] – including those of its own inhibitor IκB-α, interleukins, e.g. IL-8, or the growth factor for lymph angiogenesis, VEGF-c. NFκB is an important factor for drug resistance and cancer progression due to its target genes, which are mainly anti-apoptotic and pro-angiogenic[74].

The second or alternative NFκB pathway involves p100 dimerized with Rel-B. This signaling pathway is important for secondary lymphoid organogenesis and B-cell maturation and is activated by lymphotoxin–α/β (LTα/β) or CD40 ligand (CD40L). Activation of IKK-α dimers by NFκB kinase (NIK) induces the phosphorylation and proteolytic processing of p100 to p52, enabling the translocation of Rel-B/p52 into the nucleus[75] (figure 1.3).

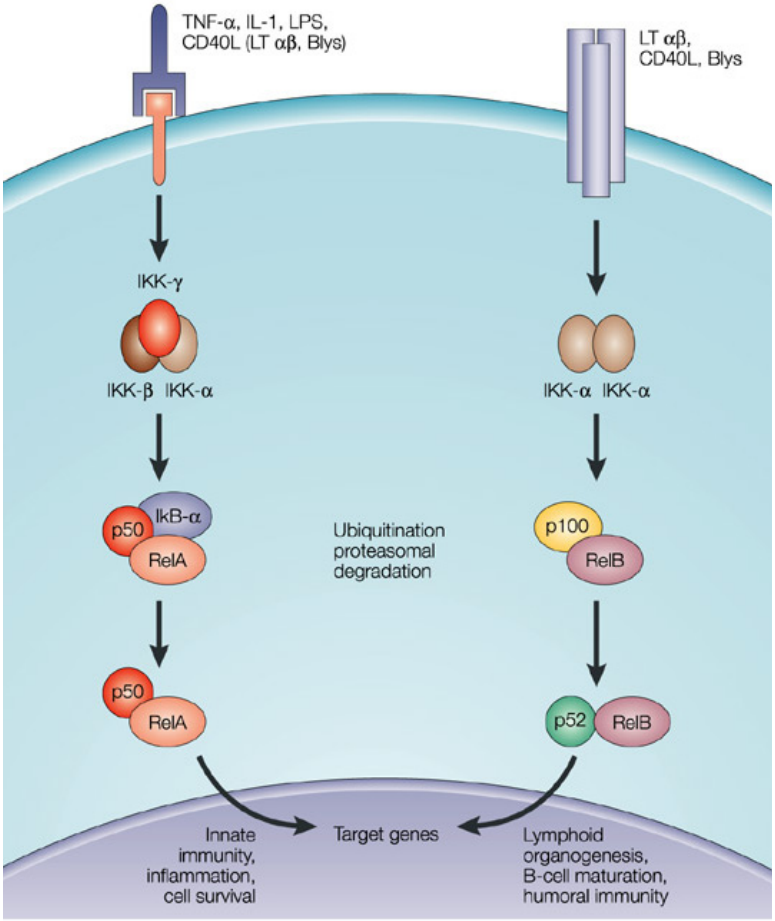

Figure 1.3: The two NFκB signaling pathways. The classical pathway (left) is activated by cytokines, e.g. TNF-α, IL-1, or LPS. This leads to the activation of the trimeric IKK complex, phosphorylation and degradation of IκB-α, and the translocation of NFκB into the nucleus. The pathway is involved in innate immunity and inflammation, and inhibition of apoptosis. The alternative pathway (right) is activated by LTα/β or CD40L. Activation of IKK-α homodimers results in p100 processing and translocation of p52/Rel-B dimers into the nucleus. This pathway is crucial for secondary lymphoid organ development, B-cell maturation, and adaptive humoral immunity (taken from Karin et al., Nat. Rev. Drug Discov., Vol. 3, 2004).

1.2.3 Signal transduction via TNF-receptors

Various stimuli activate NFκB. A very potent activator is TNF-α, a pleiotropic cytokine that regulates immune responses, inflammation, cell proliferation and differentiation, and apoptosis. Upon activation, specified immune cells secrete TNF-α, which exerts cytotoxicity on many tumor cell lines and causes tumor necrosis in certain animal models[76]. TNF-α exists as a membrane-anchored and a soluble form, both showing biological activity. Response to TNF-α is mediated through two

receptors: TNF-R1 (55 kDa) and TNF-R2 (75 kDa)[77]. Most tissues constitutively express TNF-R1, whereas mainly cells of the immune system and endothelial cells also express TNF-R2[78]. Because a great majority of cells produce TNF-R1 it appears to be the key mediator of the TNF signaling[79].

Binding of TNF-α to its receptors enables the activation of two signaling cascades:

- the activation of NFκB and induction of anti-apoptotic genes and/or
- the activation of caspases and pro-apoptotic genes

Upon binding of the TNF-α homotrimer, TNF-R1 trimerizes, which induces recruitment of several proteins to the cytoplasmic death domain of the receptor. This "complex I" and its association with TNF receptor associated protein with death domain (TRADD), receptor interacting protein (RIP), and TNF receptor associated factor 2 (TRAF2) proteins activates NFκB via the IKK complex. This results in suppression of apoptosis by expression of c-FLIP, Bcl-x_L, XIAP and other anti-apoptotic genes. "Complex II" arises by modification of the TRADD - RIP complex via ubiquitination and dissociation from the TNF-R1. Recruitment of FAS-associating death domain containing protein (FADD) to TRADD allows the activation of caspases, the release of cytochrome c, and the activation of executioner caspases[80,81]. The balance between these pathways determines death or survival. Tumor cells may evade apoptosis by activating NFκB through cytokine release by stromal cells, mutations in pathway components, or by activating NFκB in response to chemotherapeutic drugs (figure 1.4).

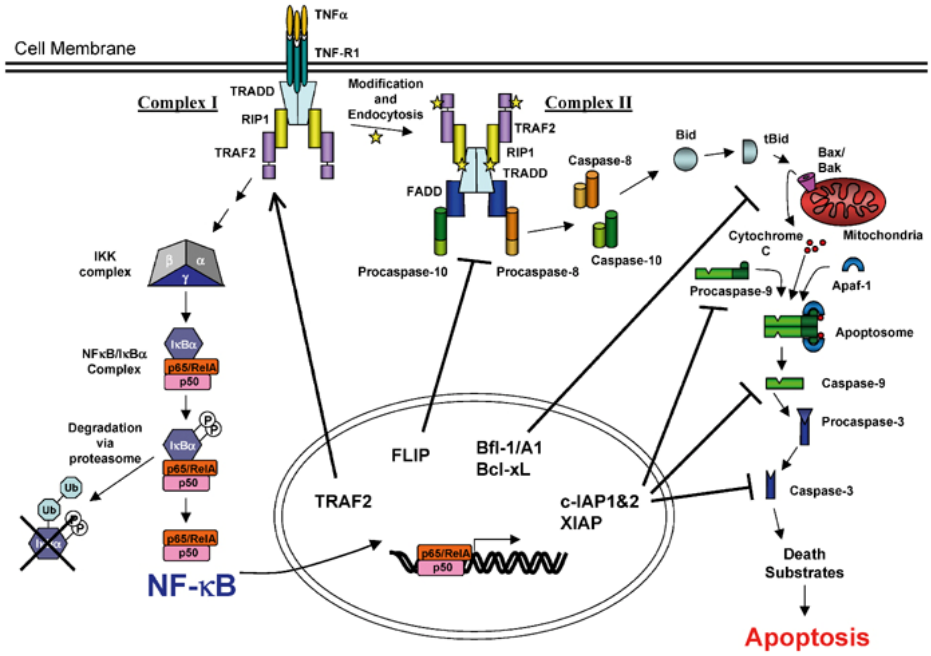

Figure 1.4: Balance between life and death decisions in the death receptor pathway.
Binding of TNF-α to the TNF-R1 may form two complexes. Complex I activates NFκB and upregulates anti-apoptotic genes. Complex II initiates the apoptotic pathway (taken from Kucharczak et al., Oncogene, Vol. 22, 2003).

1.2.4 Importance of NFκB in early embryonal development

NFκB is found in all cell types, and is essential during embryogenesis. In general, IKK-α is involved in skeletal development and epidermal differentiation[82]. IKK-α knockout mice die shortly after birth and exhibit developmental abnormalities: truncated limbs, ears, heads, and snouts due to a differentiation defect of skin epidermal cells. IKK-β deficient embryos die at embryonic day (E) 12.5 – 14.5 from excessive loss of hepatocytes due to apoptosis. Apoptosis is induced by TNF-α secretion since IKK-β and tumor necrosis factor receptor 1 (TNF-R1) double knockout mice are not affected by hepatocyte apoptosis and embryonic death[83-85]. Embryonic liver expresses tremendous amounts of TNF-α, which in the absence of NFκB activity triggers massive apoptosis. An identical phenotype is present in mice deficient in p65, which die at E14.5[86] or mice double deficient in both p65 and p50, which die at E12.5[87]. TNF-α can still activate NFκB nuclear translocation in cells from IKK-α -/- mice[88].

1.3 Histones, chromatin, and cancer

1.3.1 Chromatin structure and function

In eukaryotic cells the genetic material is packed into chromatin, a complex structure composed of DNA, histones, and non-histone proteins. The basic repeating unit of chromatin is the nucleosome, which consists of an octameric disc of histones - a H3-H4 tetramer and two H2A-H2B dimers - with about two turns of DNA wrapped around the outside. The linker histone H1 and other non-histone proteins twist and fold the chromatin fiber leading to a higher order structure[89]. The N- and C-terminal tails of core histones undergo various post-translational modifications such as acetylation, methylation, phosphorylation, ubiquitination, sumoylation, and ribosylation[90-93]. The pattern and types of modifications modulate protein-protein and protein-DNA interactions, e.g. recruitment of transcription factors. Histone acetylation, discovered more than 40 years ago[94], is a reversible modification of lysines within the N-terminal domain of core histones. In general, increasing histone acetylation enhances gene transcription by opening the chromatin, whereas decreasing acetylation represses and silences genes by condensing the chromatin (figure 1.5).

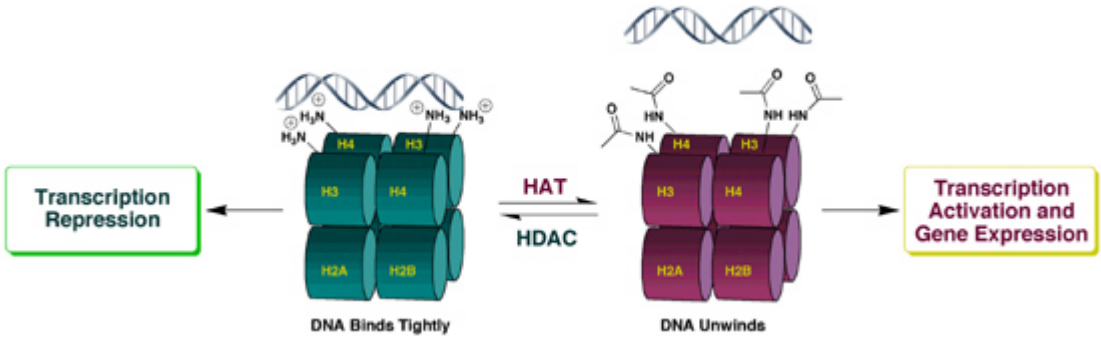

Figure 1.5: The chromatin structure regulates transcriptional activity.
Histone acetylation by histone acetyltransferases (HATs) relaxes the chromatin, enabling transcriptional activation. Histone deacetylation by histone deacetyltransferases (HDACs) leads to gene silencing (taken from G. R. Cook, Department of Chemistry and Molecular Biology, North Dakota State University).

1.3.2 Epigenetic events in cancer development and progression

Epigenetic events play an important role in the development of cancer[95-97]. Histone acetyltransferases (HATs) and histone deacetylases (HDACs) are the enzymes involved in the addition and removal, respectively, of acetyl groups at the N-terminal tails of histones. Inhibition of HDACs has emerged as a novel therapeutic strategy against cancer. The inappropriate deacetylation of tumor suppressor genes in tumor

cells may silence them, resulting in the progression of cancer. HDAC inhibitors (HDIs), in turn can switch on tumor suppressor genes, something traditional chemotherapy does not accomplish. It was shown recently, however, that HDIs influence the transcriptome of cells in a much broader manner[98].

1.3.3 Histone deacetylases (HDACs)

To date, three classes of HDACs[99,100] have been discovered in eukaryotes based on their structural homologies to yeast HDACs:

- Class I is closely related to the yeast transcriptional regulator Rpd3
- Class II has similarity to yeast Hda1
- Class III comprises homologs of yeast Sir2

Class I and II HDACs are NAD^+ independent and contain a zinc-dependent catalytic domain. The Rpd3 homologous class I comprises HDAC1, HDAC2, HDAC3, HDAC8 and the recently discovered HDAC11. Sometimes however, HDAC11 is viewed as being the sole member of class IV due to lack of sequence homology to other HDACs. Supporting this, in contrast to class I and II HDACs, HDAC11 is found in eukaryotic organisms except fungi[101]. Hda1 homologous class II includes HDAC4, HDAC5, HDAC6, HDAC7, HDAC9, and HDAC10. Crystallographic studies show that HDIs such as TSA and SAHA act by blocking the catalytic site of HDACs, inhibiting substrate access to the active zinc ion[102]. Class III HDACs[103], the so-called sirtuins, are NAD^+ cofactor dependent and are unaffected by all HDAC inhibitors (HDIs) currently under development or in clinical trials.

1.3.4 Histone acetyl transferases (HATs)

Histone acetyl transferases (HATs) also can be divided into three classes, depending on conserved structural motifs.

- GNAT family
- MYST family
- P300/CBP family

In general, HATs not only function as histone acetyl transferases, but may also act as transcriptional co-activators and co-repressors. Like GNAT members, p300/CBP has coactivator functions for transcription. They do not bind directly to DNA but are

recruited to particular promoters through interactions with DNA-bound transcription factors[104].

1.3.5 Histone deacetylase inhibitors (HDIs)

Inhibitors of HDACs class I and II are potent anti-cancer drugs, although their mode of killing tumor cells is not clear. Early models proposed that the addition of charge-neutralizing acetyl groups resulted in opening of the chromatin, increasing the access of transcription factors to the DNA, and thus augmenting gene transcription - in the case of cancer the transcription of tumor suppressor genes. Microarray data show that treatment with HDIs influences approximately 2 % of cellular genes[105], tending to downregulate as many genes as to upregulate. Different HDIs induce a similar pattern of altered genes in different cell lines[106]. Besides acetylation of histones, HDIs target many non-histone proteins, such as p53, GATA-1, ER-α, α-tubulin, nuclear receptors, Hsp90, signal transducer and activator of transcription family members, such as Stat3[107], and subunits of NFκB[108-110].

HDIs can be divided into six structural groups[111]:

- Short-chain fatty acids (e.g. Valproic acid)
- Hydroxamic-acids (e.g. SAHA, TSA)
- Cyclic tetrapeptides (e.g. Trapoxin, Apicidin)
- Benzamides (e.g. MS-275)
- Epoxyketones (e.g. TrapoxinB)
- Hybrid molecules (e.g. CHAP)

Key antitumor effects of HDIs are cell-cycle arrest and apoptosis induction. Almost all HDIs induce the transcription of CDKN1A, necessary for G1 arrest[112]. Tumor cells treated with HDIs, which do not arrest in G1, duplicate their DNA and cells subsequently undergo apoptosis[113-115]. Additionally, induction of MHC class I and II genes, of co-stimulatory molecules like CD40[116], CD80, and CD86[117] as well as of adhesion molecules, e.g. ICAM1, enhancing tumor immunogenicity is observed. Hypoxia induced expression of VEGF can be inhibited by HDIs, resulting in a suppression of angiogenesis[118].

Phenylbutyrate, a short-chain fatty acid, was the first HDI tested in patients[119]. High micromolar serum concentrations applied for therapeutic effects also had a broad spectrum of side effects. To date, the most clinically advanced HDI is the hydroxamic acid SAHA (suberoylanilide hydroxamic acid)[120], for which supposedly an NDA will be filed later this year by Merck & Co. It is effective at sub-micromolar concentrations, demonstrating significant anti-cancer activity in haematological and solid tumors at doses well tolerated by patients.

2 AIM OF THE STUDY

In recent years it has become clear that NFκB signaling has a critical role in cancer development and progression. NFκB regulated proteins are linked to cell proliferation, apoptosis inhibition, cellular transformation, invasion, angiogenesis, and metastases. Additionally, NFκB has an outstanding role in immune defense. Different research groups showed that several cancer cell lines and tumor samples of various entities exhibit increased NFκB expression and activity. Chemotherapeutic drugs and radiation therapy also activate NFκB, boosting multidrug and therapy resistance. In this context, the aims of the present work were:

1) To determine the NFκB activation status in different tumor entities. Information about the activation status might allow a reasonable selection of tumor entities for NFκB drug development and for the later application of an NFκB inhibitor in the patient.
2) To characterize several IKK inhibitors for their effects on tumor cells.
3) To analyze the induction of anti-apoptotic and pro-proliferative signaling by various chemotherapeutic drugs such as topoisomerase poisons or cisplatin.
4) To examine the influence of histone deacetylase inhibitors (HDIs) on inducibility of NFκB activity by TNF-α. HDIs are an exciting new class of anti-cancer drugs for tumor treatment and inhibition of inflammatory signaling by these molecules could prove beneficial for cancer treatment.

3 MATERIAL AND METHODS

3.1 Material

3.1.1 Chemicals

Ambion (Cambridgeshire, UK): 1x TE solution pH 8.0 (#9849)

Fluka (Seelze, Germany): bromophenolblue-xylenecyanol (#18047), DTT (#43815), Ficoll (#46324), IGEPAL CA-630 (#56741), methanol (CH_3OH, #65543), SDS solution (#71736), skim milk powder (#70166), 10x TRIS-buffered-saline (#93312), 10x TRIS-glycine-buffer (#93321), 10x TRIS-glycine-SDS-buffer (#93311)

GE Healthcare (Munich, Germany): Poly-(dI-dC) (#27-7880)

Gibco (Karlsruhe, Germany): HEPES solution (#15630-056), PBS (#14190-094)

Merck (Darmstadt, Germany): 1-Butanol (#1.01990), acrylamide-bis-acrylamide solution (#1.00639 for immunoblotting; #1.00641 for EMSA), di-sodium hydrogen phosphate (Na_2HPO_4, #1.06586), ethanol (C_2H_5OH, #1.00983), hydrochloric acid (HCl, #1.00317), magnesium chloride ($MgCl_2$, #8.14733), potassium dihydrogen phosphate (KH_2PO_4; #1.04873), sodium chloride (NaCl, #1.06404), sodium hydroxide solution (NaOH, #111584), 10x TBE buffer (#1.06177)

Molecular Probes/Invitrogen (Karlsruhe, Germany): Hoechst 33342 (#H3570)

NEB (Ipswich, MA 01938-2723, USA): BSA for EMSA (# B9001S)

Riedel-de Haën (Seelze, Germany): Potassium chloride (KCl, #31248)

Sigma-Aldrich (Munich, Germany): β-glycerophosphate disodium salt hydrate (#G-376), β-mercaptoethanol (#M6250), ammonium persulfate (APS; #A3678), bovine albumin (BSA for cellomics, #A7030, BSA for immunoblotting #A7906), bromophenolblue sodium salt (#114405), DMSO (#D2650), EDTA disodium salt solution (#E7889), fetal bovine serum (#F9665), formaldehyde solution (HCHO, #252549), glycerol (#G5516), leptomycin B (#L2913), resazurin (#199303), sodium azide (NaN_3, #S2002), sodium deoxycholate monohydrate (#238392), sodium fluoride (NaF, #S7920), sodium molybdate (Na_2MoO_4, #243655), sodium orthovanadate (Na_3VO_4, #S6508), TEMED (#T9281), Triton X-100 (#T9284), Trizma base (#T1503), TWEEN-20 (#274348)

3.1.2 Reagents

Applied Biosystems (Darmstadt, Germany): 96-well optical reaction plates (#4306737), optical adhesive films (#4311971)

Atugen (Berlin-Buch, Germany): Argfectin-50

Bio-Rad Laboratories (Munich, Germany): Extra thick blot paper (#170-3966), immun-blot PVDF membrane (#162-0177)

Dharmacon (Lafayette, CO 80026, USA): ATM siRNA (#M-003201), CHUK siRNA (#M-003473), IKBKB siRNA (#M-003503), NFKB2 siRNA (#M-003918), STAT1 siRNA (#M-003543)

Eurogentech (Liege, Belgium): q-PCR mastermix (#RT-QP2X-03-50+)

GE Healthcare (Munich, Germany): MicroSpin^{TM} G-50 columns (#27-5330-01), Protein-G Sepharose 4 Fast Flow (#17-0618-01)

Invitrogen (Karlsruhe, Germany): Custom primers for EMSA, cell culture media

Larova (Teltow, Germany): dNTP mix PCR3 (#0200/0205)

Roche Applied Science (Mannheim, Germany): Complete mini protease inhibitor cocktail (#1836153), 10x hexanucleotide mix (#1277081), Lumi-Light^{PLUS} western blotting substrate (#12015196001)

Sigma-Aldrich (Munich, Germany): Phosphatase inhibitor cocktail 2 (#P5726), protease inhibitor cocktail (#P8340)

Terumo (Frankfurt am Main, Germany): Neolus grey needles 27G (#ND-271), syringe (#BS-01T)

3.1.3 Antibodies and Molecular Weight Markers

Abcam (Cambridge, UK): IκB-β (#ab7547)

Bio-Rad Laboratories (Munich, Germany): Goat anti-rabbit IgG HRP (#170-6515), goat anti-mouse IgG HRP (#170-6516)

Calbiochem (Schwalbach, Germany): Rabbit anti-mouse IgG antibody fluorescein isothiocyanate labeled (#401219)

Cell Signaling (Danvers, MA 01923, USA): IκB-α (#9242), IKK-β (#2684), NFκB p65 (#3034), NFκB2 p100 (#4882), NFκB1 p105 (#3035), Phospho-ATM (Ser1981) (#4526), Phospho-IKK-α/β (Ser176/180) (#2687), STAT1 (#9172)

GE Healthcare/Amersham (Munich, Germany): Rainbow molecular weight marker (#RPN800)

Molecular Probes/Invitrogen (Karlsruhe, Germany): Alexa-Fluor-488 goat anti-rabbit IgG (#A11008), Alexa-Fluor-488 goat anti-mouse IgG (#A11001), Magic Mark^{TM} XP (#LC5602)

Santa Cruz Biotechnology (Heidelberg, Germany): Donkey anti-goat IgG HRP (#sc-2020), IKK-γ (FL-419) (#sc-8330), NFκB p65 (F-6) (#sc-8008), NFκB p65 (F-6) (#sc-8008x), NFκB p50 (NLS) (#sc-114x), STAT1 p84/p91 (E-23) (#sc-346), TNF-R1 (H-5) (#sc-8436)

Sigma-Aldrich (Munich, Germany): β-actin (#A5441)

Upstate (Dundee, UK): IKK-α (#05-536), IKK-β (#05-535)

3.1.4 TaqMan gene expression assays

Applied Biosystems (Darmstadt, Germany):

- Pre-designed TaqMan gene expression assay:

ATM (Hs00175892_m1), c-Flip (CFLAR, Hs00153439_m1), IκB-α (NFKBIA, Hs00153283_m1), IKK-α (CHUK, Hs00175141_m1), IKK-β (IKBKB, Hs00233287_m1), IKK-γ (IKBKG, Hs00415849_m1), p100 (NFKB2, Hs00174517_m1), p105 (NFKB1, Hs00231653_m1), STAT1 (Hs00234829_m1), TNF-R1 (TNFRSF1A, Hs00533560_m1), TRAIL-R2 (TNFRSF10B, Hs00187196_m1)

- Custom TaqMan gene expression assay:

18S rRNA, 18S rRNA-MGB, Bcl-x_L, IL-8, VEGF-c, GAPDH, β-actin

3.1.5 Peptides

Axxora (Grünberg, Germany): MG-132 (#ALX-260-092-M005)

Boston Biochem (Cambridge, MA 02139, USA): Suc-LLVY-AMC (#S-280)

Tebu-bio (Offenbach, Germany): IFN-α (#300-02A), TNF-α (#300-01A)

3.1.6 Kits

Active Motif (Rixensart, Belgium): TransAM™ NFκB p65 Chemi (#40097)

Pierce (Bonn, Germany): BCA Protein Assay Kit (#23227)

Qiagen (Hilden, Germany): QIAshredders (#79654), RNeasy Mini Kit (#74104)

Roche Applied Science (Mannheim, Germany): Cell Death Detection ELISA (#1920685)

3.1.7 Enzymes

GE Healthcare (Munich, Germany): T4 polynucleotide kinase (#70031Y)

Invitrogen (Karlsruhe, Germany): Trypsin-EDTA (#15400054)

Qiagen (Hilden, Germany): RNase-Free DNase Set (#79254)

Roche Applied Science (Mannheim, Germany): AMV reverse transcriptase (#11495062001)

3.1.8 Compounds

ALTANA Pharma: LAQ-824, Mafosfamide, MS-275, PS-1145, SAHA

Calbiochem (Darmstadt, Germany): BMS-345541 (#401480), BAY 11-7085 (##196872), SC-514 (#401479)

Sigma-Aldrich (Munich, Germany): 17-AAG (#A8476), Camptothecin (#C9911), Cisplatin (#P4394), Doxorubicin (#D1515), Etoposide (#E1383), TSA (#T8552)

3.1.9 Radiochemicals

GE Healthcare (Munich, Germany): Redivue adenosine 5'-[γ-32P]triphosphate, triethylammonium salt (#AA0068)

3.1.10 Laboratory equipment and technical devices

Blottingapparatus: Mini Protean II Electrophoresis Cell, Power Pac 200, Transblot SD Semidry Transfer Cell (Bio-Rad Laboratories GmbH, Munich, Germany)

Cell culture: Culture flasks, disposable pipettes, and plates (Corning, Kaiserslautern, Germany), plastic disposables (Greiner, Frickenhausen, Germany), HERAcell® CO_2 Incubator (Thermo Electron, Langenselbold, Germany)

Centrifuges: Eppendorf Centrifuge 5415D, Eppendorf Centrifuge 5417R (Eppendorf AG, Hamburg, Germany), Kendro Multifuge 3 S-R (Thermo Electron, Langenselbold, Germany), Sigma 4K15 Centrifuge (SIGMA Laborzentrifugen, Osterode am Harz, Germany)

EMSA equipment: baacklab® diaphragm vacuum pump, electrophoresis chamber H20 maxi, gel dryer 3545E (Armin Baack, Schwerin, Germany)

FACS: FACSCanto™ (Becton Dickinson GmbH, Heidelberg, Germany)

Heating block: Eppendorf Thermo Statplus (Eppendorf AG, Hamburg, Germany)

Imaging Systems: ArrayScan® II High Content Scan Reader (Cellomics, Berkshire, UK), FLA-5000 Phosphorimager, LAS 1000 Luminescence Image Analyzer (Fuji Photofilm, Duesseldorf, Germany)

Microscopes: Leica DM IL, Leica DM IRB (Leica Microsystems, Bensheim, Germany)

Photometers: Nano Drop ND-1000 Spectrophotometer (Peqlab Biotechnologie GmBH, Erlangen, Germany), Ultrospec 3100pro (GE Healthcare, Munich, Germany), Wallac 1420 Victor2 Multilabel Counter (Beckman Coulter, Krefeld, Germany)

Software: FlowJo Software (TreeStar, Ashland, OR, USA), GraphPad Prism 4.0 (GraphPad Software Inc., San Diego, CA 92130 USA), IM 1000 (Leica Microsystems, Bensheim, Germany)

TaqMan: ABI Prism 7700 Sequence Detector (Applied Biosystems, Darmstadt, Germany)

Ultrafiltration devices: MilliQ A10 (Millipore, Schwalbach, Germany)

3.1.11 Human cell lines

B-cell lymphoma: Pfeiffer, DB, Toledo (ATCC, American type culture collection, Wesel, Germany), KARPAS-422, OCI-LY-19 (DSMZ, German collection of microorganisms and cell cultures, Braunschweig, Germany), OCI-LY-3 (Dr. Christof Burek, Universität Würzburg, Würzburg, Germany)

Hodgkin's lymphoma: HDLM-2, KM-H2, L-1236, L-540, L-428 (Dr. Claus Scheidereit, Max Delbrueck Center for Molecular Medicine, Berlin-Buch, Germany)

Lung cancer cell lines: (a) non-small cell lung cancer: adenocarcinoma A549 (alveolar type II cells), NCI-H23 (H23), NCI-H1563 (H1563), NCI-H1703 (H1703), A-427; large cell carcinoma NCI-H460 (H460); squamous cell carcinoma NCI-H2170 (H2170), NCI-H520 (H520) (b) small cell lung cancer: NCI-H69 (H69), DMS 53, DMS 114 (all cell lines from ATCC), and SW2 (Dr. Uwe Zangemeister-Wittke, Universität Zürich, Zürich, Switzerland)

Multiple myeloma: MM.1S, MM.1R (Dr. Bisping, Universität Münster, Münster, Germany)

Pancreatic carcinoma cell lines: AsPC-1, BxPC-3, PANC-1, Capan-1, Capan-2 (ATCC), DAN-G (DSMZ)

Other cancer cell lines: A2780 (ovary, supplier unknown), U-2 OS (bone; ATCC), RKO-p21 (colon; ALTANA Pharma)

Normal cells: HFL-1 (ATCC), SAEC (Cambrex Bio Science, Verviers, Belgium)

3.1.12 Buffers and Solutions

Cytotoxicity Assay

Resazurin solution: 0.009 % resazurin in PBS

Electrophoretic Mobility Shift Assay

Annealing Buffer for Oligonucleotides: 20 mM Tris-HCl pH 8.0, 20 mM NaCl

Complete Cell Lysis Buffer (for EMSA): 20 mM HEPES, 350 mM NaCl, 20 % glycerol, 1 mM $MgCl_2$, 0.5 mM EDTA, 1% IGEPAL CA630, 1 mM DTT containing a cocktail of protease and phosphatase inhibitors

Nuclear Extraction Buffer (for EMSA):

- Hypotonic buffer: 20 mM HEPES pH 7.5, 5 mM NaF, 10 µM Na_2MoO_4, 0.1 mM EDTA, final pH 7.5

- Lysis Buffer: 20 mM HEPES pH 7.5, 400 mM NaCl, 0.1 mM EDTA, 10 mM NaF, 10 µM Na_2MoO_4, 20 % glycerol, 10 mM β-glycerophosphat, final pH 7.5

2x Shiftbuffer (EMSA): 40 mM HEPES-NaOH pH 7.9, 120 mM KCl, 8 % Ficoll

Oligonucleotides for EMSA:

NFκB sense: 5’ AGT TGA GGG GAC TTT CCC AGG C 3’

NFκB antisense: 5’ GCC TGG GAA AGT CCC CTC AAC T 3’

Gene Expression Analysis

RLT-Buffer: 400 µl β-mercaptoethanol in 40 ml RLT Buffer

Immunoblotting

Blocking buffer: 3 % BSA in 1x TTBS, 1:1000 sodium-azid

Blotting buffer for PVDF membranes: 1x Tris-glycin-buffer, 20 % methanol

5x Laemmli Buffer: 250 mM Tris-HCl pH 6.8, 5 % SDS, 5 % β-mercaptoethanol, 10 mM EDTA, 35 % glycerol, bromphenolblue

RIPA Buffer: 120 mM NaCl, 50 mM Tris-HCl (pH 7.4), 20 mM NaF, 1 % Triton-X-100, 0.5 % Na-Desoxycholat, 0.1 % SDS, 1 mM Na_3Vo_4, protease inhibitor cocktail (Roche)

SDS-PAGE running buffer (10x Tris-Glycin-SDS-Buffer): 0.25 M Tris-HCl, 1.92 M glycine, 0.1% SDS; pH 8.6

Secondary antibody solution: 3 % skim dry milk in 1x TTBS

10x Tris-Buffered Saline (TBS): 0.2 M Tris-HCl; 9.0% NaCl; pH 7.5

10x Tris-Glycin-Buffer: 0.25 M Tris, 1.92 M glycine, pH 8.6

Washing buffer 1x Tris-Buffered-Saline with TWEEN-20 (TTBS): 1x TBS, 0.05 % TWEEN-20

Immunoprecipitation

Lysis Buffer C: 1 % Triton-X-100, 0.3 M NaCl, 50 mM Tris-HCl, 5 mM EDTA, 0.1 % BSA, protease-inhibitor cocktail (Roche)

Wash Buffer: 0.1 % Triton-X-100, 0.3 M NaCl, 50 mM Tris-HCl

Nuclear Translocation Assay

Blockingbuffer: 0.3 % TWEEN-20, 1 % BSA, PBS

Fixation Buffer

3,7 % formaldehyde in PBS (37 °C preheated)

50x Permeabilisationbuffer: 1.5 M NaCl, 26.7 mM Na_2HPO_4, 15.4 mM KH_2PO_4, 5 % Triton-X-100

Proeasome Activity Assay

Incubationbuffer: 20 mM Tris-HCl pH 7.5, 0.5 mM EDTA, 200 µM Suc-LLVY-AMC

Lysis-buffer: 1 mM DTT in H_20

3.2 Methods

3.2.1 Cell Culture

Cells were grown and maintained under favorable conditions without antibiotics in a humidified incubator at 37 °C with 5 % CO_2 / 95 % air. Adherent cells were split twice a week with trypsin-EDTA. Suspension cells were grown in special culture flasks and were split by decanting a good portion of cells, which were subsequently resuspended in fresh media. For cell culture experiments, cells were seeded at least 24 hours before treatment. Drug concentrations or seeded cell numbers are listed in the results chapter.

3.2.2 Cell transfection with short interfering RNA (siRNA)

Short interfering RNA (siRNA) technology allows the specific knockdown of genes by introducing short double strands of RNA into the cell. The antisense strand binds to the sense mRNA. This complex is recognized by the cell and causes its cleavage and degradation. Lung cancer cells were seeded at 50.000 cells per 6-well plate in 1.6 ml medium supplemented with 10 % FCS. Cells were allowed to adhere 24 hours before transfection. Short interfering RNAs (siRNAs) were delivered in complex with Argfectin-50. Both the siRNA and the transfection reagent Argfectin-50 were diluted to a 10x final concentration in 200 µl culture medium containing 20 mM HEPES without FCS. siRNA and Argfectin-50 were mixed at a ratio of 1:1 in 400 µl total volume and incubated for 30 min at 37 °C for transfection complexes to be formed. The transfection complexes were added onto the cells and plates were gently swirled to ensure uniform distribution. Plates were incubated 48 hours before the addition of various drugs. Cells were either harvested for RNA and protein analysis, or were TNF-α treated (25 ng/ml, 30 min) and fixed for assaying nuclear translocation of NFκB.

3.2.3 Cytotoxicity assay

The resazurin assay is a simple way of measuring cytotoxicity and proliferation of treated versus untreated cells. Metabolically active cells reduce resazurin to resorufin which manifests as visual color change from blue (resazurin) to pink (resorufin). Cells were cultured in 96- or 6-well cell culture plates and incubated with various drugs for 24 – 72 hours. Thereafter, 1/10 volume of the resazurin dye was added to each well

and incubated at 37 °C till color change was visible. Fluorescence intensity at 590 nm - with 544 nm excitation - was monitored on a Wallac 1420 Victor2 fluorometer. Results were expressed as percentage of growth reduction versus control.

3.2.4 Nuclear translocation assay

ArrayScan technology allows to determine the distribution of fluorescence labeled components between nuclear and cytoplasmic compartments. For performing nuclear translocation assays, cells were seeded in 96- or 6-well plates. For experiments with histone deacetylase inhibitors (HDI), cells were preincubated for 24 hours with SAHA or TSA before adding TNF-α (25 ng/ml) or IFN-α (100 ng/ml) for 30 min. For inhibiting the nuclear export, leptomycin B (LMB) was added to HDI treated cells either simultaneously (for 24 hours LMB treatment), 2 hours, or 30 min before TNF-α treatment. For determining the activation status in various cell lines, cells were TNF-α stimulated for 30 min or were left untreated. After NFκB activation with cytokines, cells were fixed with 3.7 % formaldehyde at RT for 15 min, washed with blocking buffer, and permeabilised with permeabilisation buffer for another 15 min (buffers see page 21). Cells were washed twice with blocking buffer and incubated in blocking buffer containing 1:500 diluted anti-p65 antibody for TNF-α or anti-STAT1 antibody for IFN-α stimulated cells for one hour. After washing with blocking buffer twice, 1:250 diluted Alexa-Fluor-488 labeled anti-mouse IgG or anti-rabbit IgG was added together with 0.2 µg/ml Hoechst 33342 dye for one hour. After washing three times, plates were sealed and scanned using the ArrayScan® II high content reader. Data were evaluated using GraphPad Prism 4.0 software.

3.2.5 Immunoblotting

Immunoblotting is a method to detect a designated protein in a given sample. Proteins are denatured, separated by gel electrophoresis, transferred to a membrane, and probed employing antibodies against the protein of choice. For obtaining cellular extracts, cells were washed with PBS and lysed with RIPA buffer (page 20) for at least 30 min at 4 °C. Cell lysates were centrifuged at 14.000 x g/4 °C/10 min, pellet was discarded, and supernatant was used for protein concentration determination by Pierce BCA protein assay kit. 20 µg of protein lysates together with 1x Laemmli buffer (page 20) were boiled for 5 min for denaturing the proteins. Thereafter, protein

samples were subjected, depending on sizes of the studied proteins, to 5 – 12.5 % SDS-polyacrylamide gel electrophoresis:

Proteins:	≤ 40 kDa	12.5 %
	≤ 90 kDa	10.0 %
	≤ 120 kDa	7.0 %
	> 120 kDa	5.0 %

Bromphenolblue dye in the sample buffer allowed monitoring the electrophoresis process. Proteins were transferred to PVDF membranes utilizing the semidry transfer method. Transfer was performed at 150 mA current for 1½ hours. Subsequently, membranes were blocked with 3 % BSA in 1x TTBS (page 21) for one hour. Primary antibodies were incubated in blocking buffer at 4 °C over night. The following day, membranes were washed trice with 1x TTBS and incubated with secondary antibodies conjugated with horseradish peroxidase (HRP) in secondary antibody buffer for one hour at RT. Membranes were washed for another three times and developed by using the Lumi-Light^{PLUS} Western blotting substrate according to the manufacturer's protocol. Immunoblots were visualized and recorded by the LAS-1000, a chemiluminescent image analyzer. Equal loading and transfer was verified with β-actin antibody.

3.2.6 Immunoprecipitation

Immunoprecipitation allows separation of a designated protein from a cellular extract using a protein-specific antibody. This technique is employed to identify further proteins that are in complex with the precipitated protein. For immunoprecipitation experiments, cells were plated in 10 cm^2 dishes, HDI treated for 24 hours, and lysed with 500 µl ice-cold lysis buffer C (page 21). All further steps were performed on ice. Lysates were centrifuged twice at 15.000 x g/ 4 °C/10 min, the pellet was discarded, and protein concentration of the supernatant was determined employing Pierce BCA protein assay kit. Sepharose-G beads in suspension were washed trice with lysis buffer C and resuspended carefully obtaining a 50 % slurry. To minimize unspecific binding, 500 µg of protein extracts were precleared with sepharose-G beads only, rotating for 30 min. Beads were centrifuged and supernatant was incubated over night with 15 µl anti-p65 antibody on a rotator. The following day, 25 µl sepharose-G beads were added and the suspension was rotated for an additional 2 hours.

Sepharose-antibody-p65 complexes were precipitated at low speed and washed four times with wash buffer and once with PBS. The last supernatant was removed carefully. Beads were resuspended in PBS and Laemmli buffer and boiled for 5 min at 95 °C. Beads were pelleted and proteins were analyzed by subsequent SDS-PAGE and immunoblotting.

3.2.7 Gene expression analysis

Gene expression analysis by real-time PCR allows quantifying the expression of selected genes in a given sample. For NFκB target gene stimulation, cells were seeded in 6-well plates and treated with TNF-α for 4 hours. For RNA isolation, cells were washed with PBS and lysed with RLT-buffer containing β-mercaptoethanol. Total RNA was isolated with the RNeasy Mini kit according to the manufacturer's instructions, adding an additional DNase digestion step. RNA quality and quantity was specified utilizing the Nano Drop ND-1000 measuring the adsorption at 260 nm versus 280 nm. cDNA synthesis was carried out using 1 µg of RNA, 0.75x hexanucleotidmix, 500 µM dNTPs, and 20 units AMV reverse transcriptase. The cDNA mix was incubated for 1 hour at 42 °C, thereafter diluted with 0.1x TE to 2 ng/µl RNA. Quantification of mRNA expression was performed employing the Abi Prism 7700 sequence detection system. PCR-reactions for all samples were done in triplicate in 96-well optical plates using 5 ng of RNA in a total volume of 25 µl. Thermocycler conditions comprised an initial holding stage at 50 °C for 2 min and a denaturing stage at 95 °C for 10 min, followed by a 40 cycles two-step program consisting of 95 °C for 10 sec and 60 °C for 1 min. All samples were standardized with respect to 18S rRNA: ΔCt values of the target genes, which were standardized to 18S rRNA (Ct[target gene] – Ct[18S control]), were normalized to the control sample according to the ΔΔCt method (ΔCt [treated sample] - ΔCt [untreated sample]). Fold changes of relative expression were calculated by assuming duplication of mRNA for each ΔΔCt unit. For HDIs, results from three independent experiments were analyzed for statistical significance performing ANOVA with Dunnett's multiple comparison test using GraphPad Prism 4.0 software.

3.2.8 Electrophoretic mobility shift assay (EMSA)

The electrophoretic mobility shift assay allows the study of protein-DNA interactions. It determines if a protein in a cell extract is able to bind to a given DNA sequence.

Cells were seeded in 6-well plates for whole cell extracts or in 10 cm^2 dishes for nuclear extracts. Cells were incubated with or without drugs before stimulation with 25 ng/ml TNF-α for 30 min.

Nuclear extracts were prepared according to the protocol of Active Motif. Briefly, cells were washed and scraped off in ice-cold PBS, centrifuged, resuspended in 1 ml hypotonic buffer, and kept on ice for 15 min. NP-40 was added to a final concentration of 0.5 % and the suspension was re-centrifuged. Supernatant was discarded, the pellet resuspended in 50 µl complete lysis buffer (buffers see page 20), and rocked on ice for 30 min. Then, the suspension was centrifuged at 14.000 x g/4 °C/10 min and the supernatant was stored at -80 °C. Nuclear extracts were either used for electrophoretic mobility shift assays (EMSA) or for NFκB activation studies by the ELISA-based TransAM NFκB p65 kit from Active Motif.

For whole cell extracts cells were washed with PBS and lysed in complete cell lysis buffer (page 20) on ice for 30 min. Subsequently, the lysate was centrifuged for 5 min at 14.000 x g/4 °C in an eppendorf microcentrifuge. The supernatant was stored at – 80 °C for EMSA experiments.

EMSAs were performed using a double-stranded oligonucleotide containing a consensus κB-binding site from the HIV-1 LTR (5'-AGTTGAGGGGACTTTCCCAGGC-3' – consensus κB-region underlined). 1 µl of each NFκB oligonucleotide (100 µM) was annealed in a total volume of 20 µl by boiling at 95 °C for 5 min and then turning off the heating block for cooling down slowly. For end-labeling, 2 µl (10 pmol) annealed oligonucleotides were incubated with 2 µl polynucleotide kinase buffer, 3 µl [γ-^{32}P]ATP, and 1 µl T4 polynucleotide kinase in a total volume of 20 µl for one hour at 37 °C. The endlabeling reaction was purified utilizing MicroSpin G50 columns and filled with 80 µl 0.1x TE buffer. Nuclear extracts were incubated with 2x shiftbuffer adding 2 mM DTT, 0.1 µg/µl poly-(dI:dC), and 0.1 µg/ml BSA in a total volume of 20 µl at RT for 15 min. For supershift experiments, the nuclear extracts were preincubated with 4 µg anti-p65 antibody. The reaction mixture was subjected to electrophoresis on a 5 % non-denaturing polyacrylamide gel. The electrophoresis was run between 120 – 200 V

until the bromphenolblue-xylenecyanol dye, loaded into a separate well, was 3 cm from the end of the gel. Gels were dried under vacuum and exposed to phosphor screens for a few days. Radioactive signals were visualized with a FUJIFILM FLA-5000 phosphorimager.

ELISA-based measurements of NFκB DNA binding were performed according to the manufacturer's protocol. Briefly, nuclear extracts were incubated in complete binding buffer with mild agitation for one hour, allowing the binding of NFκB to its consensus sequence that is linked to the 96-well plate. Afterwards, plates were incubated with a primary anti-p65 antibody followed by an HRP-conjugated secondary antibody. After all incubation steps, plates were washed three times with wash buffer. For the chemiluminescence reaction, the substrate was added to each well and incubated in the dark for about 5 min before adding the stop solution. Chemiluminescence was deteceted at the Wallac 1420 Victor2.

3.2.9 Fluorescence flow cytometry

Flow cytometry is a method for quantifying components or structural features of cells. It detects cells or labeled particles on a cell in a fluidic system, one at a time, measuring thousands of cells in a few seconds. This technique was employed to determine the amount of the TNF-R1 at the cell surface upon drug treatment. A549 cells were plated in 10 cm^2 dishes and were either treated with HDIs for 24 h or were left untreated. Cells were rinsed with PBS, detached with a 0.2 % EDTA/PBS solution at 37 °C for about 10 - 20 min, centrifuged at 310 x g/3 min, washed with PBS, and divided into two aliquots. Cells were either incubated with 20 µl mouse IgG_{2b} anti-human TNF-R1 antibody or without for the isotype control for 30 min on ice. Thereafter, cells were washed with PBS and incubated in the dark with 10 µl rabbit anti-mouse IgG antibody labeled with fluorescein-isothiocyanate. After 30 min, cells were washed twice with PBS, resuspended in 1% formaldehyde/PBS, and analyzed using a FACS-Canto instrument. Data were analyzed employing FlowJo Software.

3.2.10 Proteasome activity assay

The proteasome activity assay is designed to measure the chymotrypsin-like peptidase activity of the 20S proteasome by cleaving the substrate Suc-Leu-Leu-Val-Tyr-AMC (Suc-LLVY-AMC) releasing the fluorophore AMC. Cells were treated with HDIs for

24 hours or MG-132 for 4 hours, washed, scraped off in PBS, centrifuged, and incubated in H_2O containing 1 mM DTT for 30 min at 4 °C. Cells were lysed by passing 25-30 times through a 27-gauge needle fitted to a syringe. The lysates were centrifuged for 10 min at 10.000 x g and supernatants were checked for protein concentration by Pierce BCA protein assay kit. Equal amounts of protein (5 µg) were incubated with 90 µl proteasome incubation buffer in a total volume of 100 µl for 30 min at 37 °C. Proteasomal activity was determined in triplicate at 355 nm excitation and 460 nm emission on the Wallac 1420 Victor2 fluorometer.

4 RESULTS

4.1 Experimental system

Usually, the transcription factor NFκB, most commonly a dimer of p65/p50, is held inactive in the cytoplasm by inhibitory proteins called IκBs e.g. IκB-α. Upon the appropriate stimulus, IκB-α is degraded and NFκB transfers to the nucleus and activates expression of its target genes. Publications on different tumor entities and cell lines report enduring NFκB nuclear activity[38,40,51]. Furthermore, it has been reported that constitutively activated NFκB is accompanied with worse outcome for tumor patients[121,122]. For this reason, the NFκB activation status in various tumor entities was tested.

NFκB activation was measured at different levels:

- phosphorylation of IKK-α/β and IκB-α in the cytoplasm (immunoblotting)
- translocation (nuclear translocation assay)
- DNA binding (EMSA, ELISA)
- target gene expression (TaqMan PCR)

A very prominent method to detect NFκB activation is the quantification of phosphorylated IKK-α/β, IκB-α, and p65 as well as IκB-α degradation by immunoblotting.

To achieve a visual impression of NFκB localisation upon various stimuli, nuclear translocation assays were performed. They measure differences in NFκB distribution between nucleus and cytoplasm upon activation.

For detecting the DNA binding capability of NFκB, electrophoretic mobility shift assays (EMSA) were employed. This technique detects the interaction of activated NFκB with its DNA recognition sequence, in both a qualitative and quantitative manner. Because IκB-α keeps NFκB in an inactive condition, nuclear extracts or whole cell extracts can be utilized. Activated NFκB binds to the radioactively labeled κB-recognition sequence forming stable complexes, which migrate slower than the

unbound oligonucleotide in a non-denaturating polyacrylamide gel. Addition of an antibody against a selected NFκB subunit before adding the labeled oligonucleotides allows the identification of the complex by an additional gelshift (supershift assay). The non-radioactive DNA binding assay "TransAM" from Active Motif is an ELISA-based NFκB activation kit. Comparable with EMSA, it also measures the ability of NFκB in cellular extracts to bind to κB-oligonucleotides. Addition of primary NFκB antibodies followed by secondary antibodies conjugated to horseradish peroxidase produces a chemiluminescence signal in NFκB activated cells.

The activation of NFκB target gene expression upon DNA binding can be either measured by PCR or by reporter gene assays. The stable transfection of reporter gene constructs into different cell lines is time consuming. Reporter gene assays are also quite sensitive to confounding factors influencing the expression level of reporter genes. Additionally, clonal selection gives rise to single clones, which may differ from the original population. And, viral promoters are often methylated or silenced by other mechanisms in mammalian cells, which requires drug treatment, e.g. HDIs to enable gene expression of the desired gene. To avoid these influences, TaqMan PCR was employed for measuring NFκB activation upon different stimuli. Different NFκB target genes are described to be upregulated upon its activation. The induction of interleukins is caused by a variety of stimuli including inflammatory cytokines. IL-8[123] is a strongly inducible target gene upon TNF-α treatment. The most prominent target gene is the inhibitor IκB-α[124,125]. NFκB activation targets IκB-α for degradation via the ubiquitin-proteasome pathway. In turn, nuclear NFκB triggers the resynthesis of IκB-α, terminating the activation process by binding to and shuttling NFκB back to the cytoplasm. Other known NFκB target genes, some of which are not activated by TNF-α, or only in a few cell lines are c-Flip[126], Bcl-x_L[127,128], and VEGF-c[129].

4.2 Activation status in different tumor entities

4.2.1 Lung cancer

Lung cancer is the leading cause of cancer death for both women and men. There are two main types of lung cancer, depending on their pathological classification: small cell lung carcinoma (SCLC) and non-small cell lung carcinoma (NSCLC). The more common NSCLC is further subdivided into squamous cell carcinoma, adenocarcinoma, and large-cell carcinoma. This classification is important for the choice of treatment and prognosis of the disease. Small cell lung carcinoma is the most aggressive form of pulmonary tumor. Early in the course of disease it develops distant metastases. Although initially responsive to chemotherapy and radiation, cells rapidly develop resistance. An accurate classification of the different tumor subclasses based on molecular markers could increase treatment options. Additionally, finding of specific factors for SCLC or NSCLC that are involved in tumor development or tumor resistance, could allow the development of new chemotherapeutic drugs. To test, if SCLC and NSCLC behave differently regarding NFκB activation, various lung cancer cell lines were analyzed.

4.2.1.1 NFκB was inducible by TNF-α in NSCLC but not in SCLC cell lines

First, the NFκB activation status in SW2 and H69 (SCLC) and in A549 and H460 (NSCLC) cells was determined, performing EMSA. Cells were seeded in 6-well plates and stimulated with TNF-α for 30 min. Whole cell extracts were prepared and EMSA was performed as described (figure 4.1). Without TNF-α, the NSCLC cell lines A549 and H460 showed only marginal NFκB DNA binding to the κB-sites. However, upon TNF-α stimulation, binding to the κB-sequence could be drastically enhanced. Thus, the two NSCLC cell lines possessed an inducible and functional NFκB pathway. Untreated SCLC cell lines exhibited none (H69) or little DNA binding (SW2), too. Yet, in contrast to NSCLC, stimulation of SCLC with TNF-α did not increase the binding of NFκB to the κB-sequences. The data demonstrated that the NFκB pathway was not inducible by TNF-α in the SCLC cell lines H69 and SW2.

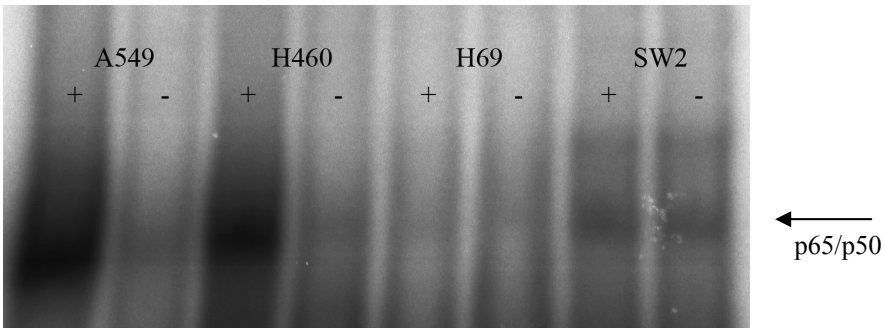

Figure 4.1: Electrophoretic mobility shift assay (EMSA) of lung cancer cell lines studying NFκB activation.
A549 and H460 (NSCLC) as well as H69 and SW2 (SCLC) cell lines were incubated with 25 ng/ml TNF-α (+) for 30 min or were left untreated (-). Whole cell extracts were prepared and incubated with radioactively labeled oligonucleotides containing the κB-binding site for complex formation and were run on a non-denaturating polyacrylamide gel. p65/p50 dimers are indicated by the arrow.

Since translocation assays require adherent cell growth and H69 and SW2 cells were growing in suspension, translocation assays could only be performed in A549 and H460, both adherent cell lines. Cells were seeded in 96-well plates and either treated with TNF-α for 30 min or left untreated. Immediately afterwards, cells were fixed and stained with an anti-p65 antibody and analyzed by an ArrayScan® II high content scan reader. In both cell lines, localization of NFκB was cytoplasmatic in unstimulated cells that rapidly translocated into the nucleus upon TNF-α treatment (figure 4.2).

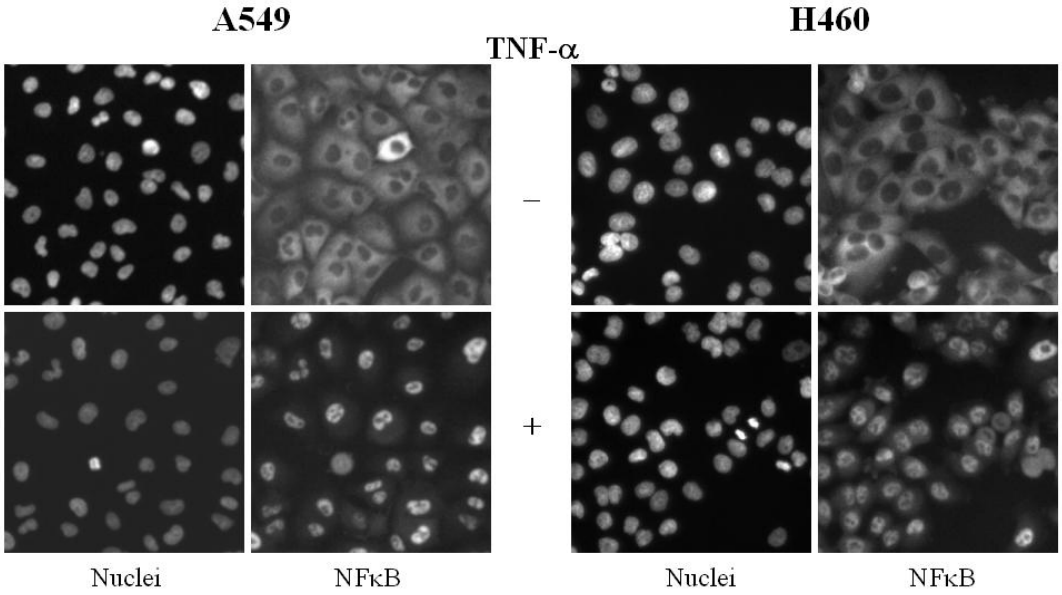

Figure 4.2: Nuclear translocation potential of NFκB in A549 and H460 NSCLC cell lines upon TNF-α stimulation.
A549 and H460 cells were TNF-α (25 ng/ml) treated (+) for 30 min, fixed, and fluorescence labeled with Hoechst dye (nuclei) and an NFκB (p65 subunit) antibody.

4.2.1.2 Absent activation of NFκB target gene expression by TNF-α in a majority of SCLC cell lines

To further examine the differences in TNF-α stimulation between SCLC and NSCLC cells, two additional SCLC cell lines were used: DMS 53 and DMS 114, which both grow adherent. To check if the lack in NFκB DNA binding translated into reduced target gene expression, TaqMan PCR was used to quantify NFκB target genes in H69, DMS 53, DMS 114, and SW2 cells in comparison to A549. Cells were treated with TNF-α for four hours, lysed, and RNA was isolated for TaqMan PCR. As predicted from the EMSA read outs, A549 cells showed significant target gene expression, whereas SCLC cell lines showed none or little upon TNF-α treatment. DMS 114, however, behaved exceptionally, i.e. it showed strongly activated IκB-α, but only slightly activated IL-8 gene expression. A549 exhibited a 9.5-fold and 340-fold induction in IκB-α and IL-8, compared to DMS 114 featuring an 8-fold and 15-fold induction, respectively. In H69, DMS 53, and SW2 cells, TNF-α could not induce IκB-α or IL-8 expression more than 1.5-fold (figure 4.3).

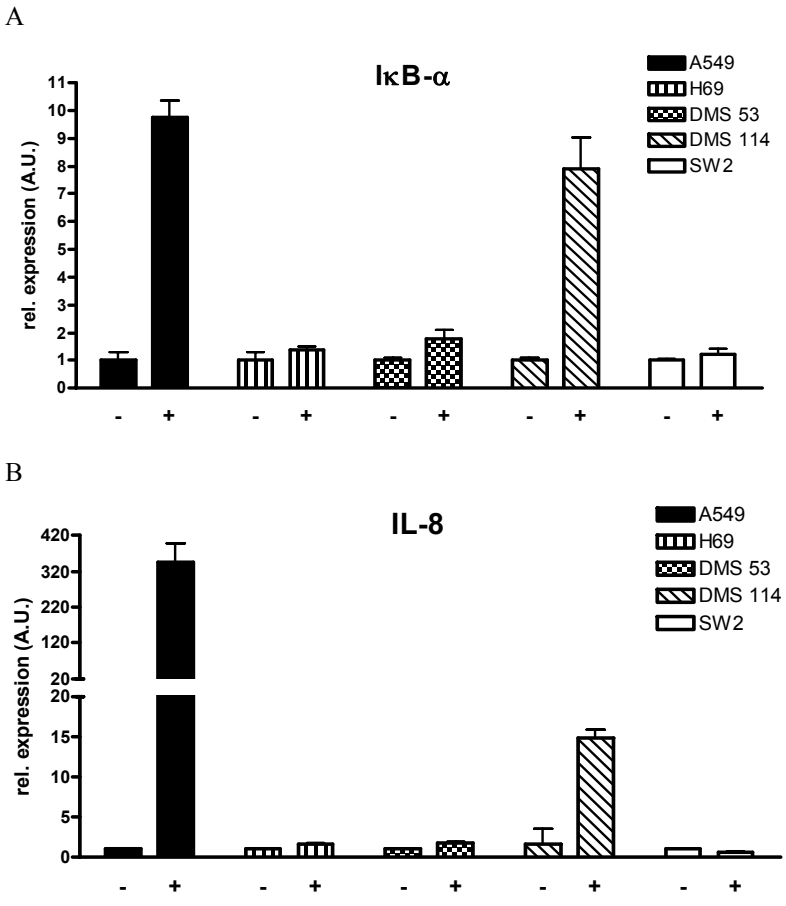

Figure 4.3: NFκB target gene expression of lung cancer cell lines upon TNF-α treatment.
Human lung cancer cells (A549, H69, DMS 53, DMS 114, and SW2) were seeded between $2x10^5$ – $1x10^6$ cells / 6-well. Cells were either left untreated (-) or stimulated with 25 ng/ml TNF-α (+) for 4 hours. Cells were lysed in RLT-buffer, total RNA was isolated, and assayed for NFκB target genes IκB-α (A) and IL-8 (B) via TaqMan PCR. Data represent mean ± SD.

4.2.1.3 Investigation of NFκB activation upon TNF-α stimulation in SCLC cell lines

To visualize NFκB nuclear translocation in SCLC, ArrayScan based measurements were performed. Cells were TNF-α treated, fixed, and antibody stained. Cell images delivered information about the amount of NFκB nuclear translocation. In DMS 53 cells, NFκB did not translocate into the nucleus at all, whereas in DMS 114 cells NFκB molecules partially shifted into the nucleus upon TNF-α stimulation. However, the amount of translocated NFκB was much lower in DMS 114 compared to A549 cells (figure 4.4).

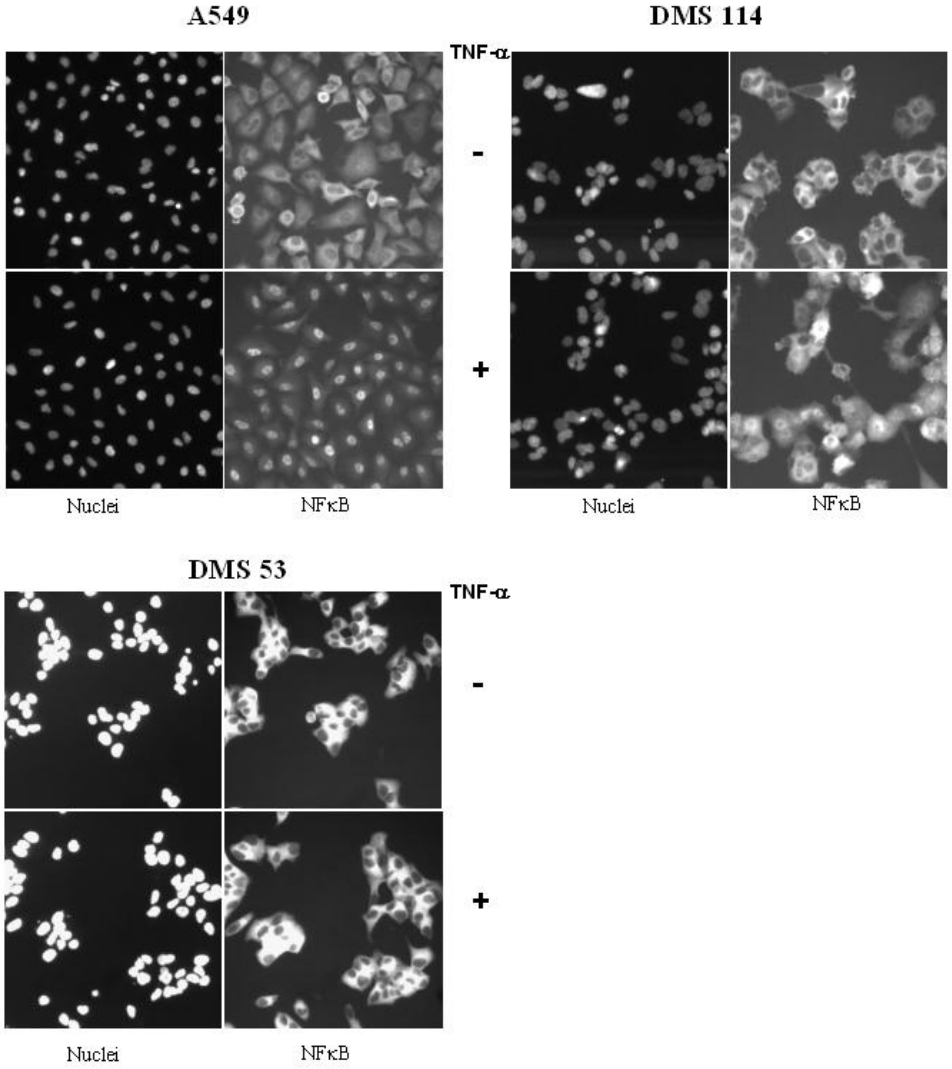

Figure 4.4: Measurements of nuclear translocation in A549, DMS 114, and DMS 53 cells upon TNF-α treatment.
A549, DMS 114, and DMS 53 cells were TNF-α (25 ng/ml) stimulated for 30 min (+), fixed, and fluorescence labeled with Hoechst dye (nuclei) and an NFκB (p65 subunit) antibody.

4.2.1.4 SCLC cells displayed reduced or absent phosphorylation of IκB-α upon the addition of TNF-α

For proof of concept, diminished NFκB activation should correlate with a lack in inhibitor phosphorylation and degradation. To test this, immunoblotting studies were performed in SCLC (figure 4.5). Cells were stimulated for 5 – 30 min with TNF-α in respect to control, lysed, and loaded onto a polyacrylamide gel. Coherent with previous data, upon TNF-α treatment A549 rapidly phosphorylated and degraded IκB-α. After 5 min a strong band of phosphorylated IκB-α was detectable, 10 min later, IκB-α was largely degraded by the proteasome, and after 15 min the inhibitor was not detectable anymore. In contrast, the SCLC cell line H69, which did not show DNA binding or target gene expression upon stimulation at all, did not exhibit inhibitor phosphorylation or degradation upon TNF-α treatment. DMS 114 cells, which exhibited medium induction of NFκB target gene expression, showed delayed IκB-α phosphorylation and degradation. Phosphorylated IκB-α could be detected after approximately 10 min. 30 min later a weak band of IκB-α was still detectable.

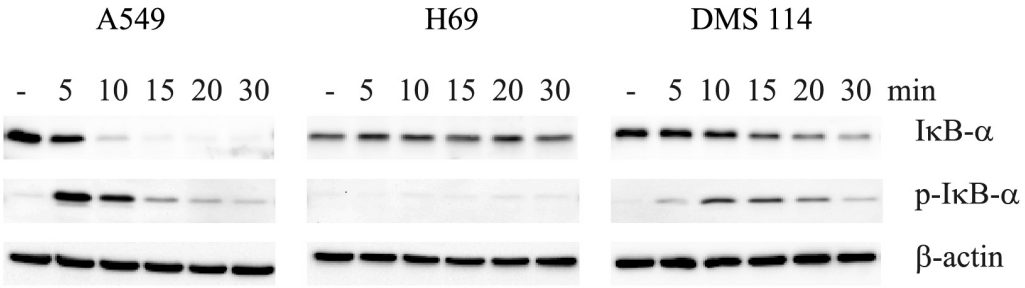

Figure 4.5: Kinetics of IκB-α phosphorylation and degradation in lung cancer cell lines upon TNF-α stimulation.
A549 ($2x10^5$), H69 ($1x10^6$), and DMS 114 ($3.5x10^5$) lung cancer cells were seeded in 6-well plates and TNF-α treated (25 ng/ml) for the indicated times (0 – 30 min). Cells were washed with PBS, lysed with RIPA buffer, and immunoblotted with antibodies against IκB-α and p-IκB-α. Loading control: β-actin.

Upstream of inhibitor phosphorylation and degradation is the binding of TNF-α to its receptor followed by the activation of the IKK complex, consisting of IKK-α, IKK-β, and IKK-γ. Immunoblotting studies revealed that all IKK subunits were still in place in SCLC cell lines, implying that the activation defect occured upstream of the kinase complex (figure 4.6).

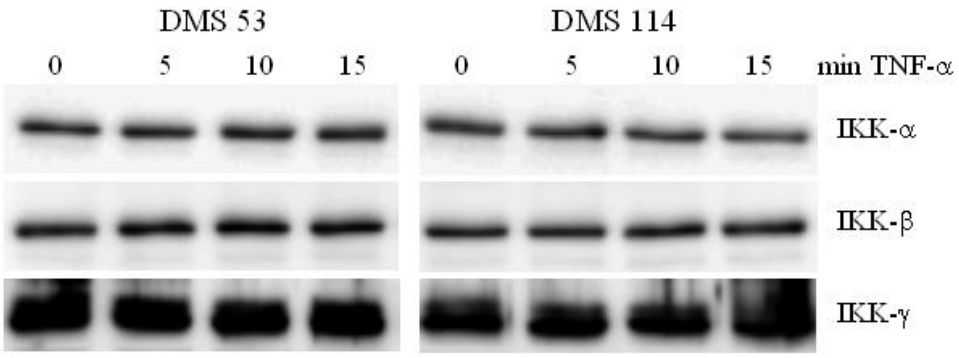

Figure 4.6: IKK status in SCLC cell lines.
DMS 53 and DMS 114 cells were seeded ($3.5x10^5$) in 6-well plates, TNF-α treated (25 ng/ml) for the indicated times (0 – 15 min), washed with PBS, and lysed with RIPA buffer. Cell extracts were run on a polyacrylamide gel and immunoblotted against IKK-α, IKK-β, and IKK-γ.

4.2.1.5 SCLC cells exhibited repressed tumor necrosis factor receptor 1 (TNF-R1) mRNA and protein expression

Experiments demonstrated that NFκB was inducible by cytotoxic substances such as etoposide or camptothecin in SCLC cell lines (chapter 4.4). One possible cause for the absent induction of NFκB upon TNF-α in SCLC could be the downregulation of tumor necrosis factor receptor 1 (TNF-R1). This possibility was checked by quantitative PCR and immunoblotting studies (figure 4.7), employing various lung cancer cell lines. In accordance with data on target gene expression and inhibitor phosphorylation/degradation, SCLC cell lines showed greatly reduced mRNA levels of TNF-R1, i.e. less than 0.5 % in comparison to A549. When assayed for protein expression, A549 cells showed a strong band at 55 kDa. While DMS 114, which could slightly activate NFκB by TNF-α, exhibited 5 % expression on the RNA level relative to A549, and a very faint band on the protein level. In H69, DMS 53, and SW2 cells TNF-R1 could not be detected by immunoblotting at all.

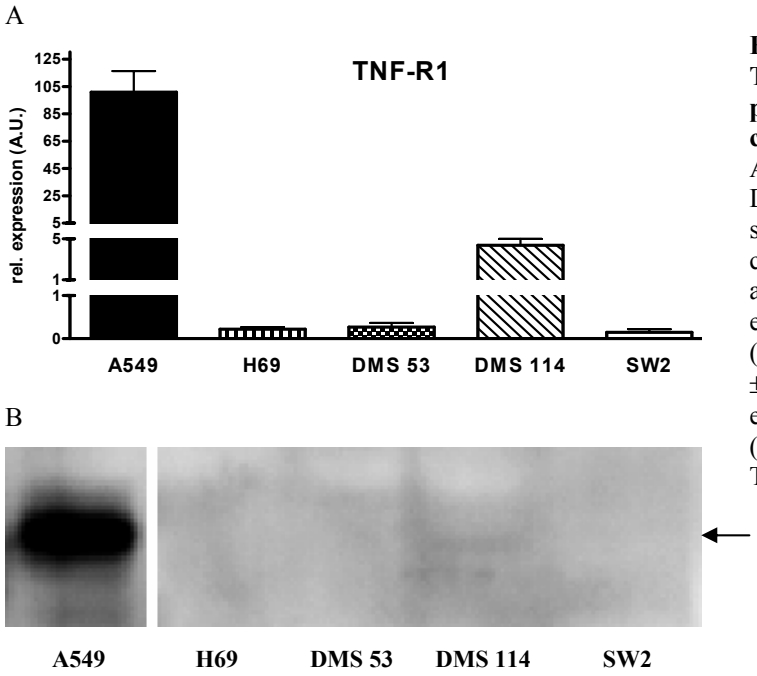

Figure 4.7: Expression of TNF-R1 on RNA and protein level in human lung cancer cell lines.
A549, H69, DMS 53, DMS 114, and SW2 cells were seeded between $2x10^5$ – $1x10^6$ cells / 6-well, washed in PBS, and either targeted for RNA expression by TaqMan PCR (A; Data represent mean ± SD) or for protein expression by immunoblotting (B). The arrow indicates TNF-R1.

Based on the data above, a panel of lung cancer cell lines was employed to test for TNF-R1 and other possibly dysregulated genes in the NFκB pathway. RNA from previously isolated cells (ALTANA RNA-panel) was used. TaqMan PCR was performed in NSCLC (H460, A549, COLO-699, A-427, BEN, LCLC-97TM1, and H226 cells) and SCLC (H69, H128, H345, SW2, and H209) cell lines. Cells were tested for TNF-R1, IKK subunits (IKK-α, IKK-β, and IKK-γ), IκB-α, and TNF-related apoptosis-inducing ligand receptor 2 (TRAIL-R2). TRAIL-R2 is a cell surface receptor that triggers cell death. Expression analysis clearly showed that TNF-R1 and also TRAIL-R2 were greatly reduced in SCLC cells, whereas NSCLC cells showed normal expression levels. In contrast to the observed receptor downregulation, components of the IKK complex (IKK-α, IKK-β, and IKK-γ) as well as the inhibitor IκB-α were observed in all lung cancer cell lines at similar RNA expression levels (table 4.1).

Lung cancer cell lines	TNF-R1	TRAIL-R2	IKK-α	IKK-β	IKK-γ	IκB-α
H460	+++	+++	++	++	++	+++
A549	+++	++	+	++	++	+++
COLO-699	+++	+++	+++	+++	++	+++
A-427	+++	+++	++	+++	+++	+++
BEN	+++	++	++	++	+++	+++
LCLC-97TM1	+++	+++	++	+++	++	+++
H226	+++	+++	+++	+++	+++	+++
H69	+	-	++	++	++	+++
H128	+	+	++	+++	++	+++
H345	+	-	++	++	+++	+++
SW2	+	-	++	++	+++	+++
H209	++	+	++	++	++	+++

Table 4.1: Gene expression of TNF-R1, TRAIL-R2, IKK-α, IKK-β, IKK-γ, and IκB-α in a panel of lung cancer cell lines.
RNA from various lung cancer cell lines was targeted for gene expression analysis. Expression of various genes: (-) not detectable, (+) very low, (++) medium, (+++) high expression.

4.2.2 Pancreatic cancer

Human pancreatic cancer is currently the fifth leading cause of cancer deaths worldwide. It has a very poor prognosis with an overall 5-year survival rate of approximately 3 %. Pancreatic cancer spreads rapidly and is rarely detected in its early stages, which is a major reason for the poor prognosis. Although the genetic profile of pancreatic cancer is emerging as a result of intensive research[130,131], so far these results could not be translated into the clinic. A number of studies show that NFκB activity is increased in human pancreatic adenocarcinomas and pancreatic cancer cell lines[38]. It has been demonstrated that constitutive NFκB activation in pancreatic carcinomas is involved in tumorigenesis and metastasis[132,133]. To verify if NFκB might be a drug target in pancreatic cancer, the activation status in pancreatic cancer cell lines was analyzed.

4.2.2.1 NFκB activity was inducible by TNF-α in pancreatic cancer cells

For this purpose, nuclear translocation and target gene expression studies in pancreatic cancer cell lines with and without TNF-α was performed. Translocation assays revealed that TNF-α addition stimulated NFκB nuclear translocation in all pancreatic cells (figure 4.8). Visually, translocation efficiency was not as good as in non-small cell lung cancer cells.

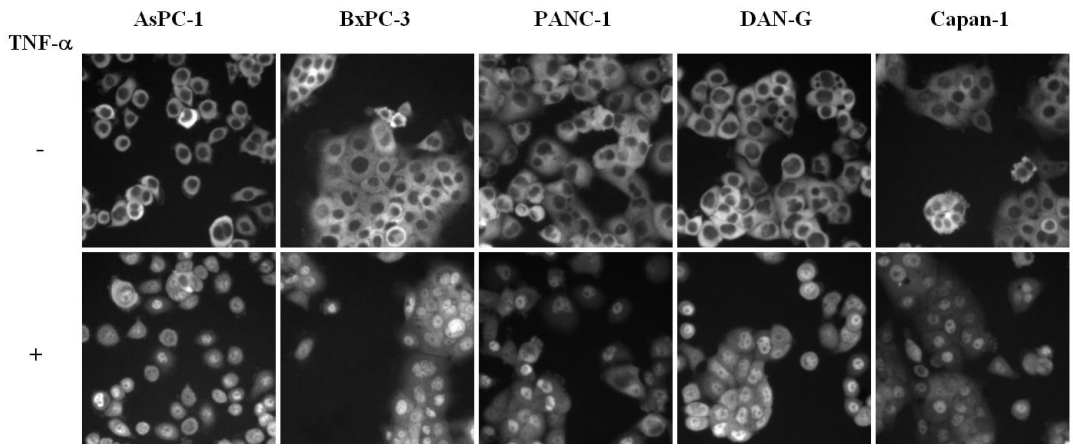

Figure 4.8: Measurements of NFκB nuclear translocation in selected pancreatic cancer cell lines upon TNF-α treatment.
Pancreatic cancer cells AsPC-1, BxPC-3, PANC-1, DAN-G, and Capan-1 were plated in 96-well plates ($1x10^4$), TNF-α stimulated (30 min, 25 ng/ml, +), fixed, and fluorescence labeled with Hoechst dye and an NFκB (p65 subunit) antibody. Images shown for NFκB staining only.

Gene expression analysis and immunoblotting studies confirmed the translocation data. Moreover, upon TNF-α treatment, all cell lines increased IκB-α and IL-8 gene expression. Induction of expression levels for IκB-α was between 4.5-fold to 10-fold, for IL-8 about 5-fold to 55-fold (figure 4.9-A,B). Next, IκB-α phosphorylation and degradation upon activation by TNF-α was tested. Immunoblotting revealed IκB-α phosphorylation within 5 min and degradation within 20 min (figure 4.9-C).

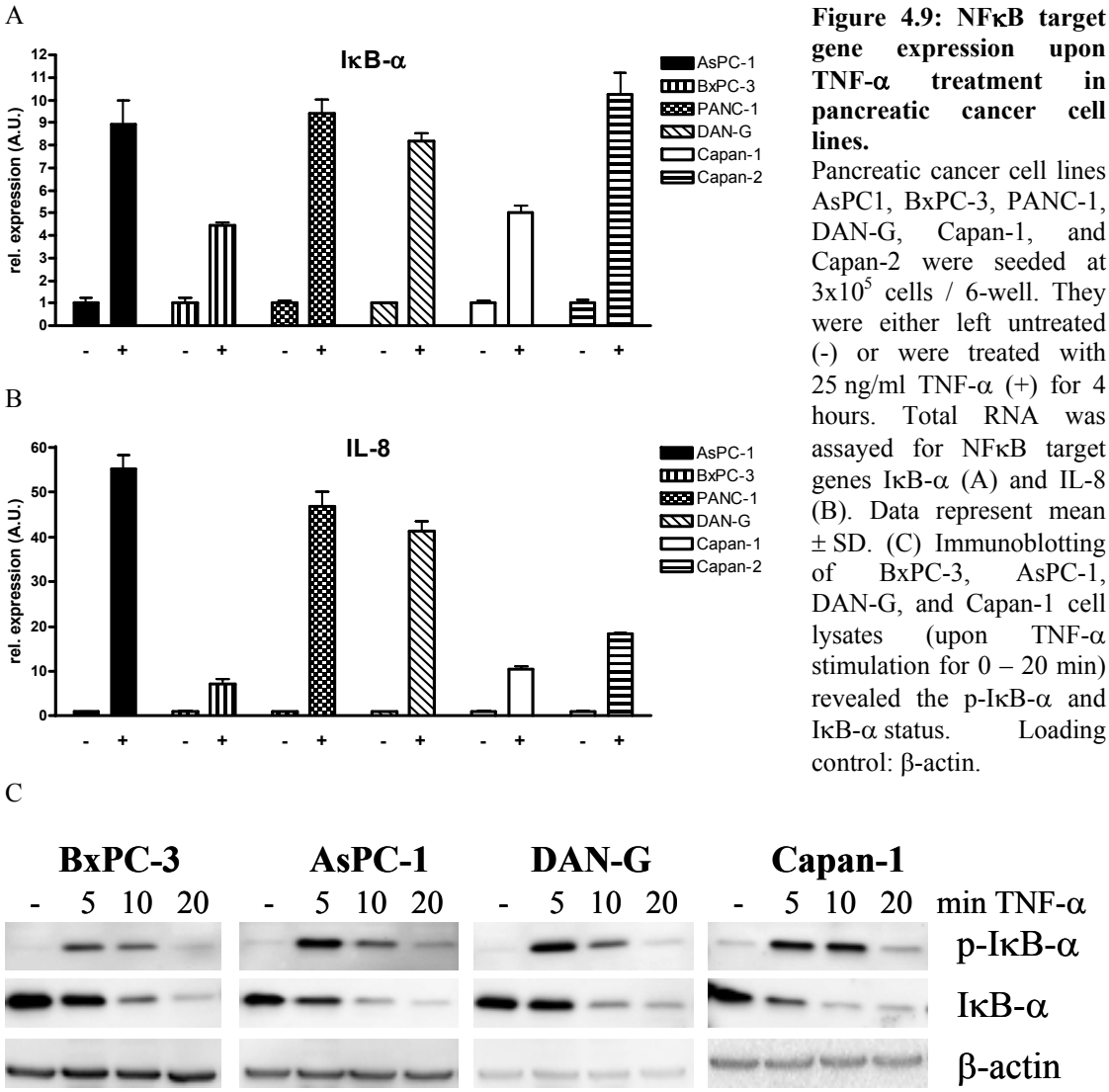

Figure 4.9: NFκB target gene expression upon TNF-α treatment in pancreatic cancer cell lines.
Pancreatic cancer cell lines AsPC1, BxPC-3, PANC-1, DAN-G, Capan-1, and Capan-2 were seeded at $3x10^5$ cells / 6-well. They were either left untreated (-) or were treated with 25 ng/ml TNF-α (+) for 4 hours. Total RNA was assayed for NFκB target genes IκB-α (A) and IL-8 (B). Data represent mean ± SD. (C) Immunoblotting of BxPC-3, AsPC-1, DAN-G, and Capan-1 cell lysates (upon TNF-α stimulation for 0 – 20 min) revealed the p-IκB-α and IκB-α status. Loading control: β-actin.

4.2.2.2 Pancreatic cancer cells showed increased DNA binding in untreated cells, which was reducible by proteasomal inhibition

EMSA assays also showed increased NFκB DNA binding upon TNF-α treatment, but even in the absence of TNF-α, in five of six cell lines increased basal NFκB activity could be observed: BxPC-3, PANC-1, DAN-G, Capan-1, and Capan-2. Only in the AsPC-1 cell line, basal NFκB activity could not be detected (figure 4.10-A).

Proteasomal degradation of phosphorylated IκB-α is key to NFκB activation. To test, if incubation with the proteasome inhibitor MG-132 could reduce increased NFκB activity in unstimulated cells, pancreatic cancer cell lines were incubated with MG-132 for two hours. Subsequently, RNA was isolated and target gene expression

was measured. In cell lines that showed enhanced NFκB DNA binding even in the absence of TNF-α, proteasome inhibition resulted in reduced target gene expression. In unstimulated AsPC-1, where basal NFκB DNA binding activity could not be detected, target gene expression was not reduced by proteasome inhibition. In contrast, in cells exhibiting increased NFκB activation levels (BxPC-3, PANC-1, DAN-G, and Capan-1), MG-132 incubation decreased IκB-α gene expression: BxPC-3 exhibited a decrease of ~ 70 %, PANC-1 ~ 85 %, DAN-G ~ 50 %, and Capan-1 ~55 %. Capan-2 cells, which also showed enhanced NFκB DNA binding activity, target gene expression could not be decreased by proteasome inhibition (figure 4.10-B).

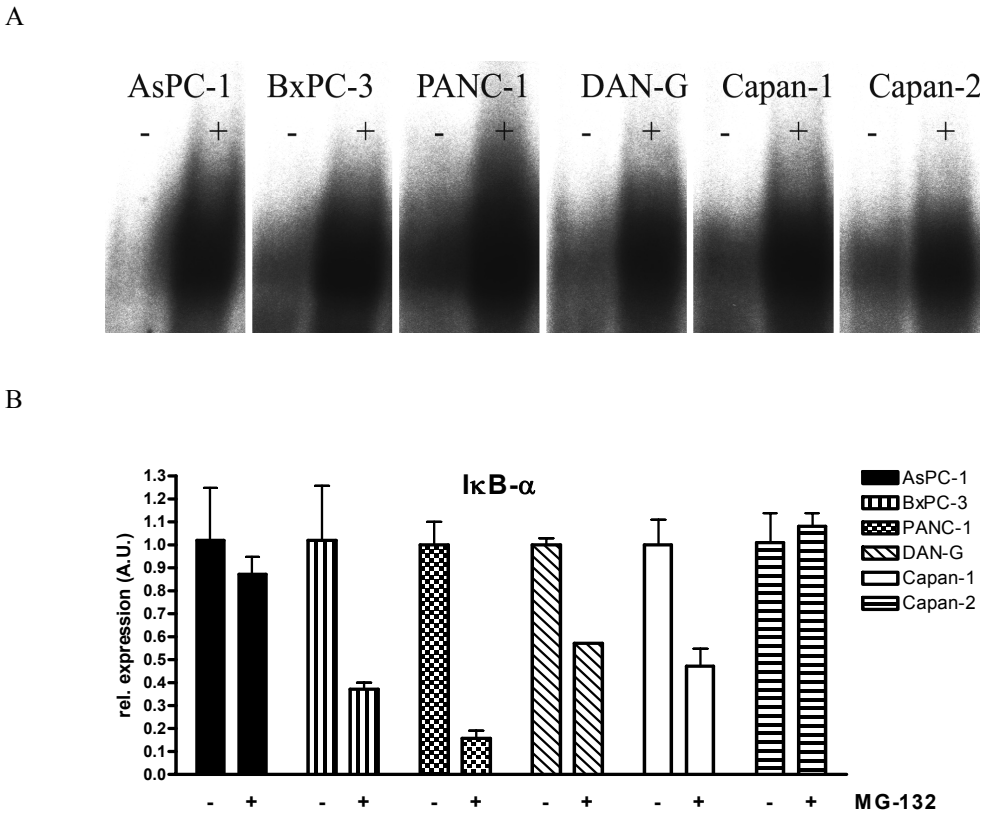

Figure 4.10: NFκB activation status in pancreatic cancer.
$3x10^5$ cells (AsPC-1, BxPC-3, PANC-1, DAN-G, Capan-1, Capan-2) were seeded into 6-well plates. (A) Pancreatic cancer cell lines were incubated with TNF-α (+; 25 ng/ml, 30 min) or were left untreated (-) and lysed with complete cell lysis buffer for EMSA. Protein concentration was determined and equal amounts were employed for NFκB DNA binding studies. (B) Cells were incubated with 5 µM MG-132 (+) for 2 hours or were left untreated (-), lysed, and assayed for IκB-α gene expression by TaqMan PCR. Data represent mean ± SD.

4.2.3 Hematopoietic cancers

Lymphomas are a group of cancer, which originate from the lymphatic system. They can be classified into two major categories:

- Hodgkin's lymphoma
- non-Hodgkin's lymphoma

Hodgkin's lymphoma is characterized by the presence of Reed-Sternberg cells and originates from lymphocytes (B and T-cells[134]). Non-Hodgkin's lymphomas include a variety of B-cell lymphomas, such as diffuse large B-cell lymphoma (DLBCL). Multiple myeloma originates from plasma cells, antibody producing immune cells.

Hodgkin´s lymphoma, B-cell lymphoma, and multiple myeloma have been described to have constitutively activated NFκB[40,48,135]. First, the NFκB activation status in different lymphoma and myeloma cell lines was evaluated. To this end, EMSA and TaqMan PCR experiments were performed and the inhibitor status was analyzed by immunoblotting.

Cell lines tested:

- Hodgkin's lymphoma: L-540, HDLM-2, L-1236, KM-H2, L-428
- Multiple myeloma: MM.1S, MM.1RL
- Diffuse large B-cell lymphoma: KARPAS-422, DB, Pfeiffer, OCI-LY-3, OCI-LY-19, Toledo

4.2.3.1 Enhanced NFκB DNA binding activity in hematopoietic cancer

For DNA binding studies in hematopoietic cancer cell lines cells were TNF-α treated or left untreated, and lysed for EMSA experiments. Even in the absence of TNF-α, all Hodgkin's lymphoma cells exhibited strong binding to the κB-sequence, which could not be further enhanced by TNF-α. B-cell lymphoma cells Pfeiffer and KARPAS-422 displayed only marginal DNA binding of NFκB with and without TNF-α. Toledo, OCI-LY-3, and DB cells on the other hand exhibited strong NFκB activation levels even without TNF-α and DNA binding could not be further enhanced by TNF-α stimulation. OCI-LY-19 cells showed increased basal NFκB levels, which were further inducible with TNF-α. Multiple myeloma cells MM.1S and MM.1RL both

exhibited strong DNA binding in the absence of TNF-α, which could be slightly increased by the addition of TNF-α (figure 4.11). A summary of the data is listed in table 4.2.

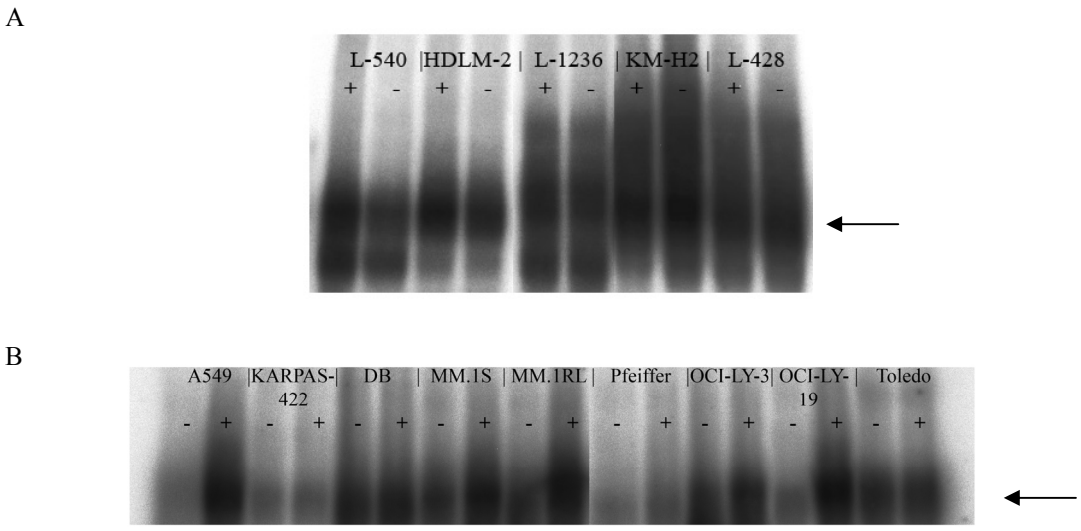

Figure 4.11: NFκB DNA binding of Hodgkin's lymphoma, B-cell lymphoma, and multiple myeloma cell lines in comparison with the lung cancer cell line A549.
Cells were seeded in 6-well plates (Hodgkin's lymphoma) or in 10 cm^2 dishes (B-cell lymphoma, multiple myeloma, A549) and TNF–α treated (+; 25 ng/ml) for 30 min or left untreated (-). Cells were washed in PBS and lysed in complete cell lysis buffer or nuclear extraction buffer, respectively. EMSAs were carried out with (A) Hodgkin's lymphoma cell lines (L-540, HDLM-2, L-1236, KM-H2, and L-428) or with (B) B-cell lymphoma cells (KARPAS-422, DB, Pfeiffer, OCI-LY-3, OCI-LY-19, and Toledo) and multiple myeloma cells (MM.1S, MM.1RL). A549 was used as control for band intensity. Equal amounts were loaded. The arrow indicates p65/p50 dimers.

4.2.3.2 IκB-α defects are the cause for elevated NFκB activation levels in a majority of lymphoma cell lines

To investigate possible mechanisms responsible for increased NFκB DNA binding activity, the IκB-α status in lymphoma and myeloma cells was determined. The inhibitor status in Hodgkin's lymphoma cells has been analyzed by Scheidereit and co-workers[48]. A summary of the data is listed in table 4.2. Immunoblotting for IκB-α (figure 4.12-A) in unstimulated cells revealed the presence of the inhibitor IκB-α in all non-Hodgkin's lymphoma cell lines and in the multiple myeloma cell line MM.1RL. IκB-α could not be detected in the multiple myeloma cell line MM.1S. Upon TNF-α treatment, IκB-α was phosphorylated and degraded in OCI-LY-19 and MM.1RL cells. This is evidence that these cells still responded to upstream activating signals and possessed a functional NFκB pathway. In all other cells neither enhanced

NFκB DNA binding nor phosphorylation of the inhibitor was observed upon stimulation with TNF-α.

Thereafter, gene expression studies (figure 4.12-B) were employed on B-cell lymphomas and multiple myelomas. OCI-LY-19 cells, which degraded IκB-α upon TNF-α treatment, also activated target gene expression (IκB-α: ~ 4.5-fold induction). Both, MM.1S and MM.1RL cells enhanced NFκB target gene expression (IκB-α: MM.1S ~ 2.5-fold; MM.1RL ~7.5-fold), although only MM.1RL degraded IκB-α upon TNF-α treatment. All other cells, including Toledo, DB, KARPAS-422, and Pfeiffer did not activate NFκB target genes upon TNF-α treatment. To further analyze the causes for increased basal NFκB DNA binding, cells were preincubated with MG-132 (proteasome inhibitor) for 2 hours (figure 4.12-C). B-cell lymphoma cells did not alter IκB-α gene expression upon proteasome inhibition, whereas in the multiple myeloma cells MM.1S and MM.1RL, proteasome inhibition led to a drastical decrease in NFκB target gene expression.

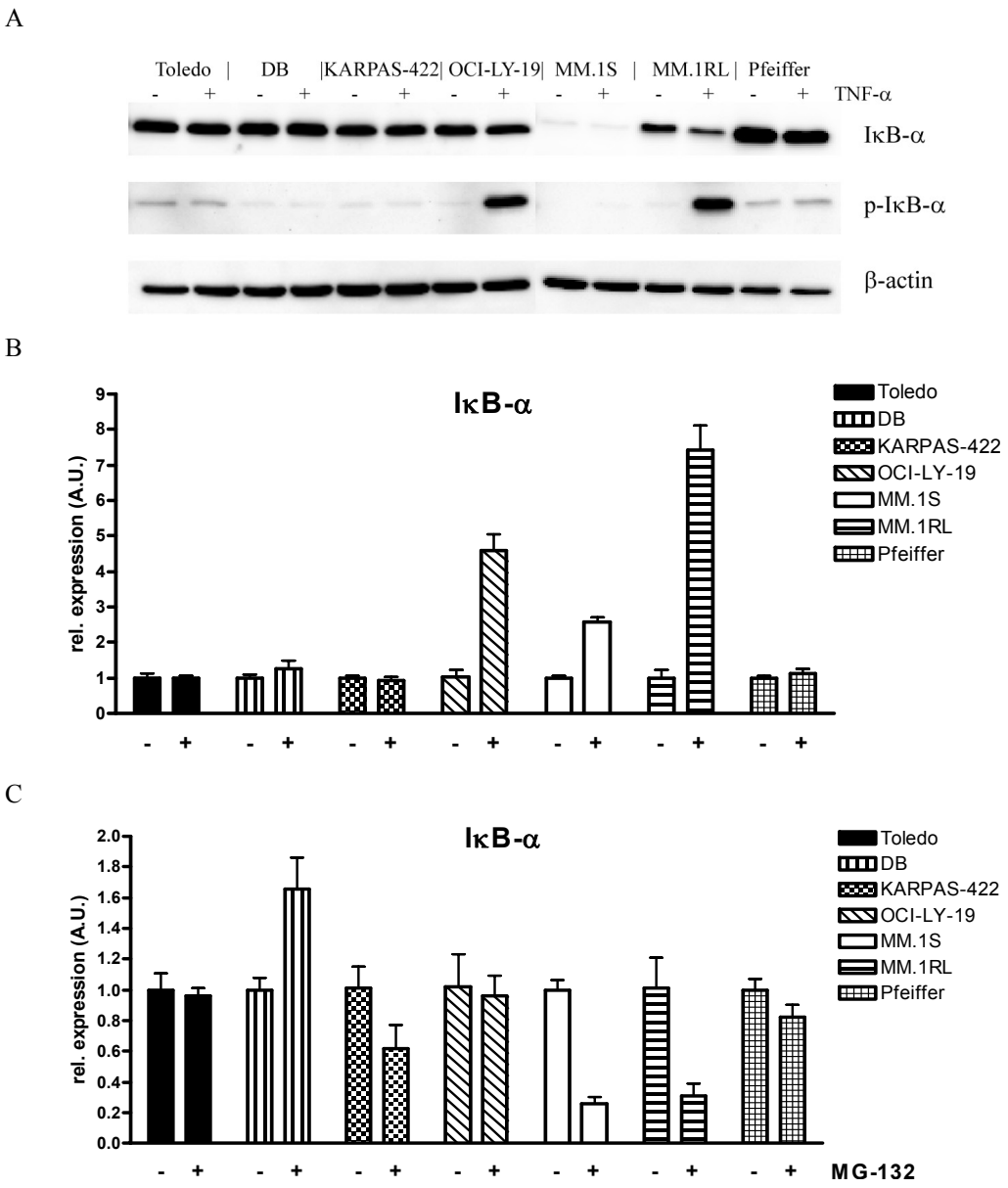

Figure 4.12: NFκB activation status in B-cell lymphoma and multiple myeloma cell lines. Between $1x10^6$ – $3x10^6$ cells (Toledo, DB, KARPAS-422, OCI-LY-19, MM.1S, MM.1RL, Pfeiffer) were seeded in 6-well plates. (A) For determining the IκB-α status, cells were stimulated with TNF-α (+, 25 ng/ml) for 8 min or were left unstimulated (-), lysed, and immunoblotted for IκB-α and p-IκB-α. Loading control: β-actin. (B) NFκB target gene induction upon TNF-α treatment (25 ng/ml, 4 hours) was determined. Cells were either left untreated (-) or were TNF-α treated (+), lysed, and assayed for IκB-α mRNA expression. (C) IκB-α gene expression upon MG-132 incubation for 2 h. Data represent mean ± SD.

A summary of NFκB DNA binding activity with or without TNF-α stimulation as well as the inhibitor status is listed in the table below (table 4.2).

		Hodgkin' lymphoma					Multiple myeloma	
	TNF-α	L-540	HDLM-2	L-1236	KM-H2	L-428	MM.1S	MM.1RL
NFκB DNA-binding	-	++	++	++	++	++	+	+
	+	++	++	++	++	++	++	++
IκB-α status		+ (wt)	+ (wt)	+ (wt)	-	-	-	+ (wt)

		B-cell lymphoma					
	TNF-α	KARPAS-422	DB	Pfeiffer	OCI-LY-3	OCI-LY-19	Toledo
NFκB DNA-binding	-	-/+	++	-/+	++	-/+	++
	+	-/+	++	-/+	++	++	++
IκB-α status		+	+	+		+ (wt)	+

Table 4.2: Summary of NFκB DNA binding activity and the IκB-α status in Hodgkin's and non-Hodgkin's lymphoma and multiple myeloma cell lines.
DNA binding: basal/marginal (-/+), increased (+), strong (++); IκB-α status: not detectable (-), detectable (+) by immunoblotting; proposed wildtype (wt). The inhibitor status in OCI-LY-3 cells has not been evaluated.

4.3 IKK inhibition

Many pharmaceutical companies are running programs for the discovery and development of small-molecule inhibitors aiming at the NFκB pathway. The most prominent target for NFκB inhibition is the IKK complex, consisting of the kinases IKK-α and IKK-β, and the regulatory subunit IKK-γ. Well-studied molecules described in the literature and proposed to specifically inhibit IKK-β were used in this study: PS-1145, BMS-345541, SC-514, BAY-11-7085 as well as IKK-β short interfering RNAs (siRNAs). A detailed view on these IKK inhibitors[136,137] is given in table 4.3:

	Comments
PS-1145	IC_{50} = 0.15 μM for IKK-β IC_{50} = 5 μM (NFκB activation in HeLa cells) Reduction of TNF-α in LPS-challenged mice
BMS-345541	IC_{50} = 0.3 μM for IKK-β IC_{50} = 4 μM for IKK-α IC_{50} = 4 μM (IκB phosphorylation in cell-based assay) Reduction of TNF-α in LPS-challenged mice
SC-514	IC_{50} = 2.7 – 11.2 μM for IKK-β IC_{50} > 200 μM selective over IKK-α and other kinases
BAY-11-7085	IC_{50} = 5 – 10 μM Inhibition of NFκB activated expression of ICAM-1, VCAM-1, IL-6 and IL-8

Table 4.3: Literature summary of utilized IKK inhibitors

4.3.1 IKK inhibition drove cells into apoptosis

First of all, the effect of IKK-β inhibition on cell growth and survival in various cancer cell lines was investigated. Therefore, siRNA technology was applied to evaluate IKK as target in cancer cell lines. Because it was impossible to chemically transfect siRNAs into lymphoma cells (data not shown), various lung, pancreatic, breast, and prostate cancer cell lines were utilized. Unfortunately, a target suppression of only about 70 % could be reached with IKK-β siRNA. The remaining 30 % activity was sufficient for fractional NFκB induction. Thus, to test IKK-β inhibition, a 72-hour cytotoxicity assay was performed, employing IKK-β inhibitors on multiple myeloma (MM.1S, MM.1RL), B-cell lymphoma (DB, KARPAS-422, Pfeiffer, Toledo, OCI-LY-19, OCI-LY-3), Hodgkin's lymphoma (KM-H2, HDLM-2), and NSCLC cell lines (A549, H460). Cells were incubated with increasing concentrations

of IKK-β inhibitors. After 72 hours, resazurin was added and proliferation was measured. Besides BAY-11-7085 and BMS-345541, data on cytotoxicity were collected on PS-1145 and SC-514, but for the latter two compounds cytotoxicity and NFκB inhibition could only be detected at saturation concentrations. EC_{50} values for BAY-11-7085 and BMS-345541 are presented in table 4.4.

Cell lines	EC_{50} BMS-345541 [M]	EC_{50} BAY-11-7085 [M]
A549	5.6×10^{-7}	1.4×10^{-6}
H460	6.4×10^{-7}	6.9×10^{-7}
HDLM-2	1.3×10^{-6}	3.8×10^{-7}
KM-H2	1.3×10^{-6}	5.4×10^{-7}
MM.1S	1.1×10^{-6}	4.3×10^{-7}
MM.1RL	1.9×10^{-6}	5.9×10^{-7}
DB	1.1×10^{-6}	4.3×10^{-7}
KARPAS-422	2.5×10^{-6}	4.4×10^{-7}
Pfeiffer	2.1×10^{-6}	4.2×10^{-7}
Toledo	9.5×10^{-7}	8.2×10^{-8}
OCI-LY-19	5.3×10^{-7}	3.3×10^{-7}
OCI-LY-3	5.3×10^{-6}	2.6×10^{-6}

Table 4.4: EC_{50} values for BAY-11-7085 and BMS-345541 in NSCLC, Hodgkin's lymphoma, B-cell lymphoma, and multiple myeloma cell lines.
Cells were seeded 24 hours before drug addition between $1x10^3$ and $3x10^4$ cells per 96-well. Plates were orbitally shaken for uniform distribution. The following day BAY-11-7085 or BMS-345541 was added. Cells were incubated for 72 hours and cytotoxicity was measured by resazurin dye.

BAY-11-7085 displayed an EC_{50} around $4x10^{-7}$ [M]. A significant difference between various cell lines and DNA binding activity could not be noticed. Only OCI-LY-3 cells were affected less, but this was due to uneven growth, possibly inhibiting the drug's action. Additionally, an increase in the resazurin readout in MM.1 cells at subtoxic dosis was noticed, which was reproducible in three independent experiments. BMS-345541 displayed an EC_{50} around $1.5x10^{-6}$ [M]. Again, differences in growth preferences upon drug incubation could not be detected, and dose-response curves were very steep.

4.3.2 IKK inhibition led to increased IKK gene expression and NFκB activity

In detail, the specificity of BMS-345541 for IKK-β inhibition in A549 was evaluated. Cells were incubated with increasing concentrations of the drug for 24 - 72 hours and

checked for NFκB inducibility. Checking for phosphorylated IKK-α/β in immunoblotting studies revealed an inhibition in p-IKK-α/β after 24 hours at concentrations around 7.5 µM and higher. Interestingly, after 48 hours this effect weakened, enabling NFκB translocation and IKK phosphorylation. The inhibitory effect was abolished after 72 hours (figure 4.13). These effects might be either due to a short half life of BMS-345541, an increase in the expression of IKK subunits, or a combination of both.

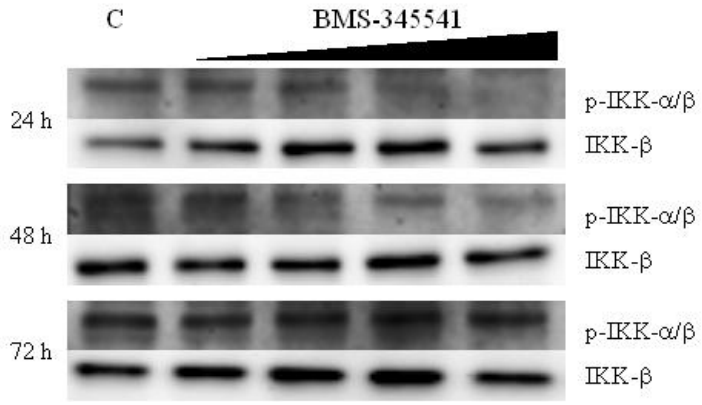

Figure 4.13: Inhibition of NFκB activation upon BMS-345541 incubation. A549 cells ($5x10^4$ seeded) were pretreated with 1 µM, 5 µM, 7.5 µM, and 10 µM BMS-345541 for 24, 48, or 72 hours before TNF-α (25 ng/ml) stimulation for 10 min. IKK-α/β phosphorylation was analyzed by immunoblotting. Control: IKK-β.

To determine, if IKK inhibition had any influence on IKK subunit expression, TaqMan analysis was performed. A549 cells were incubated with increasing concentrations of BMS-345541 for up to 72 hours, followed by gene expression analysis. BMS-345541 caused enhanced gene expression of IKK-α, IKK–β, and IKK-γ in a concentration dependent manner (figure 4.14-A,B,C). After about 48 hours, gene expression of IKK subunits was increased ~ 2-fold. Genes were normalized to 18S rRNA.

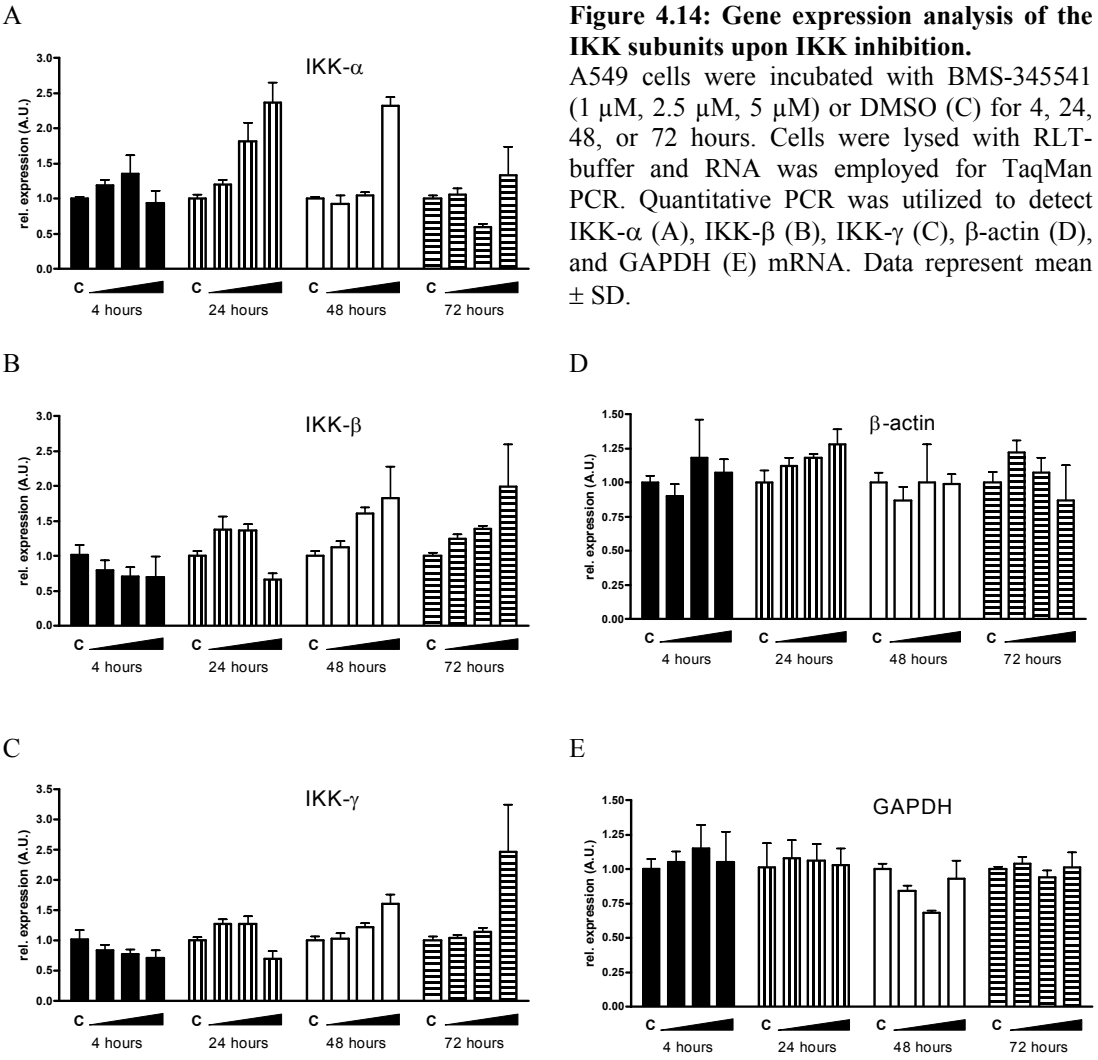

Figure 4.14: Gene expression analysis of the IKK subunits upon IKK inhibition.
A549 cells were incubated with BMS-345541 (1 μM, 2.5 μM, 5 μM) or DMSO (C) for 4, 24, 48, or 72 hours. Cells were lysed with RLT-buffer and RNA was employed for TaqMan PCR. Quantitative PCR was utilized to detect IKK-α (A), IKK-β (B), IKK-γ (C), β-actin (D), and GAPDH (E) mRNA. Data represent mean ± SD.

Because IKK inhibition was coherent with proliferation inhibition (figure 4.15-A,B), further endogenous controls were employed to probe the specificity of IKK upregulation. Control genes like β-actin and glyceraldehyde-3-phosphate dehydrogenase (GAPDH) did not change in comparison to 18S rRNA (figure 4.14-D,E).

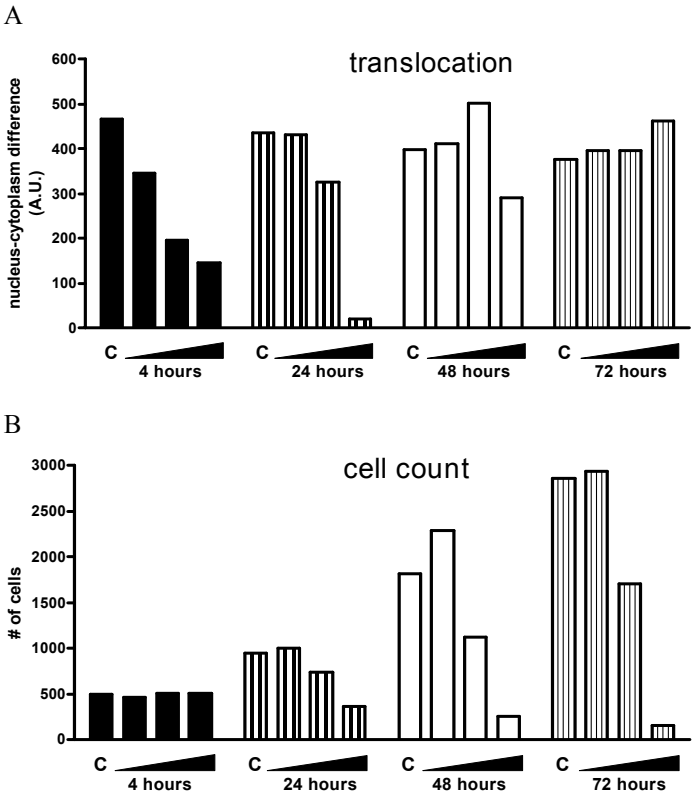

Figure 4.15: NFκB translocation and cell count upon IKK inhibition.
A549 cells were incubated with BMS-345541 (1 μM, 2.5 μM, 5 μM) or DMSO (C) for 4, 24, 48, or 72 hours. Cells were stimulated with TNF-α for 30 min, fixed, and stained with Hoechst dye and an anti-p65 antibody. Graphs represent quantitative fluorescence intensity read-outs of cell images. (A) translocation, (B) cell count.

4.4 Influence of cytotoxic drugs on the NFκB pathway

Human cells react differently to chemotherapeutic drugs depending on their genetic profile. They may undergo apoptosis, activate genes for drug resistance, or remain unaffected at all. Although these drugs are supposed to inhibit cell growth and induce apoptosis in cancerous cells, normal cells are affected as well. Additionally, tumor cells often acquire resistances to these drugs, to some extent enhanced by NFκB activation. Investigations focused on the influence of different cytotoxic drugs on the NFκB pathway.

Camptothecin and etoposide (VP16) are topoisomerase class I or class II inhibitors, respectively. Topoisomerase enzymes untangle DNA strands during cell division, thereby introducing temporary DNA strand breaks. Topoisomerase poisons bind to topoisomerase enzymes and prevent rejoining of the cut ends, thereby driving these cells into apoptosis[138-140]. Doxorubicin (adriamycin) binds directly to DNA via intercalation. It inhibits the progression of topoisomerase II enzymes and is classified as a topoisomerase II poison, although other mechanisms of action have been described as well, such as DNA cross-linking or interference with the DNA helicase[141]. The various mechanisms of action that have been ascribed to doxorubicin may be dependent on the drug concentration used. Cisplatin covalently binds to DNA producing crosslinks[142]. Mafosfamide is an alkylating agent. The drug alkylates the DNA generating crosslinks, causing erroneous DNA duplication during S-phase. These five drugs with different modes of action were tested for their influence on the NFκB signaling pathway.

4.4.1 Topoisomerase poisons induced NFκB target gene expression

To address the question if cytotoxic drugs activate NFκB, several SCLC cell lines (H69, DMS 53, DMS 114, SW2) and one NSCLC cell line (A549) were either incubated with TNF-α, etoposide, or doxorubicin for four hours. Cells were lysed for RNA and NFκB target gene expression assays were applied (figure 4.16). TaqMan PCR indicated that A549 activated the NFκB pathway and its target genes only upon TNF-α, but not upon etoposide or doxorubicin treatment. The same was true for the SCLC cell line DMS 114. In contrast, the SCLC cell lines H69, DMS 53, and SW2

activated NFκB upon etoposide incubation but not upon TNF-α or doxorubicin. In A549, TNF-α increased IκB-α and IL-8 gene expression ~ 10-fold and 300-fold, respectively. In SCLC cells, etoposide caused an induction in the range of 5 - 6-fold for IκB-α and 6 - 55-fold for IL-8. Differences were found for DMS 53 cells, which induced IL-8 expression upon etoposide only ~ 2-fold. Doxorubicin predominantly caused a reduction in NFκB target gene expression rather than an induction.

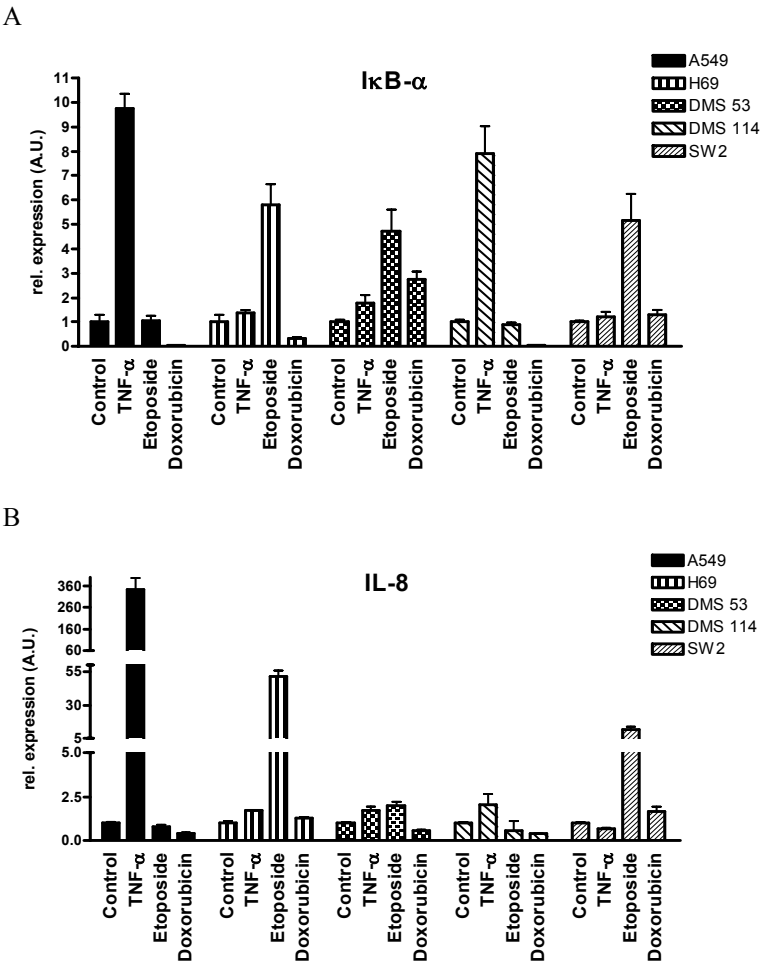

Figure 4.16: NFκB target gene expression in lung cancer cells upon TNF-α, etoposide, and doxorubicin incubation. A549, H69, DMS 53, DMS 114, and SW2 cells were incubated for 4 hours with TNF-α (25 ng/ml), etoposide (10 µM), or doxorubicin (10 µM). Cells were lysed and RNA was isolated. TaqMan PCR was applied for target gene expression analysis: IκB-α (A) and IL-8 (B). Data represent mean ± SD.

Camptothecin, cisplatin, and mafosfamide were also tested for their NFκB activating potential. Therefore, H69 and A549 cells were treated with etoposide, camptothecin, cisplatin, mafosfamide, or doxorubicin for 2 - 8 hours. Cells were harvested and analyzed for NFκB target gene expression. NFκB activation was only detectable in H69 (figure 4.17-A,B) but not in A549 cells (figure 4.17-C) and only by etoposide and camptothecin. Etoposide caused the strongest induction of ~ 11-fold and 70-fold of IκB-α and IL-8, respectively. NFκB activation was quite rapid, with a marked

increase at 2 hours, reaching a plateau after around 6 hours. The induction of NFκB upon addition of camptothecin was weak in comparison with etoposide. IκB-α was induced ~ 4-fold and IL-8 ~ 6-fold. Topoisomerase poisons activated only a subset of NFκB target genes, as they did not induce the expression of VEGF-c, c-FLIP, and Bcl-x_L at all. Cisplatin and mafosfamide had no effect on NFκB at all, resulted neither in an increase nor a decrease in expression, unlike doxorubicin, which led to a decrease in IκB-α and IL-8 gene expression in H69 and A549. A549 did not activate NFκB upon addition of chemotherapeutic drugs, but showed a decrease with doxorubicin. Cell viability was determined by resazurin dye after 72 hours. Viability was decreased to: ~ 45 % with etoposide (A549 and H69), ~ 5 % with camptothecin (A549 and H69), ~ 60 % (A549) and ~ 50 % (H69) with cisplatin, ~ 90 % (A549) and ~ 50 % (H69) with mafosfamide, and ~ 10 % (A549) and ~ 23 % (H69) with doxorubicin (figure 4.17-D).

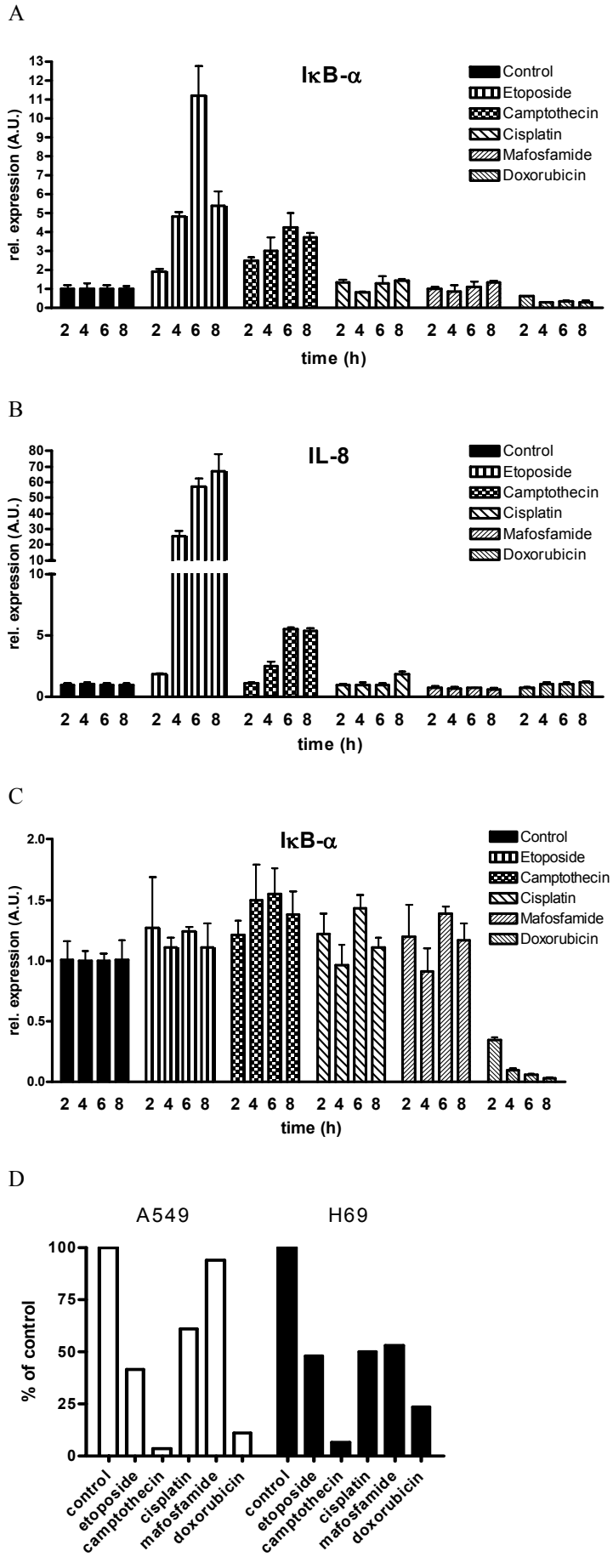

Figure 4.17: NFκB target gene expression in H69 and A549 upon drug treatment.
Cells were incubated up to 8 hours with 10 µM etoposide, 10 µM camptothecin, 10 µM cisplatin, 10 µM mafosfamide, 10 µM doxorubicin, or were left untreated. RNA was isolated and targeted in H69 for IκB-α (A) and IL-8 (B), and in A549 for IκB-α (C) expression. Data represent mean ± SD. (D) Cell viability was determined by resazurin dye after 72 hours.

4.4.2 Ataxia telangiectasia mutated (ATM) protein inhibition reduced NFκB activation upon etoposide treatment

The first connection between cellular stress, e.g. radiation and NFκB induction was identified by Jung and coworkers[143] in 1995. The group worked on ataxia telangiectasia (AT) patients, which are hypersensitive to ionizing radiation. They observed that introduction of truncated IκB-α into AT cells restored normal radiation sensitivity thereby establishing a link between radiation sensitivity and NFκB. The link between defective nuclear kinase ataxia telangiectasia mutated (ATM), responsible for the genetic disorder ataxia telangiectasia, and NFκB activation in response to radiation or topoisomerase inhibitors has been found by Lee et al.[144] and Piret and colleagues[145]. Li and coworkers[146] demonstrated that IKK activation in response to DNA double strand breaks depends on the nuclear kinase ATM. Very recently, Miyamoto's group[147,148] employed further research on this topic. They proposed that free cytoplasmatic IKK-γ becomes sumoylated promoting its nuclear translocation. In the nucleus it associates with DNA damage activated ATM protein kinase. ATM phosphorylates IKK-γ on serine 85 promoting its ubiquitination and finally nuclear export of ubiquitin marked IKK-γ and ATM. There, IKK-γ associates with the IKK complex and activates NFκB nuclear translocation.

On the basis of these publications the consequences of ATM suppression for NFκB inducibility by topoisomerase poisons were analyzed. H69 cells were transfected with siRNA against ATM for 48 hours followed by etoposide incubation for 5 hours. RNA suppression for ATM was ~ 60 % (figure 4.18-C). NFκB target gene expression upon etoposide incubation was decreased from around 7 to 4 for IκB-α and 60 to 30 arbitrary units for IL-8 (figure 4.18-A,B).

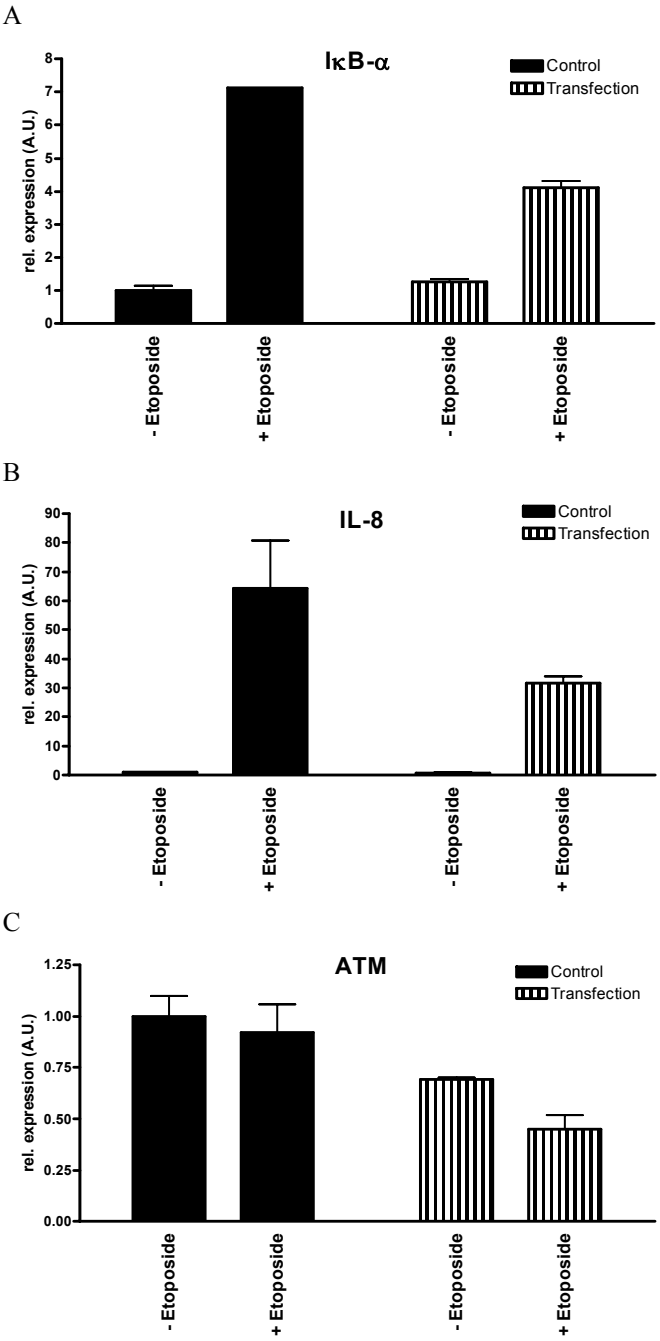

Fig. 4.18: NFκB target gene induction upon ATM siRNA transfection and etoposide treatment.
H69 were seeded at $7x10^5$ cells per 6-well plates. The following day, cells were transfected with ATM siRNA (10 nM) and 48 hours later treated with 10 µM etoposide for 5 hours. RNA was isolated and targeted for IκB-α (A) and IL-8 (B) gene expression and suppression sufficiency (C). Data represent mean ± SD.

4.4.3 A549 cells could not phosphorylate ATM and activate NFκB

Since ATM downregulation by siRNA resulted in reduced NFκB activation upon etoposide, differences for NFκB induction between A549 and H69 / SW2 cells were further investigated. Kozlov and colleagues[149] reported the identification of several phosphorylation and autophosphorylation sites on ATM in response to DNA damage. Thus, ATM activation via phosphorylation in response to etoposide was tested. Cells were incubated with 10 µM etoposide between 1 - 2 hours and lysed for

immunoblotting studies (figure 4.19). SW2 and H69 cells exhibited phosphorylated ATM within 30 min of etoposide incubation presumably leading to IKK activation and NFκB nuclear translocation. A549 cells could not phosphorylate ATM and consequently not activate NFκB.

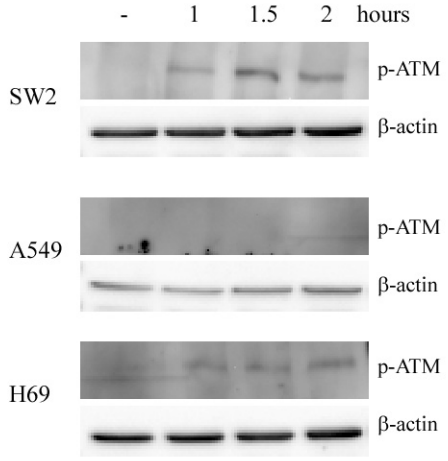

Figure 4.19: Immunoblotting for p-ATM upon etoposide incubation.
SW2, A549, and H69 lung cancer cells were incubated with 10 µM etoposide for up to two hours (1, 1.5, 2 hours) or were left untreated (-). Cells were lysed and assayed for phosphorylated ATM (p-ATM). Loading control: β-actin.

4.5 Influences of histone deacetylase inhibitors (HDIs) on the NFκB pathway

Histone deacetylase inhibitors (HDIs) are a new class of anticancer agents, which lead to hyperacetylation of histones. However, little is known about their action on non-histone targets. The aim of this project was to analyze the impact of HDIs on the NFκB pathway. First, histone acetylation may lead to modifications in promoter accessibility and in turn to the activation or inactivation of the pathway. Direct acetylation of NFκB subunits again may influence NFκB activity. Additionally, the alteration of nuclear import or export pathways may impact NFκB as well. Previous reports do not give a clear, unified picture about NFκB and HDIs. Therefore, the influence of HDIs on the NFκB pathway in non-small cell lung cancer was analyzed.

4.5.1 HDIs inhibited NFκB target gene expression due to decreased DNA binding

First, NSCLC cell lines A549 and H460 were incubated with SAHA and TSA for 24 hours, stimulated with TNF-α for four hours, and lysed for NFκB target gene expression. TaqMan PCR revealed a drastical decrease in relative expression of NFκB target genes IκB-α, c-Flip, Bcl-x_L, and VEGF-c. In detail, IκB-α mRNA expression was decreased to ~ 20 – 30 %, c-FLIP was lowered to 5 %, Bcl-x_L was decreased to ~ 20 %, and VEGF-c was reduced to less than 10 % in comparison to the DMSO control (figure 4.20).

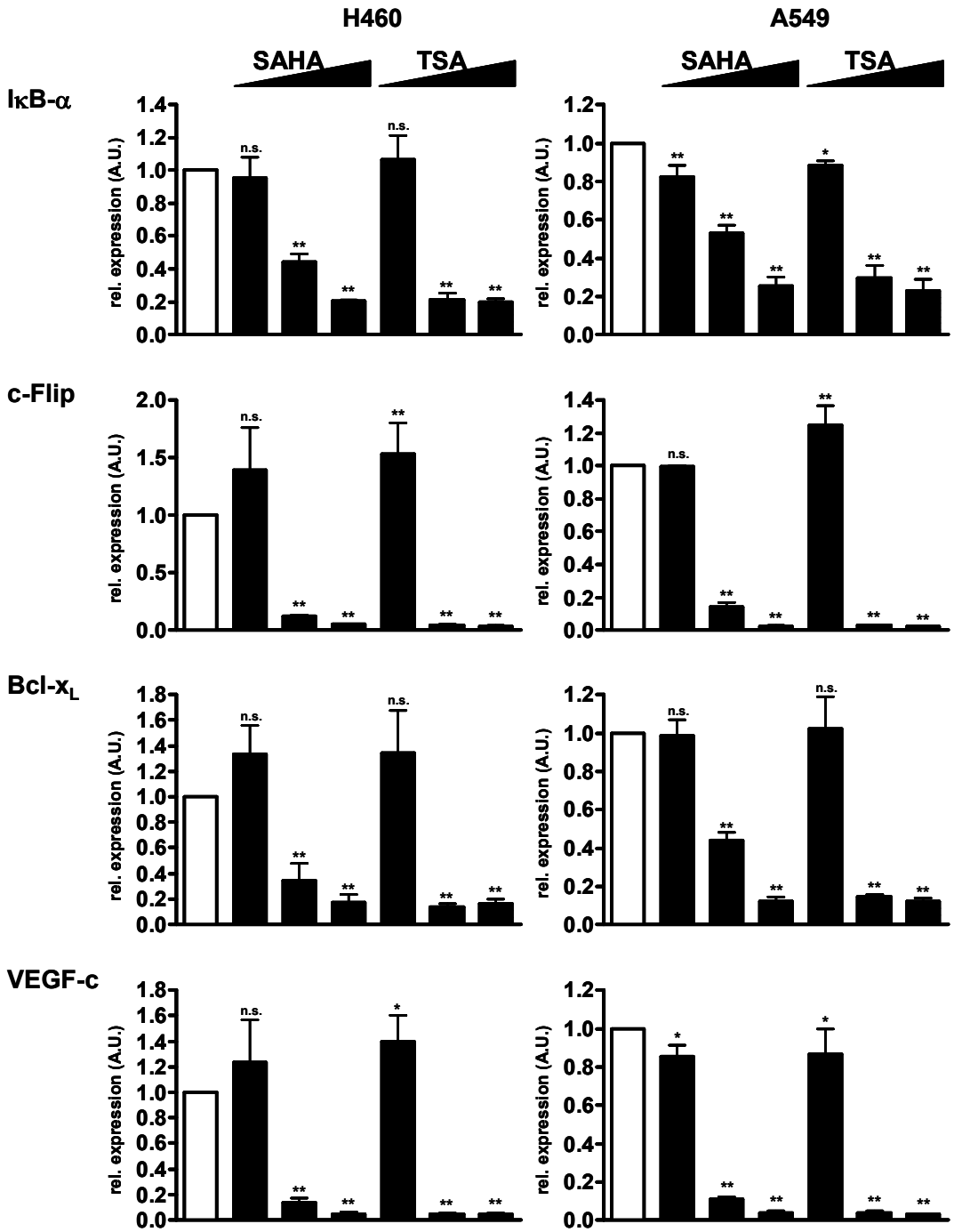

Figure 4.20: NFκB target gene expression upon HDI incubation.
A549 ($2.5x10^5$) and H460 ($3x10^5$) non-small cell lung carcinoma cells were seeded into 6-well plates, pretreated with SAHA (1 µM, 10 µM, 50 µM) or TSA (200 nM, 2 µM, 4 µM) for 24 hours, and stimulated with TNF-α (25 ng/ml) for 4 hours. Cells were washed, lysed in RLT-buffer, and employed for TaqMan PCR. Data represent mean ± SD from 3 independent experiments. Statistical significance: n.s., not statistically significant; *, $P < 0.05$; **, $P < 0.01$.

NFκB target gene expression requires NFκB nuclear translocation and DNA binding. To determine if the gene expression effects were due to altered NFκB DNA binding,

EMSA measurements were employed. Thus, NSCLC cells were incubated with SAHA and TSA for 24 hours and stimulated with TNF-α. Nuclear extracts were obtained and used for DNA binding studies. In TNF-α treated cells, increasing concentrations of SAHA and TSA reduced the amount of NFκB bound to DNA below the level seen in untreated, but TNF-α stimulated cells (figure 4.21-A). Supershift experiments identified the shifted band as p65-containing NFκB (figure 4.21-B). To verify these data, nuclear extracts were utilized for an ELISA-based quantification of NFκB using the NFκB p65 TransAM kit. Again, TNF-α stimulated H460 and A549 cells reduced NFκB activation by HDI incubation (figure 4.21-C,D).

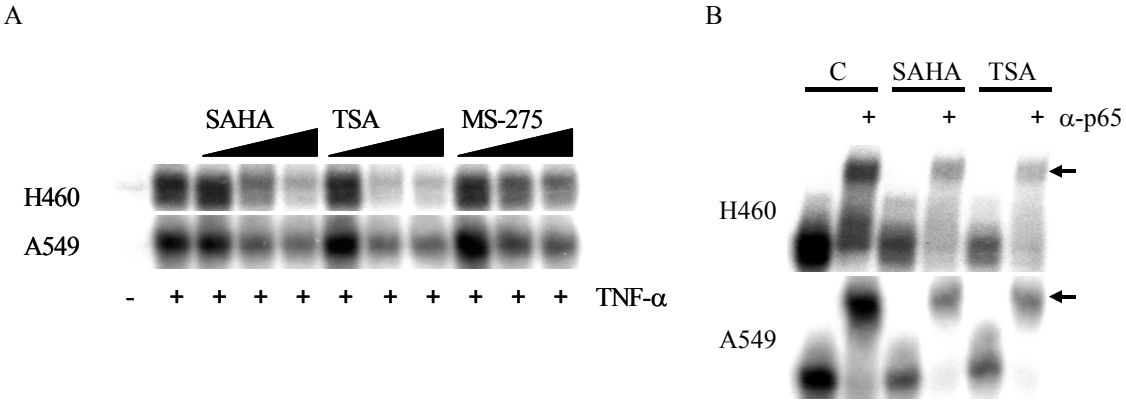

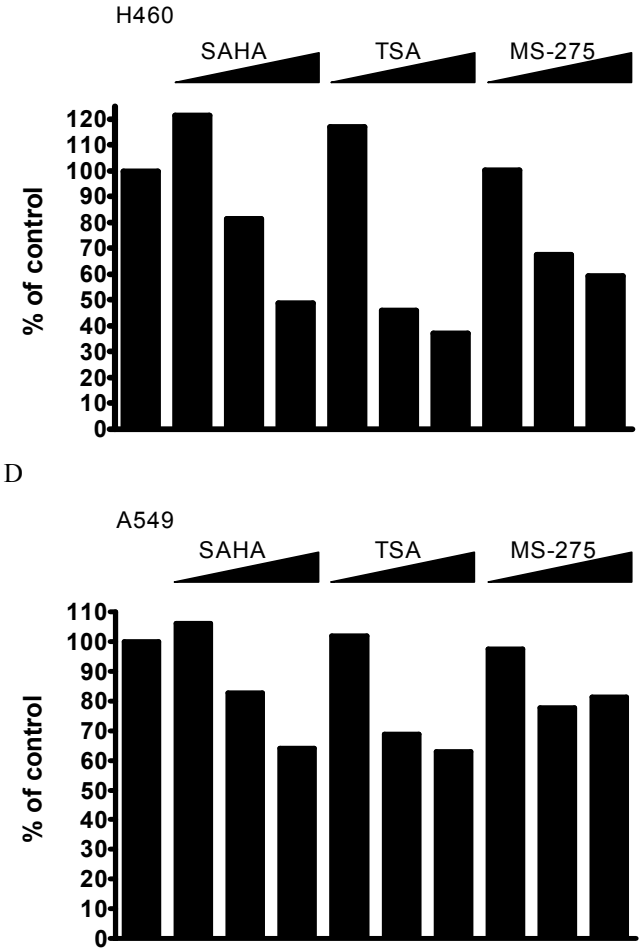

Figure 4.21: Analysis of DNA binding activity in H460 and A549 cells upon HDI treatment.
Cells were seeded in 10 cm^2 dishes ($1x10^6$), pretreated with SAHA (1 µM, 10 µM, 50 µM), TSA (200 nM, 2 µM, 4 µM), or MS-275 (100 nM, 20 µM, 50 µM) for 24 hours, TNF-α (25 ng/ml) stimulated for 30 min (+) or left untreated (-), and lysed. Nuclear extracts were employed for EMSA (A) or EMSA supershifts (B). For supershifts, TNF-α treated extracts (control, SAHA 50 µM, TSA 4 µM) were preincubated with anti-p65 antibody, permitting complex formation between NFκB and the anti-p65 antibody, before adding the radioactively labeled oligonucleotide probe. ELISA based quantification of NFκB was performed using the TransAM NFκB activation kit for H460 (C) and A549 (D) cells.

4.5.2 Viability was largely unaffected upon HDI incubation

To test for cytotoxicity at these concentrations, viability was measured by resazurin assay after 24 hours of HDI incubation. Viability was between 70 – 90 % for SAHA, TSA, and MS-275. Pictures of cells revealed that cells were greatly unaffected after 24 hours of HDI incubation, demonstrating that the observed effects were NFκB specific (figure 4.22-A,B).

A

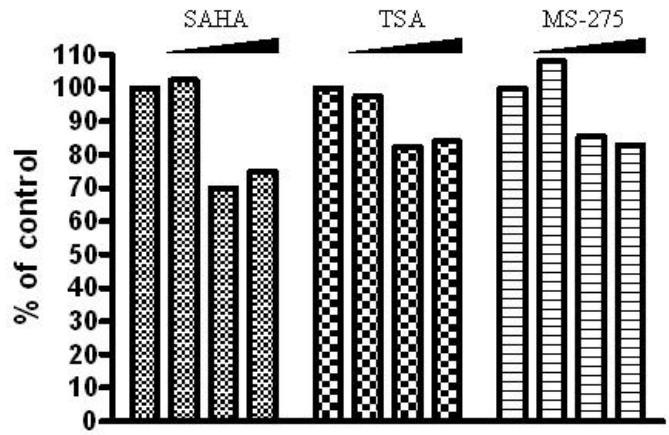

B

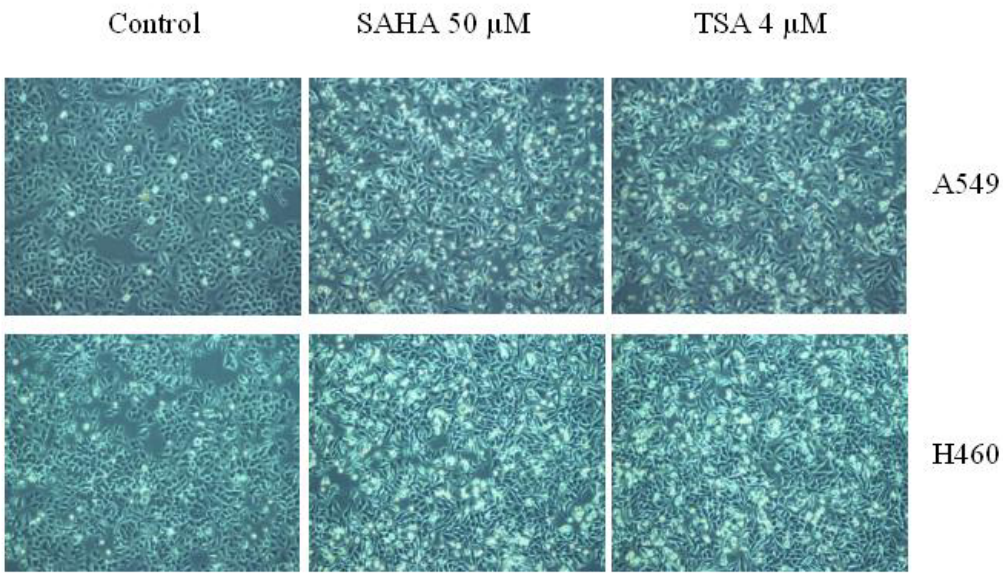

Figure 4.22: Viability measurements in A549 and H460 cells.
(A) A549 and H460 cells were seeded in 6-well plates and incubated with SAHA (1 µM, 10 µM, 50 µM), TSA (200 nM, 2 µM, 4 µM), or MS-275 (100 nM, 20 µM, 50 µM) for 24 hours. Viability was determined by using the resazurin dye. Data shown for A549. (B) Images of A549 and H460 cells incubated with SAHA or TSA were taken using the Leica DM IRB microscope.

4.5.3 HDIs decreased nuclear translocation of NFκB

NFκB nuclear translocation marks an early event in the activation of NFκB. To solve the question if reduced target gene expression and DNA binding was due to decreased cytosol to nuclear translocation, ArrayScan based measurements, quantifying the cytosolic and nuclear fractions of NFκB upon stimulation, were applied. To test if various HDIs changed NFκB nuclear translocation, A549 cells were incubated with SAHA, TSA, or MS-275 and stimulated with TNF-α. Upon HDI incubation, nuclear translocation was decreased (figure 4.23). SAHA treated cells exhibited a decrease in nuclear translocation at a concentration of 10 µM, TSA between 200 nM – 800 nM, and MS-275 at 2 µM.

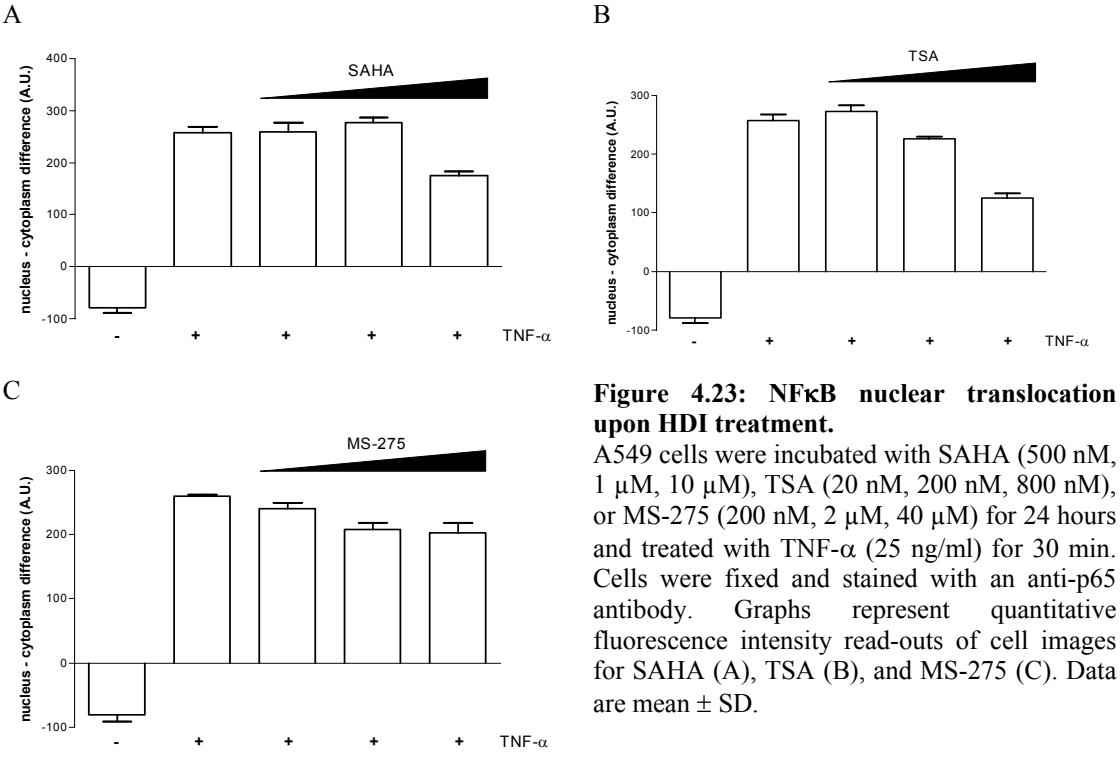

Figure 4.23: NFκB nuclear translocation upon HDI treatment.
A549 cells were incubated with SAHA (500 nM, 1 µM, 10 µM), TSA (20 nM, 200 nM, 800 nM), or MS-275 (200 nM, 2 µM, 40 µM) for 24 hours and treated with TNF-α (25 ng/ml) for 30 min. Cells were fixed and stained with an anti-p65 antibody. Graphs represent quantitative fluorescence intensity read-outs of cell images for SAHA (A), TSA (B), and MS-275 (C). Data are mean ± SD.

For a more detailed study, A549 and H460 cells were seeded in 96-well plates, pretreated with HDIs, stimulated with TNF-α, fixed, and stained against NFκB. Indeed, at the same concentrations at which NFκB DNA binding was decreased, HDIs led to a reduction of nuclear NFκB upon TNF-α versus control cells. Without HDIs, NFκB nuclear translocation upon TNF-α treatment was quite rapid. After approximately 10 min, a sizeable amount of NFκB had translocated into the nucleus. Translocation reached its maximum at about 30 min. HDI treated cells differed in two

aspects: first, there was a lag phase of several minutes for the onset of translocation, secondly, the overall level of translocated NFκB was much lower in HDI treated cells than in control cells. Data shown for A549 (figure 4.24).

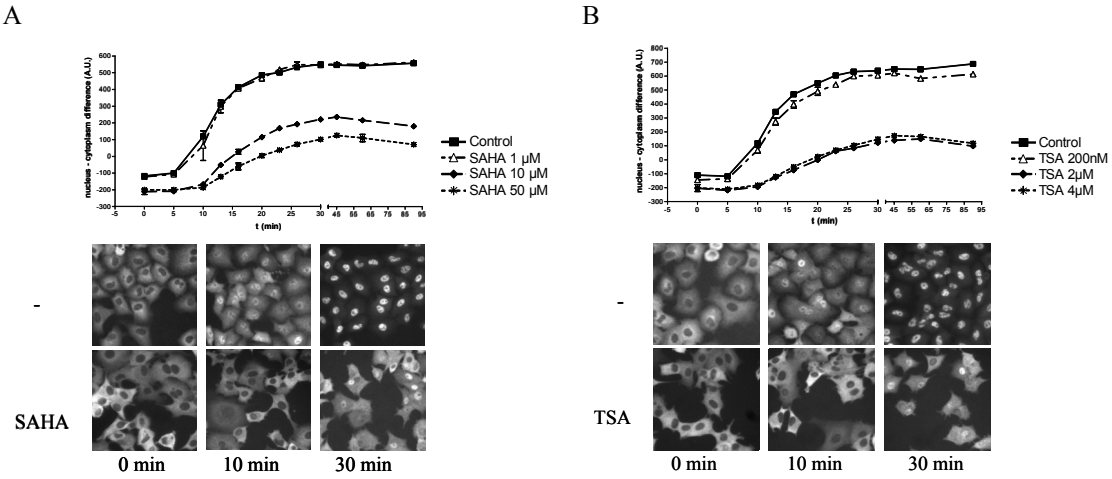

Figure 4.24: NFκB nuclear translocation measurements upon HDI treatment.
A549 cells were incubated with SAHA and TSA for 24 hours, TNF-α (25 ng/ml) treated for indicated times (0 min – 90 min), fixed, and stained with anti-p65 antibody. Graphs represent quantitative fluorescence intensity read-outs of cell images. Data are mean ± SD.

To check if these effects were specific for the NFκB pathway, the translocation potential of STAT1, another transcription factor that translocates from the cytoplasm to the nucleus mediating interferon (IFN) response was tested. No inhibitory effect for STAT1 translocation was detected in SAHA pretreated and IFN-α stimulated cells. The activation potential of STAT1 was even slightly increased (figure 4.25). In HDI pretreated but unstimulated cells, NFκB as well as STAT1 were found exclusively in the cytoplasm. This indicates that HDIs specifically blocked NFκB but not STAT1 nuclear translocation.

A

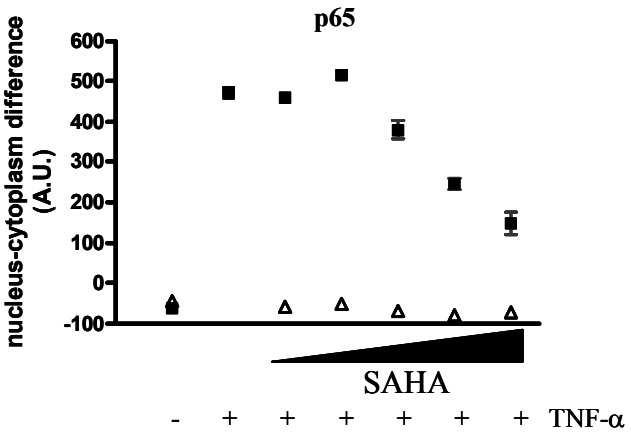

Figure 4.25: IFN-α induced STAT1 nuclear translocation upon HDI treatment.
A549 cells were incubated with SAHA (100 nM, 1 µM, 5 µM, 10 µM, or 50 µM) for 24 hours, which were subsequently treated (filled squares) with 25 ng/ml TNF-α (A), or 100 ng/ml IFN-α (B). Unstimulated cells are represented by empty triangles. Cells were fixed and stained with either anti-p65 or anti-STAT1 antibodies, respectively. Graphs represent quantitative fluorescence intensity read-outs of cell images. Data are mean ± SD.

B

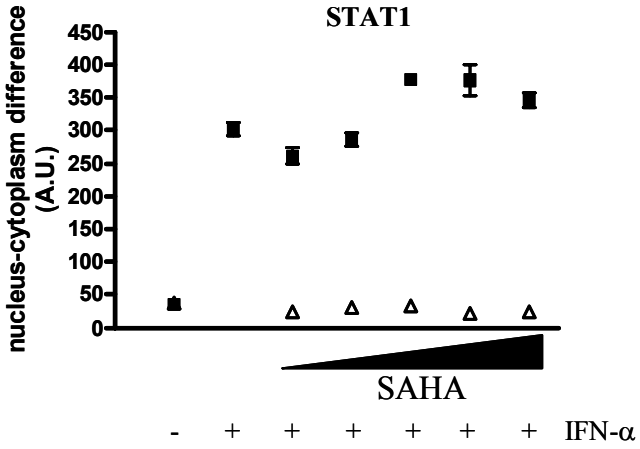

4.5.4 Incubation with HDIs did not change proteasome activity

Other research groups also proposed reduced NFκB signaling upon HDI incubation. Giardina's lab[150] proposed reduced proteasome activity upon HDI incubation. This could be an explanation for the reduction in nuclear translocation and DNA binding, as inhibition of IκB-α degradation leads to stabilization of the NFκB/IκB-α complex. To evaluate this possibility for the situation in NSCLC, A549 cells were treated with HDIs for 24 hours or the proteasome inhibitor MG-132 for 4 hours. Only a slight proteasomal inhibition after 24 hours HDI treatment versus control could be detected. In contrast, the proteasome inhibitor MG-132 reduced the catalytic activity to approximately 5 % (figure 4.26).

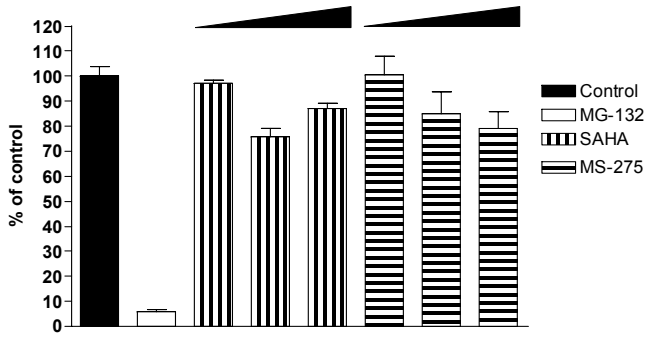

Figure 4.26: Proteasomal degradation of the substrate Suc-LLVY-MCA upon HDI incubation.
A549 cells were incubated with MG-132 (10 µM), SAHA (1 µM, 20 µM, 50 µM), or MS-275 (100 nM, 20 µM, 50 µM) for 24 hours, scraped off, lysed, and incubated with the 20S proteasomal substrate Suc-LLVY-MCA for 30 min. Fluorescence readouts were taken on the Victor2 fluorometer. Data represent mean ± SD.

4.5.5 STAT1 had no influence on the NFκB pathway

Because proteasomal inhibition could be ruled out regarding NFκB inhibition, increased export of activated NFκB out of the nucleus could be an explanation for the observed phenomenon. Kramer and coworkers[151] postulated that STAT1 becomes acetylated upon HDI treatment and may then interact with NFκB. This interaction removes nuclear NFκB thereby inhibiting DNA binding in melanoma cell lines with constitutive NFκB activity. This hypothesis was tested by p65 co-immunoprecipitation and siRNA experiments, targeting STAT1. Employing p65 immunoprecipitation experiments, co-immunoprecipitated STAT1 could not be detected in HDI treated cell lines (data not shown). Additionally, targeting STAT1 by siRNA did not reconstitute the translocation potential of NFκB upon TNF-α treatment (figure 4.27). Also binding of other STATs to p65 could not be detected by co-immunoprecipitation experiments (data not shown).

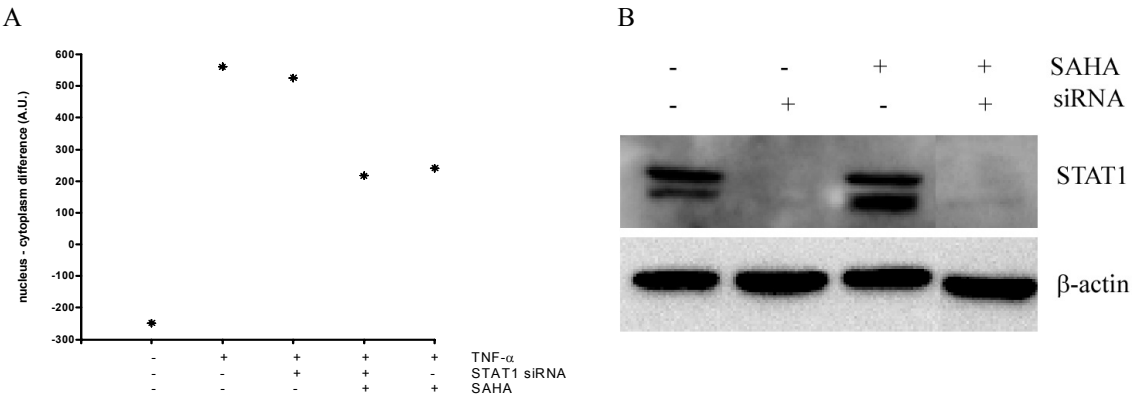

Figure 4.27: TNF-α induced p65 nuclear translocation upon HDI treatment and STAT1 suppression.
A549 cells ($5x10^4$) were transfected with STAT1 siRNA for 48 hours followed by a 24 hours treatment with SAHA (50 µM). Cells were stimulated with TNF-α (25 ng/ml) for 30 min, fixed, and p65 stained. Graph represents quantitative fluorescence intensity read-outs of cell images (A). Transfection efficiency was checked by immunoblotting against STAT1. Loading control: β-actin (B).

4.5.6 Reduced NFκB activity was due to reduced nuclear translocation and not enhanced export

To gain a more detailed insight into the mechanism of nuclear import reduction, further studies using leptomycin B (LMB), a Streptomyces metabolite that inhibits the function of the chromosome region maintenance protein 1 (CRM1), a receptor for nuclear export[152], were performed. A549 cells were seeded into 96-well plates and pretreated with HDIs for 24 hours. LMB was either added 30 min, 2 hours, or 24 hours before TNF-α treatment (figure 4.28). Without TNF-α, LMB caused an accumulation of NFκB in the nucleus, already visible after 30 min, reaching a maximum after 24 hours. Upon TNF-α stimulation, nuclear translocation inhibition was detectable in SAHA treated in comparison to DMSO control cells. Thus, the proposed mechanism for NFκB inhibition upon TNF-α stimulation was located upstream of NFκB nuclear translocation. Additionally, these experiments showed that in cells not stimulated by TNF-α, NFκB shuttles through the nucleus. By inhibiting nuclear export, NFκB rapidly accumulates in the nucleus.

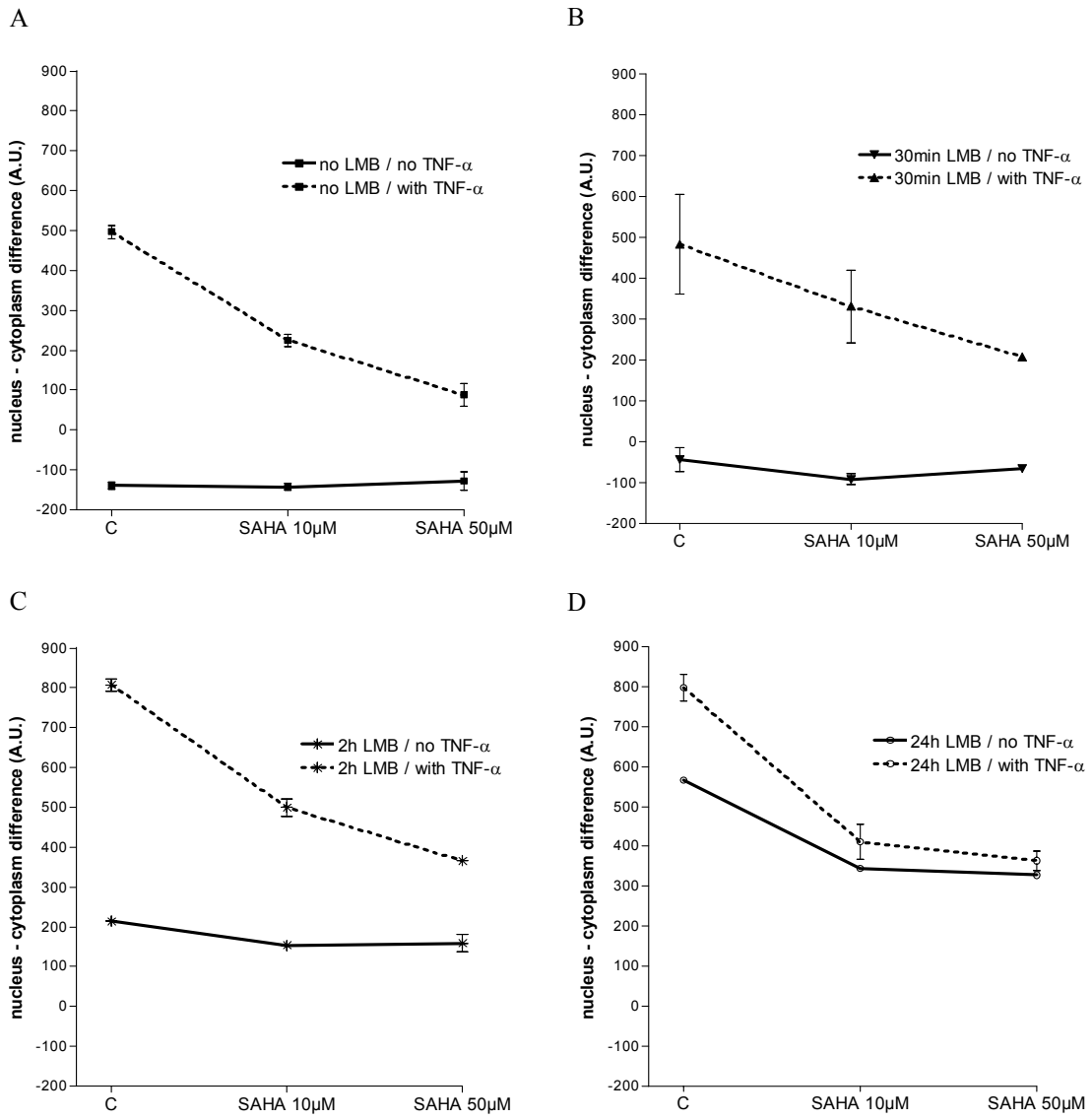

Figure 4.28: Measurements of NFκB nuclear export upon HDI and LMB co-treatment.
A549 cells were incubated with SAHA for 24 hours together with leptomycin B (20 ng/ml) for the indicated times, followed by a stimulation with TNF-α (25 ng/ml) for 30 min. Cells were fixed and stained with anti-p65 antibody. Graphs represent quantitative fluorescence intensity read-outs of cell images: (A) no LMB, (B) 30 min LMB, (C) 2 hours LMB, (D) 24 hours LMB treatment.

4.5.7 Expression of the NFκB subunits p100 and p105 was influenced by HDIs

In mammals there are five NFκB subunits: p65, c-Rel, Rel-B, p100/p52, and p105/p50. The latter two are produced as larger precursors, possessing the potential to bind to the p65 subunit via ankyrin repeats[153], thereby inhibiting p65 nuclear translocation. It was tested, if p100 or p105 expression was changed by HDIs. To this end, H460 cells were incubated with increasing concentrations of SAHA, TSA, or MS-275 and RNA was analyzed by TaqMan PCR. In a dose dependent manner, p100

expression was increased whereas p105 mRNA expression decreased upon 24 hours HDI treatment (figure 4.29-A,C). During a 24 hours time course, gene expression analysis revealed on the one hand a steady increase in p100 and on the other hand a more immediate decrease in p105 gene expression (figure 4.29-B,D). Expression changes initiated in the hydroxamic acid treated cells were obvious after 4 hours, while reactions to MS-275 were delayed by several hours. Further it was checked if altered mRNA expression translated into changes in protein expression. In accordance with RNA data, immunoblotting revealed increased p100 (figure 4.29-E) and reduced p105 protein levels in unstimulated H460 cells (data not shown). To assay if increasing levels of p100 resulted in enhanced p100-p65 binding, co-immunoprecipitation experiments were performed. Native p65 was immunoprecipitated from whole cell extracts with an anti-p65 antibody and in a concentration dependent manner, p100-p65 binding was increased in H460 cells. This effect was enhanced upon the addition of TNF-α. The data showed that TNF-α stimulation was not required for the formation of the p65-p100 complex, but enhanced complex formation (figure 4.29-F).

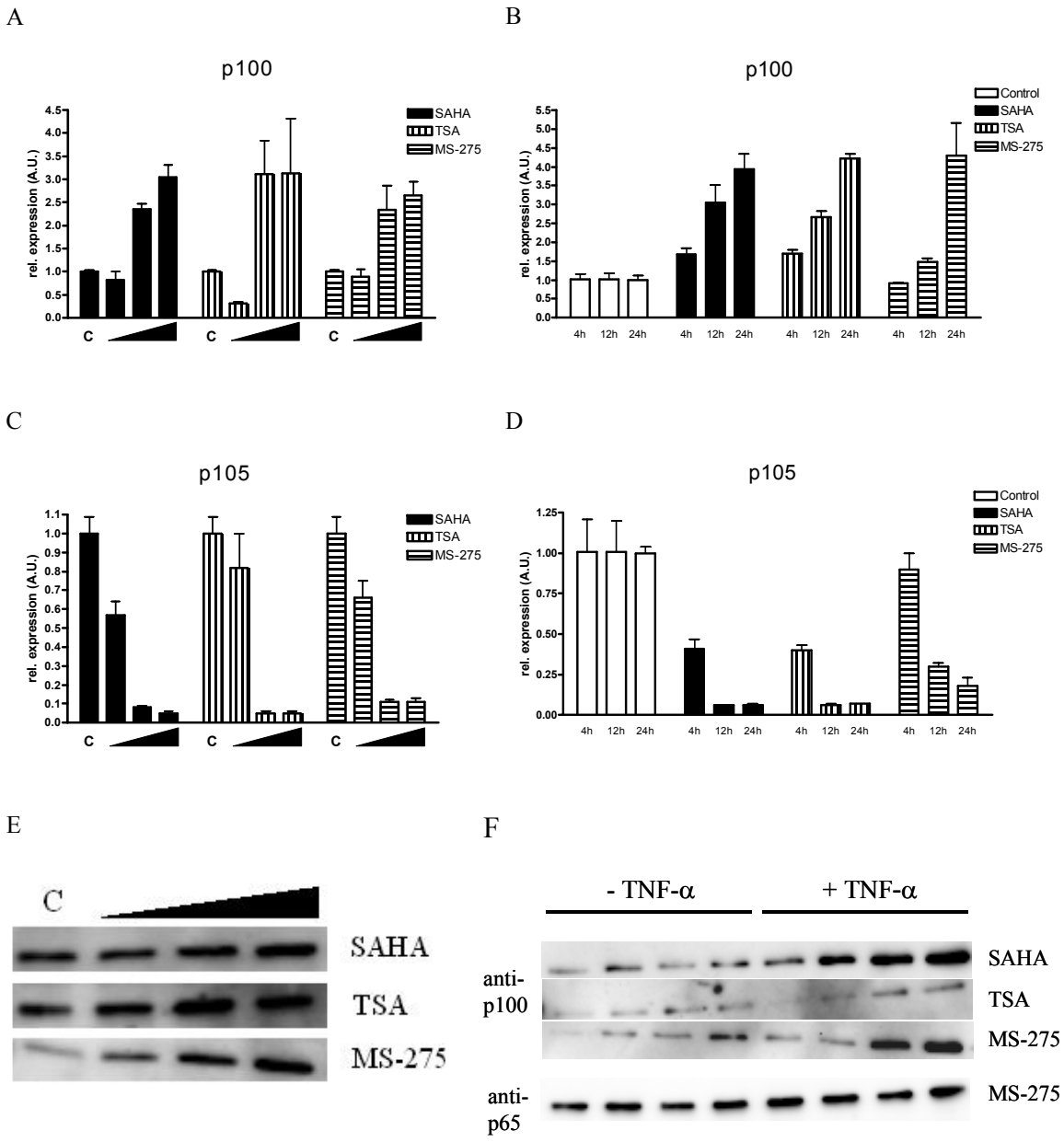

Figure 4.29: Gene expression analysis of NFκB subunits p100 and p105 upon HDI treatment. H460 cells were incubated with HDIs (SAHA 1 µM, 10 µM, 50 µM ; TSA 200 nM, 2 µM, 4 µM ; or MS-275 100 nM, 20 µM, 50 µM) for 24 hours, lysed for RNA, and targeted for p100 (A) and p105 (C) gene expression. Additionally, H460 cells were treated with HDIs (SAHA 50 µM, TSA 4 µM, MS-275 50 µM) for the indicated times (4h, 12h, 24h) and p100 (B) and p105 (D) gene expression levels were measured. Data represent mean ± SD. (E) p100 protein levels (concentrations see A) after 24 hours HDI incubation were determined as well. (F) H460 cells were incubated with HDIs (SAHA 1 µM, 10 µM, 50 µM; TSA 200 nM, 2 µM, 4 µM; MS-275 100 nM, 20 µM, 50 µM) for 24 hours, TNF-α treated (25 ng/ml) for 30 min and p65 was targeted for immunoprecipitation, followed by immunoblotting studies against p100. Control for equal loading: p65.

To test for the functional implications of this finding, short interfering RNAs targeting p100 expression were applied. A549 and H460 cells were transfected with p100 siRNA for 48 hours. HDIs were added for 24 hours and cells were subsequently

treated with TNF-α for 30 min and fixed for ArrayScan analysis. p100 knock-down could be demonstrated by immunoblotting. The fact that knock-down of p100 did not reconstitute NFκB translocation implies that the increase in p100 was not responsible for the HDI induced suppression of NFκB signaling (figure 4.30).

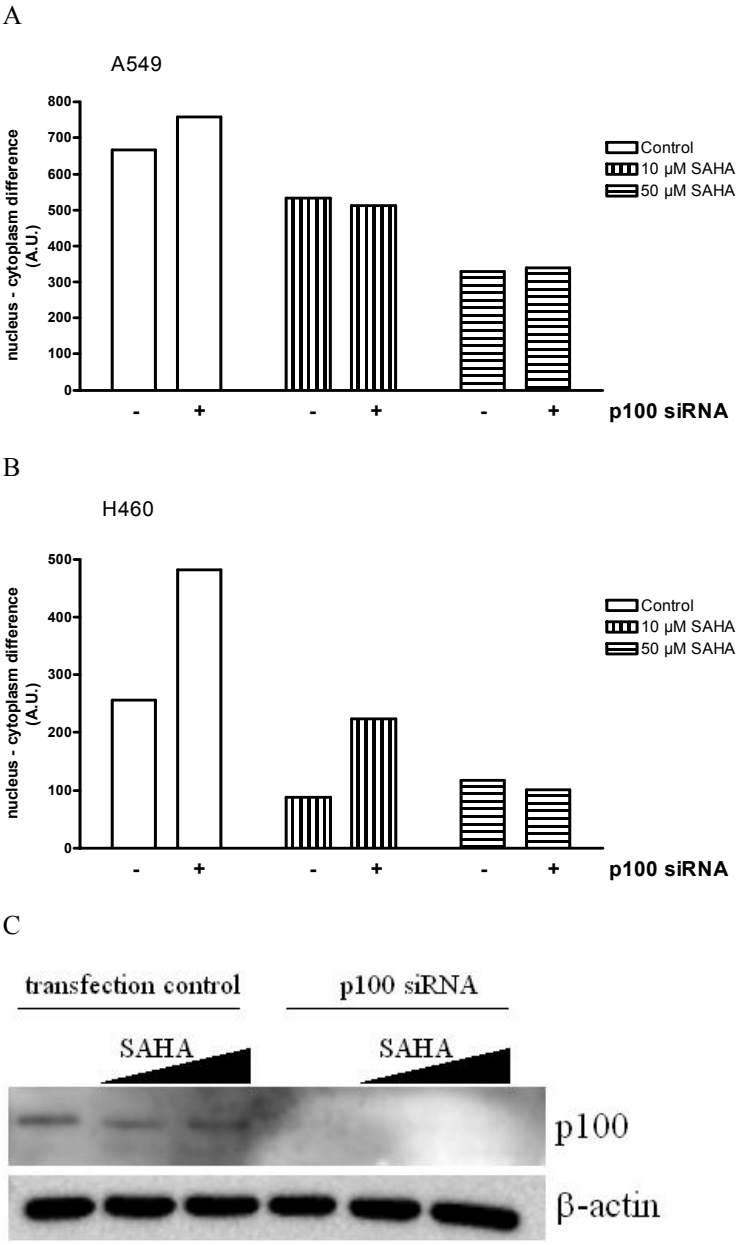

Figure 4.30: NFκB nuclear translocation measurements upon p100 suppression, HDI treatment, and TNF-α stimulation.
(A) A549 ($5x10^4$) and (B) H460 cells ($3x10^4$) were seeded in 6-well plates and transfected with p100 siRNA (10 nM). After 48 hours, SAHA (10 µM, 50 µM) was added for an additional 24 hours. Cells were either stimulated with TNF-α for 30 min, fixed, and p65 stained (translocation: A, B), or lysed for immunoblotting studies against p100 and β-actin (C). Suppression of p100 was shown in A549.

4.5.8 Incubation with HDIs changed IKK activation and reduced IκB-α phosphorylation and degradation

Although p100 expression and binding to p65 was increased, inhibition of NFκB translocation upon TNF-α could not be ascribed to p100 induction. In order to translocate to the nucleus, NFκB needs to be activated. TNF-α treatment leads to the activation of the IKK-complex, consisting of the kinases IKK-α and IKK-β, and the regulatory subunit IKK-γ. Activation of the IKK-complex by TNF-α is ascribed to the phosphorylation of the kinase subunits IKK-α and IKK-β on serines 176/180 and 177/181, respectively, resulting in the phosphorylation of the inhibitory protein IκB-α. Phosphorylated IκB-α becomes ubiquitinated and degraded by the proteasome. Previous experiments showed that proteasome activity was not inhibited by HDIs. To sheed light on the activation process in the presence of HDIs, immunoblotting studies were performed. A549 and H460 cells were incubated with SAHA or TSA for 24 hours, TNF-α treated for 4 min or 10 min, and lysed for immunoblotting. Cells preincubated with HDIs had reduced levels of phosphorylated IKK-α and IKK-β 10 min after the addition of TNF-α compared to control cells (figure 4.31-A). To test, if the reduction was due to reduced levels of IKK, cell lysates were blotted for the three subunits of the IKK complex. Immunoblotting showed that IKK levels were unaffected upon HDI treatment (figure 4.31-B). This rules out that inhibition of NFκB signaling could be due to lack of IKK protein.

Next, the possibility of Hsp90 acetylation and influence on NFκB was investigated. Hsp90 is required to stabilize and activate the IKK complex[154] and has been described to be regulated by acetylation[155,156]. In contrast to HDIs, 17-AAG, a specific Hsp90 inhibitor, led to a complete ablation of IKK-β expression (figure 4.31-C). Acetylation of Hsp90 was not tested directly, but this data favor the idea that HDIs do not acetylate Hsp90 or acetylation does not inhibit Hsp90 chaperone activity.

The lack of activated IKK could be translated into reduced inhibitor phosphorylation. Immunoblotting experiments revealed that in SAHA and TSA pretreated cells, IκB-α phosphorylation was largely undetectable upon 4 minutes TNF-α stimulation as compared to control cells, which showed a strong phosphorylated band of IκB-α at

4 min. After 10 min TNF-α excitement, IκB-α was largely undetectable in control cells, whereas a protein band was still present under increasing concentrations of SAHA and TSA (figure 4.31-D).

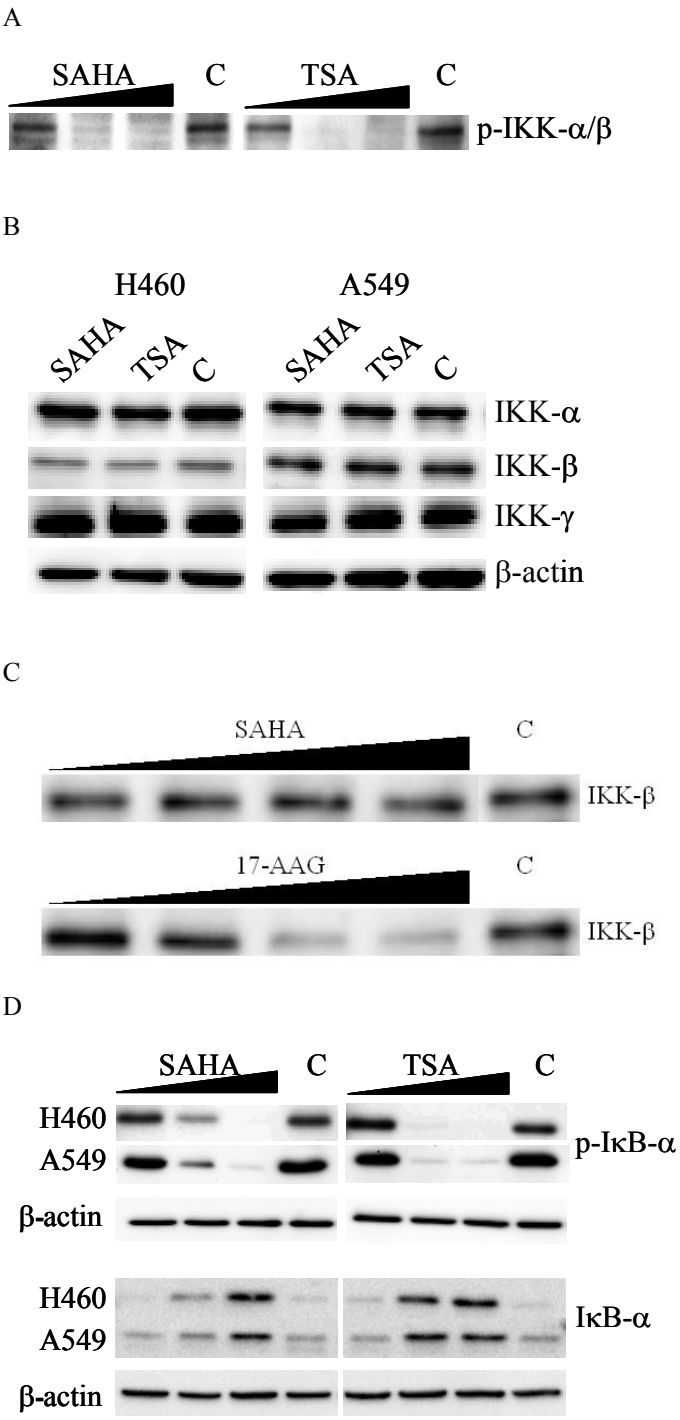

Figure 4.31: IKK activation, and IκB-α phosphorylation upon HDIs.
A549 and H460 cells were preincubated with SAHA and TSA for 24 hours and stimulated with TNF-α (25 ng/ml). (A) A549 cells were stimulated with TNF-α for 10 min, lysed, and immunoblotted against p-IKK-α/β. Concentrations: SAHA 1 µM, 10 µM, 50 µM; TSA 200 nM, 2 µM, 4 µM, or DMSO control. (B) Protein levels of IKK-α, IKK-β, and IKK-γ were determined upon TNF-α incubation for 10 min. Concentrations: SAHA 50 µM, TSA 4 µM, or DMSO control. (C) IKK-β quantification by immunoblotting in A549 cells incubated with SAHA or 17-AAG. Concentrations: SAHA 1 µM, 10 µM, 20 µM, 50 µM; 17-AAG: 5 nM, 50 nM, 100 nM, 500 nM. (D) IκB-α phosphorylation (4 min TNF-α) and degradation (10 min TNF-α) were determined. Concentrations: see A. Loading control: β-actin.

4.5.9 HDIs suppressed TNF-R1 expression and surface exposure

Immunoblotting clearly indicated that reduced NFκB activation was due to decreased IKK phosphorylation. Activation of NFκB by TNF-α requires TNF-receptors at the cell surface, whereas TNF-R1 initiates the majority of TNF's biological activities[79]. To obtain evidence if the activation and translocation defect might be caused by downregulation of the TNF-R1, A549 and H460 cells treated with SAHA or TSA for 24 hours were analyzed for TNF-R1 expression by TaqMan PCR, immunoblotting, and FACS. Experiments were performed in triplicate to perform statistical analysis. In a dose dependent manner SAHA and TSA decreased mRNA levels of TNF-R1 after 24 hours. As an internal control TRAIL-R2 expression was measured, which was previously shown to increase upon HDI treatment[157-159]. Indeed, at concentrations at which TNF-R1 expression was decreased, TRAIL-R2 expression was increased (figure 4.32-A,B): TNF-R1 was reduced to 10 % of control cells, while TRAIL-R2 increased around 2-fold in H460 and 3.5-fold in A549 cells. The reduced mRNA levels of TNF-R1 were accompanied by reduced protein levels (figure 4.32-C).

A

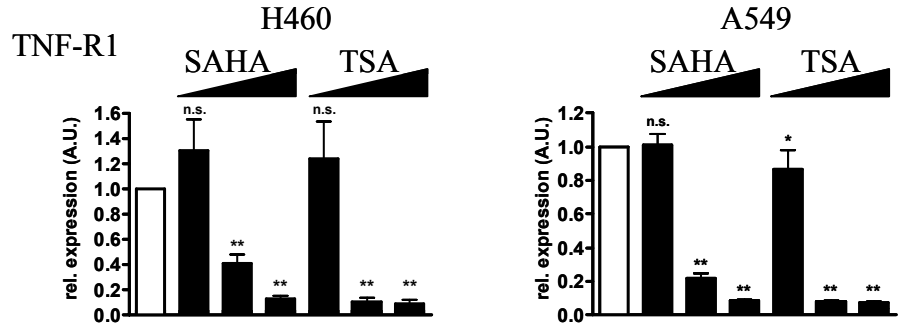

B

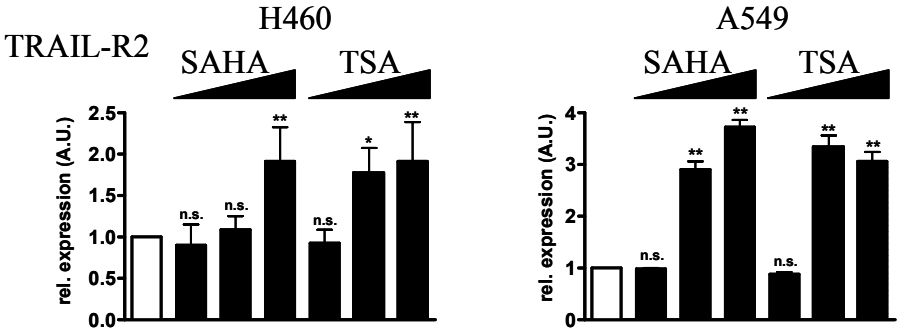

C

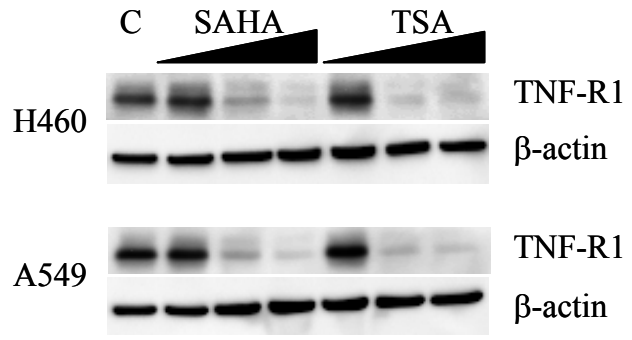

Figure 4.32: TNF-R1 mRNA and protein expression upon HDI incubation.
H460 and A549 cells were incubated with SAHA (1 µM, 10 µM, 50 µM) and TSA (200 nM, 2 µM, 4 µM) for 24 hours, lysed, and assayed for RNA and protein expression. TNF-R1 (A) and TRAIL-R2 (B) mRNA quantified by TaqMan PCR. Data represent mean ± SD from 3 independent experiments. Statistical significance: n.s., not statistically significant; *, $P < 0.05$; **, $P < 0.01$. (C) TNF-R1 protein expression was checked by immunoblotting. Loading control: β-actin.

If functionally important, the strong downregulation of TNF-R1 mRNA and protein should correlate with reduced surface exposure of the receptor. Thus, expression of surface TNF-R1 was checked employing FACS measurements. A549 lung cancer cells were carefully detached from 10 cm^2 culture dishes and incubated with anti-TNF-R1 antibody. In line with the findings for TNF-R1 mRNA and protein expression, increasing concentrations HDIs reduced the surface exposure of TNF-R1.

The main fluorescence intensity shifted from 10^4 as observed in untreated cells towards 10^3, the value also seen for the isotype control sample (figure 4.33).

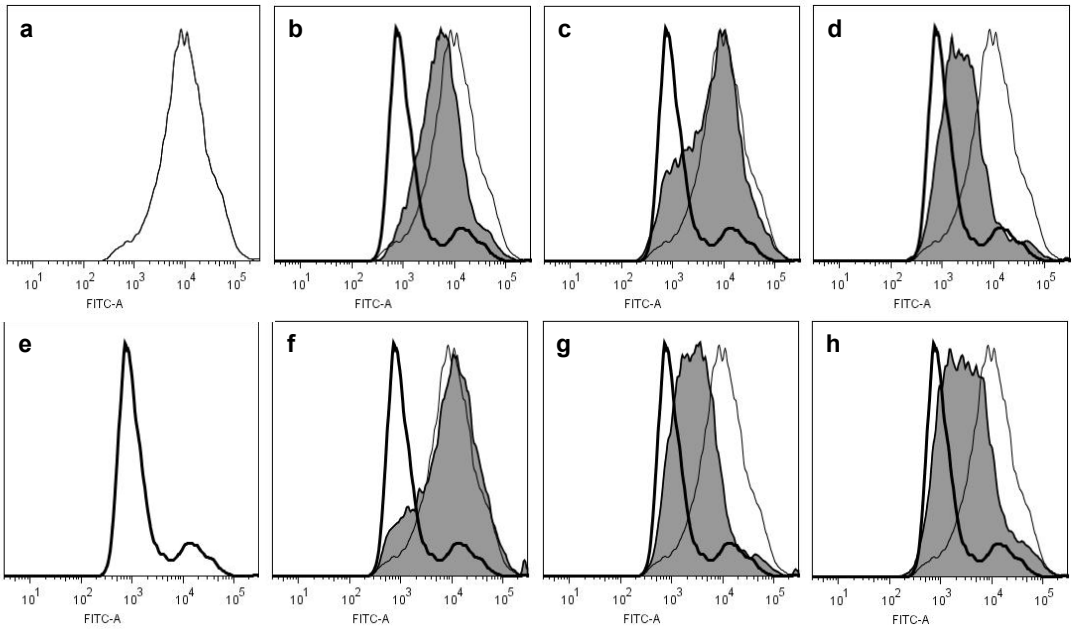

Figure 4.33: TNF-R1 surface exposure upon SAHA and TSA.
A549 cells were seeded in 10 cm^2 dishes and incubated with SAHA and TSA for 24 hours, detached and reacted with mouse anti-TNF-R1 antibody and FITC conjugated anti-mouse antibody. Labeled cells were analyzed on a BD FACS-Canto: a. no HDI, b-d. SAHA 1 µM, 10 µM, 50 µM, e. isotype control, f-h. TSA 200 nM, 2 µM, 4 µM.

Furthermore, the kinetics of TNF-R1 downregulation on RNA and protein level was investigated. Therefore, A549 cells were incubated with SAHA, TSA, and MS-275 for 4, 12, or 24 hours. Cells were lysed and RNA was used for TaqMan PCR. Reduction in TNF-R1 RNA expression occured quite rapidly. After around 4 hours, receptor expression was reduced to ~ 70 %, after 12 hours to ~20 %, reaching its minimum after 24 hours of about 10 % compared to control cells (figure 4.34-A). TRAIL-R2 showed a similar kinetic with a significant increase after around 12 hours, reaching a maximum after 24 hours with an induction between 3 – 7 fold (figure 4.34-B). Reduction of TNF-R1 protein levels was apparent after 7 hours, and was further attenuated after 14 hours (figure 4.34-C).

A

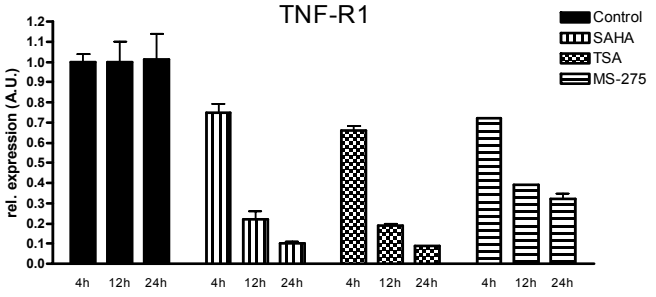

B

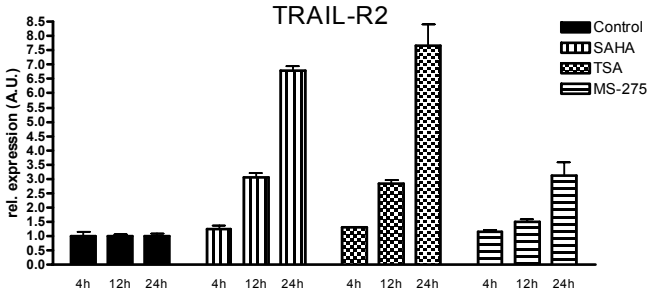

Figure 4.34: Kinetics of TNF-R1 downregulation upon HDIs.
A549 cells were treated with SAHA (50 µM), TSA (4 µM), and MS-275 (50 µM) for 4, 12, or 24 hours. Cells were lysed with RLT-buffer für RNA isolation and gene expression analysis of TNF-R1 (A) and TRAIL-R2 (B). Data represent mean ± SD. Additionally, cells were treated with SAHA (1 µM, 10 µM, 50 µM) for 4 – 14 hours, lysed with RIPA buffer, und targeted for TNF-R1 protein by immunoblotting (C). Loading control: β-actin.

C

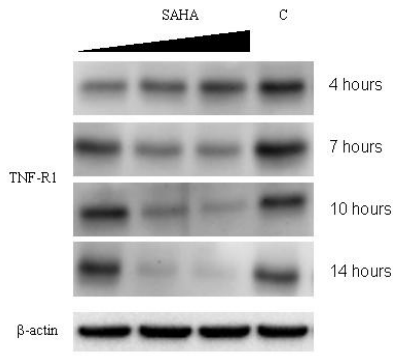

4.5.10 TNF-R1 downregulation by HDIs: a general cellular response mechanism

To address whether this was a singular finding specific for A549 and H460, the number of NSCLC cell lines was expanded and tested for TNF-R1 down-regulation upon HDI incubation. Treatment with SAHA and TSA caused an overall reduction of TNF-R1 mRNA to ~ 10 % - 40 % (table 4.5).

Cell line	NSCLC subtype	rel. expression of TNF-R1 (% of untreated control ± SD)			
		10 µM SAHA	50 µM SAHA	2 µM TSA	4 µM TSA
A-427	Adenocarcinoma	36 ± 6	21 ± 1	20 ± 3	25 ± 2
A549	Adenocarcinoma	29 ± 4	13 ± 2	12 ± 1	12 ± 2
NCI-H23	Adenocarcinoma	21 ± 1	7 ± 1	6 ± 1	7 ± 1
NCI-H1563	Adenocarcinoma	91 ± 5	29 ± 3	21 ± 2	26 ± 2
NCI-H1703	Adenocarcinoma	35 ± 1	15 ± 2	18 ± 2	17 ± 1
NCI-H460	Large cell carcinoma	24 ± 1	9 ± 1	6 ± 1	6 ± 1
NCI-H520	Squamous cell carcinoma	23 ± 1	9 ± 1	8 ± 0	7 ± 0
NCI-H2170	Squamous cell carcinoma	40 ± 2	10 ± 1	10 ± 1	9 ± 1

Table 4.5: TNF-R1 expression in NSCLC cell lines upon HDI treatment.
Various NSCLC cell lines were incubated with SAHA and TSA with indicated concentrations for 24 hours, lysed, and assayed for TNF-R1 mRNA expression.

In A549 and H460 cells TRAIL-R2 upregulation was detected at concentrations at which TNF-R1 was downregulated. Out of the additional cell lines tested, TRAIL-R2 upregulation was only seen in H520, H2170, and H1703 lung cancer cells (table 4.6).

Cell line	NSCLC subtype	rel. expression of TRAIL-R2 (% of untreated control ± SD)			
		10 µM SAHA	50 µM SAHA	2 µM TSA	4 µM TSA
A-427	Adenocarcinoma	57 ± 1	69 ± 6	62 ± 10	66 ± 3
A549	Adenocarcinoma	331 ± 89	550 ± 40	541 ± 25	726 ± 56
NCI-H23	Adenocarcinoma	71 ± 3	80 ± 23	69 ± 9	67 ± 10
NCI-H1563	Adenocarcinoma	58 ± 2	90 ± 15	87 ± 4	137 ± 5
NCI-H1703	Adenocarcinoma	149 ± 8	265 ± 3	238 ± 32	223 ± 11
NCI-H460	Large cell carcinoma	190 ± 15	340 ± 45	339 ± 26	297 ± 4
NCI-H520	Squamous cell carcinoma	725 ± 45	2370 ± 19	2582 ± 79	2729 ± 83
NCI-H2170	Squamous cell carcinoma	293 ± 33	448 ± 30	438 ± 2	433 ± 12

Table 4.6: TRAIL-R2 expression in NSCLC cell lines upon HDI treatment.
Various NSCLC cell lines were incubated with SAHA and TSA with indicated concentrations for 24 hours, lysed, and assayed for TRAIL-R2 mRNA expression.

To check, if the effect was restricted to lung tumor cells, TNF-R1 gene and protein expression was examined in other cancer cell lines. PANC-1, a pancreatic cancer cell line, A2780, an ovarian cancer cell line, U-2 OS, which originated from a bone osteosarcoma epithelia, and RKO-p21, an engineered colon cancer cell line, were tested. Moreover, to determine, if HDIs also affected normal cell lines regarding TNF-R1, HFL-1 and SAEC cells were assayed as well. In all tumor entities and normal cells a reduction in TNF-R1 mRNA expression was found (table 4.7).

Cell line	Cell type	rel. expression of TNF-R1 (% of untreated control ± SD)			
		10 µM SAHA	50 µM SAHA	2 µM TSA	4 µM TSA
PANC-1	Pancreatic cancer	39 ± 3	14 ± 2	99 ± 6	35 ± 6
A2780	Ovarian cancer	80 ± 4	25 ± 3	132 ± 12	27 ± 3
U-2 OS	Osteosarcoma	20 ± 2	6 ± 1	9 ± 0	4 ± 0
RKO-p21	Colon cancer	89 ± 8	26 ± 3	23 ± 2	15 ± 1
HFL-1	Normal tissue	106 ± 2	41 ± 3	44 ± 8	32 ± 3
SAEC	Normal tissue	79 ± 6	30 ± 2	39 ± 4	26 ± 4

Table 4.7: TNF-R1 expression in various cell lines upon HDI treatment.
Various cancer and normal cell lines were incubated with SAHA and TSA with indicated concentrations for 24 hours, lysed, and assayed for TNF-R1 mRNA expression.

4.5.11 HDIs had no effect on NFκB activity in Hodgkin's lymphoma cell lines

Hodgkin's lymphoma cell lines possess constitutive NFκB activity (chapter 4.2.3). KM-H2 and L-1236 cells differ by their IκB-α status. KM-H2 cells do not contain functional IκB-α, whereas L-1236 cells express wild type IκB-α, but constitutive NFκB activity is caused by deregulation of upstream regulatory pathways, such as a constitutively active IKK. Different classes of HDIs and 17-AAG, a specific Hsp90 inhibitor controlling IKK biogenesis and enzymatic activity[154], were utilized to examine their influence on constitutive NFκB. Kovacs and coworkers[160] proposed that hyperacetylation of Hsp90, by inactivation of the histone deacetylase HDAC6, leads to loss of chaperone activity. To test the influence of HDIs in general and a possible downregulation by Hsp90 acetylation, Hodgkin's lymphoma cells were incubated with the hydroxamic acids SAHA, TSA, and LAQ-824, the benzamide MS-275, and the Hsp90 inhibitor 17-AAG for 24 hours. Total cell extracts were prepared and employed for DNA binding studies. Both cell lines, L-1236 and KM-H2, did not display reduced NFκB DNA binding activity upon HDI treatment. In contrast, L-1236 but not KM-H2 cells reduced NFκB binding activity when incubated with the Hsp90 inhibitor 17-AAG (figure 4.35).

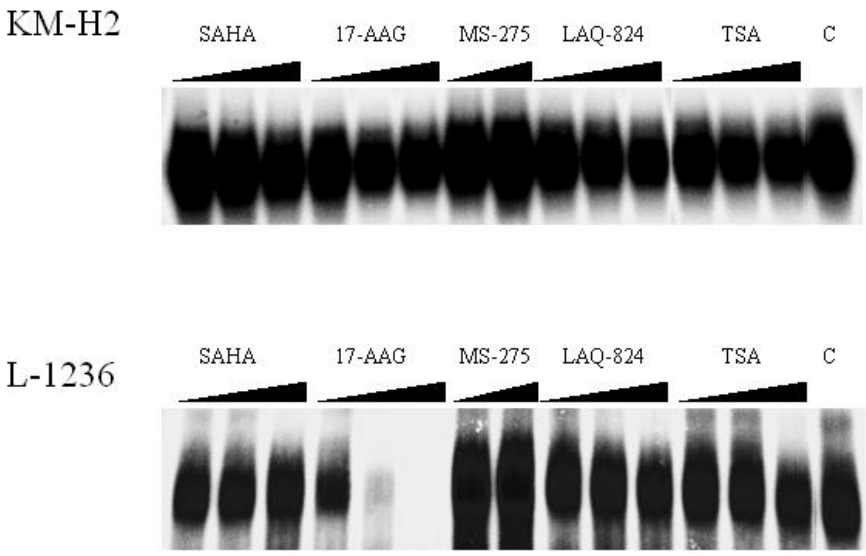

Figure 4.35: NFκB DNA binding of Hodgkin's lymphoma cell lines upon 24 hours HDI incubation.
KM-H2 and L-1236 cells were incubated for 24 hours with HDIs (SAHA 500 nM, 2 µM, 10 µM; MS-275 6 µM, 10 µM; LAQ-824 30 nM, 80 nM, 120 nM; TSA 30 nM, 100 nM, 300 nM) and the Hsp90 inhibitor 17-AAG (500 nM, 3 µM 15 µM) for 24 hours. Cells were lysed for whole cell extracts and assayed for DNA binding capability.

5 DISCUSSION

5.1 NFκB inducibility by TNF-α and chemotherapeutic drugs in different tumor entities

In normal human cells the activity of the transcription factor NFκB is tightly regulated. NFκB heterodimers are kept inactive in the cytoplasm by IκB inhibitory proteins until an activating stimulus leads to rapid degradation of the inhibitor IκB and translocation of NFκB into the nucleus. One target gene of NFκB is IκB itself, the expression of which results in a negative feedback loop by binding to and actively transporting NFκB out of the nucleus[125]. Activated NFκB also induces inhibitors of the activated IKK complex such as A20[161]. Despite the existing negative feedback mechanisms, activated NFκB has been found in various human cancer cell lines and tumor tissues derived from patients. Rayet and Gélinas[42] summarized persistent nuclear NFκB activity in several human cancer cell types, e.g. Hodgkin's lymphoma, multiple myeloma, diffuse large B-cell lymphoma, as well as breast, colon, ovarian, pancreatic, bladder, prostate, or melanoma cancers. Activation might be either due to chromosomal amplifications or rearrangements in NFκB genes, constitutive activation of upstream signals, or mutations in inhibitory IκB molecules.

The 5-year survival rate for lung cancer is around 14 %, which is low in comparison to the outcome of breast cancer or Hodgkin's lymphoma. When I started this Ph.D. thesis project in 2003, little was known about the activation status of NFκB in NSCLC and SCLC cell lines. Most publications in this area aimed at NFκB activation by chemotherapeutic drugs and possibilities for NFκB inhibition in tumor therapy[162]. Therefore, the initial focus of this work was the evaluation of the importance of NFκB signaling for cell growth and drug resistance in lung cancer cells, and accordingly, the first experiments were directed at determining NFκB activation levels in lung cancer cell lines, both from NSCLC and SCLC. Subsequently, the reaction of NFκB to chemotherapeutic drugs e.g. topoisomerase poisons, alkylating or crosslinking agents, and HDIs was analyzed. In further studies the reasons for the lack of NFκB inducibility in SCLC cells upon TNF-α was worked out.

In contrast to lung cancer, NFκB activation in pancreatic cancer cell lines is well described in the literature. In 1999, Wang and colleagues[38] showed the persistent activation of NFκB in pancreatic tumor tissues and cell lines. To this day, pancreatic cancer has the lowest survival rate of all cancer entities, and constitutive NFκB activation might be a contributory factor for drug resistance and bad prognosis. To verify the data and to establish model systems for future experiments with increased NFκB activity, a set of pancreatic cancer cell lines was tested for their activation status and the effects of NFκB inhibition.

Certain leukemias and lymphomas have been described to possess activated nuclear NFκB. Bargou and coworkers[163] showed activated NFκB to be characteristic for Hodgkin's/Reed Sternberg cells. NFκB activation in this cancer type has been further analyzed by various groups, ascribing persistent activation back to IκB-α mutations and increased signals upstream of NFκB[41,48].

Ni and coworkers[40] showed constitutively active NFκB in multiple myeloma cell lines, which could be reduced by proteasome and IκB-α phosphorylation inhibitors and led to apoptosis induction. Velcade, a proteasome inhibitor, is in clinical trials for the treatment of multiple myeloma. Inhibition of the proteasome impedes IκB-α degradation, thereby preventing NFκB nuclear translocation and activation of NFκB target genes which act mainly anti-apoptotic.

Diffuse large B-cell lymphoma (DLBCL) is the most common subtype of non-Hodgkin's lymphoma. It is subdivided into "activated B-cell-like" (ABC) DLBCL associated with persistent NFκB activation as well as worse outcome and into "germinal centre B-cell-like" (GCB) DLBCL accompanied with better outcome and inactive NFκB[135,164]. By anyalzing above named tumor entities, cell lines with different NFκB activation statuses were identified, which allowed to work on various model systems and test the impact of drugs on cell survival depending on NFκB.

In the literature, the term NFκB activity is not clearly defined. Many publications show the "constitutive" activation of NFκB in different tumor entities by EMSA

experiments[38,48,165]. Other groups describe a "basal" or "increased" NFκB activity[166,167]. For this work NFκB activity was classified as "basal", "increased" and "constitutive".

- In some cell lines tested, a low basal NFκB DNA binding activity could be detected, i.e. in EMSA experiments binding of NFκB to κB sequences was very weak comparable to normal cells.
- Stronger DNA binding in EMSAs demonstrated increased NFκB activity. Usually, cytokines or drugs could further activate NFκB in cells with a basal or increased NFκB pathway.
- Strong NFκB DNA binding accompanied by a lack of further activating potential was a hallmark of cell lines with constitutively active NFκB.

It is important to notice at this point that DNA binding is not always predictive for subsequent NFκB activation, as shown by Ho and coworkers[168]. They demonstrated that doxorubicin activates NFκB nuclear translocation and DNA binding which leads to NFκB target gene repression. Zhong and colleagues[169] also published exceptions where NFκB DNA binding does not result in transcriptionally active NFκB proteins. Yet, in general NFκB DNA binding yields NFκB target gene expression. If stimulation with TNF-α leads to IκB-α phosphorylation and degradation, DNA binding always induces target gene expression. In these cases, EMSA is highly predictive for NFκB activation. However, incubation with chemotherapeutics, intercalating into the DNA or inducing DNA damage, does not always lead to NFκB target gene expression. Therefore it is necessary or at least useful to measure NFκB activation at multiple steps along the pathway, such as IκB-α phosphorylation and degradation, NFκB translocation into the nucleus, DNA binding, and target gene expression.

TNF-α was used to determine the NFκB activation status in various cells. In 1975, TNF-α was identified as "tumor necrosis factor"[76] exhibiting cytotoxicity in two neoplastic cell lines, but not in mouse embryonic culture. Although TNF-α has systemic toxicity, it is still a potent cytokine in tumor treatment[170] when selectively

delivered to the tumor. Han et al.[171] claimed that NFκB activation decreased the sensitivity of colon cancer cells to TNF-α. Inhibition of the NFκB pathway in combination with TNF-α may increase the antitumor potential of TNF-α. Furthermore, Yasui and coworkers[172] described that NFκB inhibition in combination with TNF-α treatment enhances apoptosis in the human gastric carcinoma cell line MKN45. Additionally, in vivo tumor growth of MKN45 cells could be inhibited. These data are further supported by the publication of Kucharczak and colleagues[81]. They summarized that binding of TNF-α to its receptor leads to the formation of two complexes. The first complex activates NFκB and its anti-apoptotic genes, the second complex activates an apoptotic signaling cascade with caspase activation and cytochrome c release. Inhibition of NFκB probably shifts the action of TNF-α towards the proapoptotic pathway.

The activation of NFκB upon binding of TNF-α to the receptor is still not fully understood, but researchers suggest activation of a signaling cascade. Many members of the mitogen-activated protein kinase kinase kinase (MAP3K) family activate IKK when overexpressed, e.g. MEKK1[173], MEKK2[174], MEKK3[174], TGF-β-activating kinase 1 (TAK1)[175], NIK[176], and NFκB activating kinase (NAK)[177]. However, recent studies indicate that MEKK3 is the key signaling molecule in TNF-α induced NFκB activation[178]. Blonska and colleagues[179] propose that upon binding of TNF-α to its receptor, TRADD, TRAF2, and RIP are recruited to the death domain. MEKK3 connects RIP to the IKK complex via TAK1.

5.1.1 Lung cancer

Conventional treatment of lung cancer has reached a plateau of effectiveness in increasing the patient's survival. New treatments are eagerly sought. The importance of NFκB in this disease was analyzed by determining the activation status in non-small cell lung cancer (NSCLC) and small cell lung cancer (SCLC) cell lines by TNF-α, and by testing the inducibility of NFκB by cytotoxic drugs.

5.1.1.1 NFκB inducibility by TNF-α

Unstimulated NSCLC A549 and H460 cell lines showed only negligible DNA binding, hence only low basal NFκB activity. In both cell lines NFκB was excitable by TNF-α, yielding strong κB DNA binding as well as target gene expression. In contrast, DNA binding and target gene expression in SCLC cell lines could not or only slightly be further enhanced upon TNF-α treatment. H69 showed no DNA binding activity in unstimulated cells, whereas increased NFκB activity was detected in SW2 cells. The latter cell line originates from a small cell lung cancer metastasis post chemotherapy and thus might have gained increased NFκB activity during chemotherapy. Activation of NFκB target gene expression upon TNF-α treatment in the SCLC cell lines H69, DMS 53, and SW2 was around 1.5 fold, in DMS 114 approximately 8-fold for IκB-α and 17-fold for IL-8, and in the NSCLC cell line A549 the induction of NFκB target genes was around 10-fold (IκB-α) and 320-fold (IL-8). The cause for the lack of NFκB activation upon TNF-α stimulation in the majority of SCLC cell lines is the low expression level of TNF-R1. Hopkins-Donaldson and co-workers[180] showed reduced levels of death receptors FAS/CD95 and TRAIL-R1 and methylation specific PCR demonstrated the methylation of CpG islands in promoter regions of these genes, characteristic for SCLC cells. Moreover, literature suggests the absence of other receptors such as the TNF-R1 in SCLC[181]. In this study it could be demonstrated that a lack of TNF-R1 mRNA accompanied by diminished protein expression was the cause for missing NFκB activation upon TNF-α treatment in H69, DSM 53, and SW2 cells. There is a clear correlation between cell lines expressing TNF-R1 and the ability to activate NFκB upon TNF-α treatment. All NSCLC cell lines tested so far (see chapter 4.5.10) showed sufficient TNF-R1 expression on the RNA and protein levels, which could be reduced by HDIs. Only the SCLC cell line DMS 114 exhibited TNF-R1 expression for NFκB activation by TNF-α. The low relative amount of TNF-R1 of 5 % at the RNA and around 0.5 % at protein level as compared to A549 was sufficient to yield such a strong induction of inhibitor phosphorylation and NFκB target gene expression in DMS 114 cells. It thus appears as if NFκB induction via TNF-R1 was quite sensitive to TNF-α binding. Analysis of a lung cancer cell line panel showed, that besides TNF-R1, TRAIL-R2 expression was drastically decreased in SCLC but not in NSCLC cell lines.

Interestingly, in the SCLC cell lines H69, DMS 53, and SW2 signaling in the NFκB pathway downstream of the kinase complex IKK was still intact as was demonstrated by NFκB activation in response to topoisomerase poisons.

5.1.1.2 NFκB inducibility by cytotoxic drugs

One possible mechanism by which tumor cells gain resistance to cytotoxic drugs and prevent apoptosis is the activation of NFκB. Affymetrix data obtained in-house revealed the induction of an NFκB gene cluster, containing genes such as NFKBIA (IκB-α) and RELB (Rel-B), in the SCLC cell line SW2 and the ovary cancer cell line A2780 incubated with etoposide and camptothecin (Gekeler et al., unpublished data). This was an important hint to establish the NFκB activating potential of chemotherapeutic drugs. Various other publications also showed NFκB activation by therapeutically used drugs[182-184]. Inhibition of components of the pathway in combination with chemotherapeutic agents improves cytotoxicity in cell culture[185,186] and may be important for future treatment options in the patient.

Different drugs were tested for their capability to induce NFκB, including topoisomerase I and II poisons, alkylating and crosslinking agents. Not all drugs had the potential to activate NFκB. Although cytotoxicity in A549 and H69 was comparable, only topoisomerase poisons etoposide and camptothecin could activate NFκB quite rapidly in H69 cells. Cisplatin and mafosfamide had no effect on the NFκB pathway within 8 hours, and doxorubicin incubation reduced NFκB target gene expression. Still, it is possible that DNA-crosslinking or alkylating agents activate NFκB later on, when cells undergo cell division. This question could be addressed in further studies, exposing cells to cisplatin or mafosfamide for a longer time period. It could be shown that NFκB activation was cell line dependent. The NSCLC cell line A549 and the SCLC cell line DMS 114 did not activate NFκB upon etoposide incubation, whereas the SCLC cell lines H69, DMS 53, and SW2 activated NFκB. These data emphasize the importance to figure out which underlying molecular mechanisms allow the activation of NFκB in only a subset of cancer cells by chemotherapeutic drugs.

Although doxorubicin is grouped into the category of topoisomerase poisons, its mode of action on cells differs from etoposide and camptothecin. There are many studies describing various effects of anthracycline antibiotics such as doxorubicin on survival, gene transcription, and also NFκB. These effects can be related back to the different drug concentrations applied in experiments. Gewirtz[141] summarized these effects depending on drug concentration. In this study, 10 μM doxorubicin was employed for 2 - 8 hours before assaying for NFκB target gene expression. One possible mechanism for reduced NFκB target gene expression is a general inhibition of transcription caused by doxorubicin treatment. Doxorubicin is known to induce DNA crosslinks at 5'-GC sequences, which are often found in untranslated regions such as transcription factor binding sites and promoter regions. Adducts at GC sites may affect the binding of DNA interacting proteins inhibiting the expresssion of genes. Cutts and colleagues[187] observed that doxorubicin induced GC-adducts inhibit the binding of octamer transcription factors to their consensus motifs containing a single GC dinucleotide. The possibility of downregulation of gene transcription has to be taken into consideration for the observed phenomenon of doxorubicin induced NFκB target gene repression.

Another explanation for the observed transcriptional effects is an inhibitory NFκB dimer on the DNA resulting in reduced NFκB target gene expression. In contrast to our results, Bottero et al.[188] showed increased NFκB DNA binding upon two hours incubation with 5 μM doxorubicin associated with IκB-α phosphorylation and degradation arguing for NFκB activation. They did not check for NFκB target gene expression, instead demonstrating increased luciferase reporter gene activity. Andriollo and co-workers[189] found that doxorubicin induced IκB-α degradation and activated NFκB DNA binding in doxorubicin sensitive, but not in resistant GLC_4 human SCLC cell lines, arguing for an NFκB independent resistance mechanism. This publication again is contradictory to Das and White[182], suggesting that NFκB activation by antitumor drugs, including doxorubicin, was specific. The results presented here clearly indicate that incubation with doxorubicin drastically decreased NFκB target gene expression, whereas incubation with other antitumor drugs, e.g. etoposide, increased NFκB target gene expression. These findings are in agreement with Ho et al.[168], indeed proposing activated NFκB signaling upon doxorubicin

treatment, with NFκB competent for DNA binding in vitro. Yet, as previously mentioned, these complexes could not activate NFκB dependent gene transcription, but rather suppressed it. Our observations support these findings, as we could also not detect activation of NFκB target genes. Instead, reduced target gene expression could be shown, arguing for an inhibitory NFκB protein binding to the DNA.

A very recent publication from 2006 by Campbell and colleagues[190] outlined the various NFκB responses to chemotherapeutic drugs. Although a majority of topoisomerase II poisons resulted in NFκB DNA binding, some of them yielded repression and others activation of NFκB target gene transcription. Their data indicate that compounds capable of intercalating into DNA, e.g. doxorubicin, induced NFκB DNA binding together with repression of NFκB target genes, whereas DNA damage caused e.g. by etoposide, resulted in DNA binding and target gene activation. Already in 1997, Zhong and coworkers[169] demonstrated that activation of NFκB by various stimuli, e.g. LPS or IL-1, combined with an inhibition of p65 phosphorylation resulted in NFκB DNA binding but not in transcriptionally active NFκB proteins and target gene expression. In their experiments, Jurkat cells were transfected with an NFκB dependent reporter construct, stimulated with phorbyl myristate (PMA) in the absence or presence of protein kinase A (PKA) inhibitors. PKA was proposed to be a mediator of p65 phosphorylation, which was necessary for activating NFκB's transactivation domain. Incubation of cells with PKA inhibitors and stimulation with PMA led to NFκB DNA binding, but not to the activation of luciferase activity. Manna and colleagues[191] confirmed this theory, testing the compound P(3)-25 inhibiting PKA or other upstream kinases of p65 phosphorylation, resulting in a lack of p65 phosphorylation and transcriptionally inactive NFκB proteins. The possibility of an NFκB that translocates and binds DNA, but lacks p65 phosphorylation, could be addressed in further studies and may shed light on NFκB regulation.

It was proposed that ATM, a nuclear protein kinase, mediates the NFκB response to double strand breaks, arising from topoisomerase poisons or ionizing radiation[144]. Latest studies[147,148] suggest IKK-γ sumoylation, followed by phosphorylation and ubiquitination in the nucleus. Activated ATM and IKK-γ are then translocated into the

cytoplasm. There, IKK-γ integrates into the IKK complex and activates NFκB. Although the data presented are consistent, it is questionable how additional IKK-γ molecules can infiltrate into a stable IKK complex consisting of two IKK core subunits[192] resulting in IKK-$\alpha_{(2)}$-IKK-$\beta_{(2)}$-IKK-$\gamma_{(4)}$[193]. Possibly, IKK-γ modification is accidental and activated ATM by itself facilitates IKK activation. Alternatively, interchange of IKK subunits in the complex could be more likely than previously assumed.

Our data raise the question if phosphorylation differences between cell lines lay within ATM itself, possibly by mutations of phosphorylation and autophosphorylation sites in ATM, or more likely upstream of ATM activation. Lee and Paull[194] reported that the MRN complex, consisting of Mre11, Rad50, and Nbs1, senses DNA breaks. This complex binds to DNA, unwinds the ends, recruits ATM multimers and dissociates them into monomers. Possibly by autophosporylation, ATM becomes activated which eventually leads to NFκB activation. To resolve the question of genetic differences in cell lines, which do or do not activate NFκB upon DNA damaging agents, the short time span of approximately 30 min between drug addition, DNA-damage, and ATM itself has to be studied. One explanation for the observed phenomenon is that A549 and DMS 114 cells increase DNA repair enzymes impeding with double strand breaks. Also imagineable is the possibility that the MRN complex cannot forward the DNA damage signal. For cancer therapy these results may have implications, since inhibition of activated NFκB or avoiding NFκB activation by cytotoxic drugs presumably reduces drug resistance and improves therapy responses.

To address these questions, these assays have to be applied to cell lines from various tumor entities to test NFκB activation by therapeutically used drugs and clearify the mechanism. Treatment with topoisomerase poisons such as etoposide or camptothecin activates NFκB and as a consequence a series of anti-apoptotic target genes. Drug resistance and apoptosis prevention might therefore be decreased by cotreatment with NFκB inhibitors.

5.1.2 Pancreatic cancer

Several lines of evidence indicate the importance of NFκB in pancreatic cancer. Chronic inflammation has been identified as a possible factor in the development of some tumors and in tumor promotion. The link between inflammation and tumor progression is the activation of the transcription factor NFκB by the kinase complex IKK. First of all, Farrow and coworkers[195] summarized that chronic pancreatitis, an inflammation of the pancreas, increases the risk to develop pancreatic cancer by 10 – 20 fold. They demonstrated that inflammatory mediators are expressed in chronic pancreatitis, providing a potential explanation for the higher rate of pancreatic cancer found in patients with chronic pancreatitis. In line with these findings, Greten and colleagues[196] demonstrated in a colitis-associated cancer model that in tumor cells IKK-β contributed to apoptosis suppression by activation of anti-apoptotic genes. Moreover, in myeloid cells IKK-β was involved in the production of inflammatory mediators, which promote tumor growth. Inactivation of NFκB in two different cell types may attenuate the formation of inflammation-associated tumors, such as gastrointestinal cancers.

5.1.2.1 NFκB inducibility by TNF-α

In all pancreatic cancer cell lines tested, NFκB was further inducible with TNF-α. Additionally, increased NFκB activity was present in five of six pancreatic cancer cell lines tested. The causes for increased NFκB activity can be manifold, but are mostly ascribed to upstream activating signals or mutations in IκB-α or NFκB itself. Fujioka and co-workers[133] demonstrated the abolishment of the increased NFκB DNA binding activity by introducing an IκB-α phosphorylation defective mutant into PANC-1 cells, arguing for upstream activating stimuli in pancreatic cancer. In fact, in BxPC-3, PANC-1, DAN-G, and Capan-1 cells NFκB binding activity could be decreased by proteasome inhibition possibly on account of degradation inhibition of IκB-α. Yet, our data is in contrast to Wang and colleagues[38] who demonstrated that all pancreatic cancer cell lines have constitutive NFκB, i.e. not further inducible by TNF-α or TPA. They showed IκB-α mRNA, a target gene of NFκB, which did not increase with any of the two activators. Our experiments demonstrated basal or increased NFκB activity in all six cell lines, which was further inducible by TNF-α as measured in DNA

binding, mRNA expression, and translocation assays. Furthermore, upon TNF-α treatment IκB-α was phosphorylated and degraded, a prerequisite for subsequent NFκB translocation and DNA binding. This strongly argues for an inducible NFκB system. This is consistent with Arlt et al.[186] who showed increased basal NFκB DNA binding activity, which could be inhibited by MG-132, and was further inducible with etoposide or doxorubicin in pancreatic carcinoma cells.

5.1.3 Hematopoietic cancers

Certain lymphomas and multiple myelomas are described to have NFκB constitutively active[163,197,198]. Here, Hodgkin's lymphoma, non-Hodgkin's B-cell lymphoma, and multiple myeloma cell lines were tested. NFκB activation was evaluated in these entities to establish in-house model systems for potential drug candidates interfering with the NFκB pathway.

5.1.3.1 NFκB inducibility by TNF-α

Very strong DNA binding without TNF-α stimulation could be detected in Hodgkin's lymphoma cells and the B-cell lymphoma cell lines DB, OCI-LY-3, and Toledo. Increased DNA binding was observed in the multiple myeloma MM.1S and MM.1RL cells and basal NFκB activation in the B-cell lymphoma cell lines KARPAS-422 and Pfeiffer.

The increase in NFκB DNA binding and target gene expression in the MM.1S cell line upon TNF-α treatment might be due to p65 phosphorylation, which is a further activating stimulus for NFκB DNA binding and target gene expression, shown by Naumann and Scheidereit[199] in HeLa cells. Incubation of B-cell lymphoma and multiple myeloma cells with MG-132, a proteasome inhibitor, did not decrease NFκB target gene expression in B-cell lymphomas, but in multiple myeloma. These results argue for defective IκB-α in B-cell lymphomas, impeding with NFκB binding and inhibition and, taken as a sole indication, would argue against the use of proteasome inhibitors for treating patients with non-Hodgkin's B-cell lymphomas.

The MM.1 cell line was derived from the peripheral blood of a patient with immunoglobulin A myeloma[200]. Through addition of the glucocorticoid dexamethasone, 85 % of the initial cell population was killed over a one-week period. A small population of dexamethasone resistant cells was subcultured continuously exposing cells to dexamethasone, giving rise to the cell line MM.1R[201]. MM.1S, a sensitive clone to dexamethasone gained from the original culture MM.1, was obtained by soft agar technique. MM.1R cells were kept in culture without dexamethasone for an additional 6 months and were then reexposed to the drug. The MM.1R cell line had retained its resistance to the hormone and was renamed MM.1RL. Resistance to glucocorticoids such as dexamethasone is due to downregulation of the glucocorticoid receptor mRNA.

The analysis of the inhibitor status IκB-α revealed peculiar differences: In MM.1S cells, the inhibitor IκB-α was completely absent, whereas in MM.1RL cells, IκB-α could be detected by immunoblotting and degraded upon stimulation with TNF-α. It seems unlikely that the initial cell line MM.1 had no inhibitor IκB-α, which MM.1RL gained through reverse mutation during the resistance process. Also possible is that IκB-α was epigenetically silenced in MM.1 cells, which was reverted during the resistance process. This could be analyzed by ordering the original cell lines MM.1 and testing for the IκB-α status. More feasible is the interpretation that the MM.1RL cell line is composed of a variety of different clones differing in their IκB-α status. By picking a single MM.1S clone, an IκB-α mutant clone was selected. Alternatively, in MM.1S an IκB-α mutation could have changed the epitope of the protein impeding with detection by immunoblotting. The data shown, with reduced NFκB target gene expression in MM.1S and MM.1RL cells upon proteasome inhibition by MG-132, would argue for this. Because in the two multiple myeloma cell lines NFκB activity could be reduced by MG-132, the application of proteasome inhibition could be beneficial for the patient. The proteasome inhibitor PS-341, known as “Velcade” developed by Millennium Pharmaceuticals, is in clinical trials for multiple myeloma targeting the ubiquitin pathway, primarily the degradation of IκB-α, thereby inhibiting NFκB and enhancing sensitivity to other chemotherapeutic drugs[202].

Still, the implications of increased basal NFκB activity, whether in pancreatic, colon, breast or other tumor entities, have to be analyzed. Presumably, NFκB activation is a growth advantage for tumor cells, especially in vivo, which can be reduced by NFκB or IKK inhibition.

5.1.4 IKK inhibitors

Having established the NFκB activation status in lung, pancreatic, and hematopoietic cancer cell lines, the next step was to address whether inhibition of key pathway components would influence cell viability. To this end the effects of IKK inhibition on tumor cells were evaluated. Because it was not possible to chemically transfect blood cells with siRNA e.g. against IKK-β, the following IKK inhibitors were employed: BMS-345541, BAY-11-7085, PS-1145, and SC-514. Interestingly, although NSCLC, Hodgkin's lymphoma, B-cell lymphoma, and multiple myeloma cell lines vary greatly in their NFκB activity, no differences in cytotoxicity could be detected. A549 and H460 non-small cell lung cancer cell lines, both possessing a functional NFκB pathway with basal NFκB activity, did not show differences compared to constitutively activated NFκB cell lines such as Hodgkin's lymphoma, B-cell lymphoma, or multiple myeloma. Also, the EC_{50} for Pfeiffer or KARPAS-422, exhibiting basal NFκB DNA binding activity, was similar to the EC_{50} for DB or HDLM-2, both expressing NFκB constitutively.

Several studies about the efficacy of IKK inhibitors in apoptosis induction in cancer cells are published so far. BMS-345541 is proposed to specifically inhibit IKK-β, inhibiting TNF-α, LPS, and interleukin induced NFκB activity[203]. Mabuchi et al.[204] propose that BAY-11-7085 could decrease paclitaxel induced NFκB activity. Noteworthy, BAY-11-7085 induced apoptosis is NFκB independent as shown by various studies[205,206], pointing to the lack of specificity of this inhibitor.

The IKK inhibitor BMS-345541 was analyzed in greater detail. Therefore, A549 cells were incubated with increasing concentrations of BMS-345541 for up to 72 hours. A very small cytotoxicity window between 1 μM, where no effect on toxicity and NFκB inducibility, and 5 - 10 μM where major effects on cytotoxicity and IKK activity

could be detected, was observed. NFκB nuclear translocation and IKK phosphorylation inhibition could be detected after about 4 – 12 hours of drug incubation, which returned to normal levels with respect of IKK phosphorylation after 72 hours. Possible explanations for this phenomenon could be the upregulation of IKK subunits, degradation of the compound, or the positive selection of cells that did not react to the drug or possibly degrade the drug. In experiments checking for IKK subunit expression, upregulation of IKK-α, IKK-β, and IKK-γ was detected. Quite interesting is the fact that IKK inhibition by BMS-345541 was not detectable in NSCLC cells until drug concentrations were toxic. This was determined in a 72-hours cytotoxicity assay. Both, A549 and H460 cells possess basal NFκB activity, thus inhibition of NFκB per se should theoretically not lead to apoptosis induction. This also favors the view that the chosen drugs are unspecific at concentrations where they inhibit NFκB activation upon TNF-α treatment. The use of a specific IKK-β inhibitor would supposedly have no effect on cell proliferation or apoptosis in NSCLC, as NFκB is not activated in this tumor entity.

5.2 Histone deacetylase inhibitors (HDIs)

Histone deacetylase inhibitors (HDIs) are a new class of anticancer drugs, which hold promise for the treatment of hematologic and solid tumors. Their proposed mechanism of action is the inhibition of histone deacetylation leading to hyperacetylation of histones and the transcription of previously silenced tumor suppressor genes. Additionally, selected proteins can become acetylated, modifying their mode of action in the cell. One protein that was discussed to become acetylated is p65. This acetylation may have an effect on NFκB activity and HDIs might up- or downregulate NFκB activity in the cancerous cell. Analysis of the literature revealed opposing views, whether HDIs suppress or activate NFκB. Some studies report a suppression of NFκB activation[109,150], whereas others show the induction of NFκB[108,207,208]. Regarding the issue of NFκB acetylation, Chen et al.[108,209] observed enhanced TNF-α induced NFκB DNA binding upon one-hour incubation with TSA in 293T cells. This effect was proposed to be due to nuclear p65 being acetylated by p300 resulting in worse binding to newly synthesized IκB-α transporting activated NFκB back to the cytoplasm. Acetylated forms of p65 again are substrate for deacetylation by HDAC3, leading to IκB-α dependent nuclear export of NFκB, allowing the system to regulate NFκB action. Adam and colleagues[210], however, were unable to detect increased p65 acetylation upon TNF-α. Nevertheless, they described potentiation of TNF-α induced NFκB activation caused by 4 hours HDI incubation, associated with a delayed cytoplasmic reappearance of IκB-α. They identified a prolonged activation of the IKK complex upon TNF-α treatment, causing persistent IκB-α phosphorylation and degradation. This resulted in increased target gene expression. Yin and co-workers[150] found HDIs to be inhibitory concerning NFκB activity upon TNF-α stimulation in colon cancer, demonstrating that butyrate negatively influenced proteasomal activity. Catley et al.[211] also detected reduction of the proteasome chymotrypsin-like activity increasing cellular polyubiquitin conjugates. Mitsiades and co-workers[98] utilized microarray analysis on MM.1S, the previously described multiple myeloma cell line exhibiting increased NFκB activity, to detect up- and downregulated genes upon HDI incubation. They showed a reduction of NFκB DNA binding activity, supported by the finding that components of the ubiquitin-proteasome pathway were downregulated. There are several studies

on the influence of HDIs on cytokine release in the mouse model system[212,213]. Leoni and colleagues[214] studied the influence of HDIs measuring the cytokine release in BALB/c mice treated with LPS and SAHA. In this study, SAHA had an inhibitory effect on cytokine release, arguing for a suppression of NFκB activation by SAHA.

5.2.1 Influence of HDIs on NFκB pathway components

Several NSCLC cell lines as well as cell lines from other tumor entities and normal cells were used to test the influence of HDIs on the NFκB pathway. It could be shown, that incubation of NSCLC cells with HDIs reduced the responsiveness of NFκB to TNF-α. This reduction was due to drastic downregulation of TNF-R1. The consequence of reduced TNF-R1 levels were an almost abolished NFκB activation pathway through limited phosphorylation of the kinases IKK-α and IKK-β, yielding delayed and weakened phosphorylation and degradation of the inhibitor IκB-α. This resulted in reduced NFκB translocation and DNA binding, and a suppression of NFκB target gene expression. Cellular viability at the concentrations used was determined for every experiment after 24 hours of HDI incubation and was slightly decreased to ~ 80 % of control cells as measured by resazurin assay.

In this study the suppression of NFκB activation upon TNF-α stimulation in NSCLC was shown. This finding is in contrast with two studies about HDIs in NSCLC from one laboratory, describing the stimulation of NFκB target genes, arguing for synergy between HDIs and NFκB[207,208]. Mayo and colleagues[207] showed a 3-fold increase in expression of the κB luciferase construct and of the NFκB target gene IL-8. An around 5-fold increase in IL-8 expression upon HDI treatment could be confirmed in this work, but this was considered marginal when compared to the 200-fold increase upon TNF-α stimulation. Additionally, IκB-α mRNA, a highly specific target gene, was not increased by the addition of HDI alone. In the study by Mayo and colleagues it was proposed that the transactivating potential of p65 was modulated, as increased IκB-α degradation or DNA binding could not be detected. This suggests an NFκB independent induction of IL-8. Indeed, Ashburner et al.[215] showed that HDAC1 and HDAC2 negatively regulated NFκB dependent gene expression. TSA at 100 nM caused an increase in the basal and TNF-α induced expression of IL-8, caused by

hyperacetylation of the IL-8 promoter. Rundall and co-workers[208] showed that SAHA activated NFκB and proposed that inhibition of NFκB by BAY-11-7085 sensitized NSCLC cells to SAHA induced cell death. As discussed previously, BAY-11-7085 is a highly unspecific NFκB inhibitor, as apoptosis induction occurs prior to NFκB inhibition in non-small cell lung cancer. Possibly BAY-11-7085 interfers with another cellular signaling pathway, thereby sensitizing cells for SAHA induced death.

In HDI treated cells, employing various acetyl-lysine specific antibodies in immunoblotting studies using whole cell extracts as well as in p65 immunoprecipitation assays (data not shown), acetylated p65 could not be detected. Chen et al.[108] showed enhanced TNF-α induced NFκB DNA binding due to p65 acetylation within one hour of HDI incubation. The apparent differences in the results could be explained by the time of incubation with HDIs. The same is true for the work of Adam and coworkers[210], who proposed potentiation of NFκB activation after 4 hours HDI incubation due to prolonged IKK activity upon TNF-α treatment. Kiernan and colleagues[109] claimed that acetylation of p65 upon HDI treatment had an inhibitory effect. They showed that p65 acetylation reduced the binding to κB sequences and promoted binding to IκB-α. This led to nuclear export and the turn-off of NFκB mediated gene expression. They demonstrated that p65 acetylation was a nuclear event. In unstimulated Jurkat cells, where NFκB resided in the cytoplasm, treatment with TSA did not yield detectable p65 acetylation. Cotreatment of TSA with the NFκB activator PMA, on the other hand, led to significant p65 acetylation due to NFκB nuclear localisation. Because the NSCLC cell lines tested in this work have only basal NFκB activity, it is thus unlikely to detect acetylated p65. Nevertheless, it might be possible that in cells possessing constitutive NFκB activity, acetylation of p65 is a regulatory event.

Several reports in the literature[98,150,211] demonstrated a negative influence on proteasome activity in other cell lines than lung. Adam and colleagues[210], however, showed prolonged TNF-α induced NFκB DNA binding activity in the presence of TSA due to increased IKK activity and thus increased proteasomal degradation of IκB-α. Proteasomal activity was analyzed in this study by assaying the potential to degrade the substrate Suc-LLVY-MCA after HDI incubation. MG-132, a potent

proteasome inhibitor, could strongly inhibit the conversion of the substrate Suc-LLVY-MCA by approximately 95 %, whereas HDIs only showed a very weak reduction, which was negligible in comparison to MG-132. Possibly, the different model systems used account for the discrepancy in the cellular output caused by HDIs.

To further investigate the inhibitory effect on NFκB in non-small cell lung cancer, the NFκB subunits p100 and p105 were analyzed. The precursor forms, p100 and p105 possess inhibitory function and can be activated by proteolytic removal of their ankyrin repeats. This process is insensitive to TNF-α stimulation or IKK-β mediated phosphorylation[153,216]. Giardina's lab[150] showed increased p100 expression upon butyrate incubation. In the presented work an increase in p100 and decrease in p105 levels upon HDIs could be demonstrated. Furthermore, in H460 cells increasing concentrations of HDIs enhanced binding of p100 to p65. This effect was amplified upon TNF-α stimulation, suggesting the replacement of IκB-α in its complex with p65 by p100. Short interfering RNA experiments targeting p100 revealed no influence on NFκB inducibility. This made p100 up-regulation an unlikely explanation for the reduced NFκB nuclear translocation upon TNF-α treatment. Still, it might have consequences on NFκB activity as replacement of IκB-α by p100 might decrease stimulation.

Kramer et al.[151] investigated the mechanisms for apoptosis induction and the modulation of signaling pathways by HDIs in melanoma cell lines. There, they found increased export of nuclear NFκB upon HDI incubation. To check this possibility, experiments inhibiting nuclear export by leptomycin B (LMB) were employed. Interestingly, in cells that were not stimulated with TNF-α, LMB itself caused an accumulation of NFκB in the nucleus. Shuttling of inactive NFκB between the nucleus and the cytoplasm has been previously described[217-219]. Miyamoto's group[219] suggested that NFκB/IκB-α complexes shuttle between the cytoplasm and the nucleus. These complexes are unable to bind to DNA and activate target gene transcription. Carlotti[218] proposed the dissociation of NFκB/IκB-α complexes in the cytoplasm, followed by a separated nuclear import of NFκB and IκB-α. Inhibition of nuclear export traps and accumulates NFκB in the nucleus, which can be measured by

translocation assays. In this study, LMB coincubation with SAHA did not show a difference after 2 hours. In TNF-α unstimulated, HDI treated and control cells the same amount of NFκB moved into the nucleus. After 24 hours, control cells showed increased nuclear NFκB in comparison to SAHA treated ones, which might be due to p100 upregulation. As previously discussed, upregulation of p100 possibly could lead to replacement of IκB-α, thereby inhibiting nuclear shuttling of p65. Even in unstimulated cells, p100 complex formation with p65 was increased. This possibly trapped NFκB in the cytoplasm and did not allow shuttling between cytoplasm and nucleus. HDI and TNF-α treated cells showed differences in the amount of translocated NFκB compared to only TNF-α treated control cells. In HDI pretreated cells, TNF-α stimulation led to reduced nuclear accumulation of NFκB in comparison to DMSO control cells. The experiment employing LMB confirmed that the translocation phenotype was due to reduced nuclear translocation rather than to increased export, as regular import would result in equal amounts of nuclear NFκB upon HDI and TNF-α co-treatment in LMB experiments.

Kramer and co-workers[151] found significant upregulation of STAT1 mRNA in melanoma cells sensitive to HDIs. Furthermore, they detected that STAT1 becomes acetylated upon HDI incubation. They demonstrated that constitutive NFκB DNA binding was inhibited in those cell lines incubated with TSA and VPA. A strong interaction between acetylated STAT1 and p65 exerted a negative effect on NFκB activity by exporting NFκB back into the cytoplasm. STAT1 knock-down employing siRNA tools could neither reconstitute NFκB activity upon TNF-α treatment in our model system NSCLC, nor could STAT1 be detected in immunoprecipitated p65. These data highlight the differences in various model systems. Given the vast amount of results on HDIs and NFκB presented in the literature, it is important to carfully define the NFκB activation status, the incubation time with HDIs, and the alterations in the pathway of different cell lines.

Compared to the effects at higher HDI concentrations, slightly increased TNF-R1 mRNA and protein levels were found at lower concentrations in H460 but not in A549 cells. To investigate the significance of these observations, three independent replicates of gene expression measurements were performed. ANOVA followed by

Dunnett's multiple comparison test revealed that the observed increases were not statistically significant for TNF-R1 as well as for two of four NFκB target genes. Although the upregulation of TNF-R1 did not reach significance it cannot be excluded that selected cell lines exhibit receptor upregulation at very low doses. Further studies on other cell lines indicated that in several other NSCLC but not in normal cells, a slight upregulation of TNF-R1 (1.2 – 2 fold) was also observable (data not shown). This could be explained by the co-repressor function of HDACs 1, 2, and 3. Since HDAC1, HDAC2, and HDAC3 have all been reported to inhibit NFκB dependent gene expression[108,215], inhibition of these HDACs by HDIs might lead to an imbalance of activating and deactivating signals, increasing NFκB target genes expression.

Kim and colleagues[157] demonstrated for the first time the selective upregulation of TRAIL-R2 (DR5), a cell surface receptor described to induce apoptosis upon ligand binding, upon HDI treatment. Incubation with sodium butyrate and TRAIL enhanced TRAIL-mediated apoptosis. In this study, upregulation of TRAIL-R2 mRNA with various HDIs could be confirmed in A549 and H460 cells. At concentrations in which TNF-R1 expression was suppressed, TRAIL-R2 expression was increased. Additionally, TNF-R1 downregulation and TRAIL-R2 upregulation was detected in a panel of cell lines. TNF-R1 suppression could be found in all cell lines tested, whereas TRAIL-R2 upregulation could be only detected in a subset of NSCLC and normal cell lines. It appears, that TRAIL-R2 upregulation by HDIs is not a universal process as is the downregulation of TNF-R1.

One would expect that HDI treatment leads to the activation of genes due to histone hyperacetylation. Nevertheless, literature suggests that HDIs influence various genes, which can be either up- or downregulated. An explanation for the downregulation of genes might be the overexpression of signal repressors, influencing the promoter region of e.g. TNF-R1. Also possible is the acetylation of transcription factors that negatively influences their activity. Analysis of the causes for TNF-R1 downregulation on the promoter level would give a great insight into the mechanisms of HDIs and their impact in cancer therapy.

In conclusion, in this study it became obvious that HDIs do not directly affect NFκB in NSCLC, but rather impact the expression of cell surface receptors. By causing reduced expression of TNF-R1, HDIs inhibit NFκB inducibility upon TNF-α stimulation.

6 SUMMARY

The transcription factor nuclear factor kappa-B (NFκB) plays a pivotal role in the immune response but is also involved in cancer development and progression. In unstimulated cells NFκB is kept inactive in the cytoplasm by inhibitor of NFκB (IκB) proteins. Dysregulation of the pathway or activation of NFκB by chemotherapeutic agents may lead to cancer progression or drug resistance.

The NFκB activation status was investigated in human lung cancer, pancreatic cancer, and hematopoietic cancer cell lines. Non-small cell lung cancer (NSCLC) cells possess a functional NFκB pathway exhibiting basal NFκB activity in unstimulated cells and a strong increase upon stimulation. NFκB in small cell lung cancer (SCLC) cells could not be activated by tumor necrosis factor alpha (TNF-α) due to absence of the TNF-receptor 1 (TNF-R1). Other components of the pathway such as the inhibitor of NFκB kinase (IKK) complex or IκB-α were functional in SCLC, as topoisomerase poisons could activate the NFκB pathway in these cells.

Pancreatic cancer cells exhibited increased NFκB activity in unstimulated cells, possibly due to upstream activating signals. On the one hand, NFκB activity could be decreased by proteasome inhibition, yet on the other hand it could be further enhanced by TNF-α treatment.

Investigation of hematopoietic cancer cells demonstrated that Hodgkin's lymphoma, many B-cell lymphoma or multiple myeloma cell lines showed strong NFκB activity in untreated cells. There, cells acquired constitutive NFκB activity possibly due to mutations in the IκB-α protein or activation of upstream signals. Treatment with IKK inhibitors in above mentioned cell lines caused cellular toxicity, but EC_{50} was similar in all cell lines checked, independent of their NFκB activation status.

In lung cancer cells, activation of NFκB by cytotoxic drugs was confined to topoisomerase poisons such as etoposide or camptothecin, but could not be detected in cells incubated with DNA crosslinkers such as cisplatin or alkylating agents such as

mafosfamide. Additionally, activation of NFκB by the topoisomerase poisons was cell line dependent.

Furthermore, the influence of histone deacetylase inhibitors (HDIs) on the NFκB pathway in human NSCLC cell lines was investigated. Incubation of NSCLC cells with HDIs reduced the responsiveness of NFκB to TNF-α. It was shown that this reduction was due to drastic downregulation of TNF-R1 by HDIs. After 24 hours of HDI treatment, mRNA levels of TNF-R1 were lowered to approx. 10%, protein levels and cell surface expression were decreased as well. Substantially, the consequence of this reduced TNF-R1 level was an almost abolished activation of the NFκB pathway by TNF-α through limited phosphorylation of the kinases IKK-α and IKK-β, yielding delayed and weakened phosphorylation and degradation of the inhibitor IκB-α. This resulted in reduced NFκB translocation and DNA binding, and strongly diminished target gene expression upon stimulation. Downregulation of TNF-R1 by HDIs could also be shown for other tumor entities and normal cell lines. In contrast, TRAIL-R2 expression was increased in response to HDIs. The results clearly demonstrate that HDIs do not directly affect NFκB or downstream signaling, but affect receptors at the cell surface due to a reprogramming of gene expression.

7 ZUSAMMENFASSUNG

Der Transkriptionsfaktor NFκB (nuclear factor kappa-B) ist ein zentraler Mediator des Immunsystems. NFκB ist aber auch in der Krebsentstehung und im Fortschreiten der Krebserkrankung involviert. In unstimulierten Zellen liegt NFκB, an seinen Inhibitor IκB gebunden, im Zytoplasma vor. Seine fehlerhafte Regulation sowie die Aktivierung durch Zytostatika kann zur Entstehung von Krebs sowie Resistenzen gegenüber diesen Medikamenten führen.

Eine zentrale Aufgabenstellung in der vorliegenden Arbeit war die Bestimmung des NFκB Aktivierungsstatus in menschlichen Krebszelllinien aus folgenden Geweben: Lunge, Pankreas sowie hämatopoetischen Zellen. Experimente zeigten einen funktionalen NFκB Signalweg im nicht-kleinzelligen Lungenkarzinom (NSCLC), d.h. in der unstimulierten Zelle liegt NFκB inaktiv im Zytoplasma vor und kann durch Stimulation mit TNF-α aktiviert werden und in den Zellkern gelangen. NFκB im kleinzelligen Lungenkarzinom (SCLC) hingegen konnte nicht mit TNF-α aktiviert werden. Als Ursache wurde die fehlende Expression des TNF-R1 nachgewiesen. Andere Proteine im Signalweg wie der IKK-Komplex oder der Inhibitor IκB-α sind in SCLC funktionell, da die Behandlung dieser Zellen mit Topoisomerase Inhibitoren den NFκB Signalweg anschaltete.

Pankreaskrebszelllinien zeigten eine erhöhte NFκB Aktivität im unstimulierten Zustand. Das ist möglicherweise auf NFκB vorgeschaltete aktivierende Signale zurückzuführen. Es wurde gezeigt, dass die verstärkte NFκB Aktivität durch Proteasominhibition reduziert, aber mit TNF-α weiter stimuliert wird.

Blutkrebszelllinien abgeleitet von Hodgkin's Lymphom, verschiedene B-Zell Lymphome sowie im Multiplem Myelom zeigten eine starke NFκB Aktivität im Zellkern auch im nicht stimulierten Zustand. Dies ist vermutlich auf Mutationen im Inhibitor IκB-α oder durch Aktivierung von vorgeschalteten Signalen zurückzuführen. Die Toxizität von IKK Inhibitoren zeigte sich in allen Zelllinien, jedoch lag der EC_{50} unabhängig vom NFκB Aktivierungszustandes im gleichen Bereich.

Eine Aktivierung von NFκB im Lungenkarzinom durch Zytostatika konnte mit Topoisomerase Inhibitoren wie Etoposid und Camptothecin, aber nicht mit DNA vernetzenden Medikamenten wie Cisplatin oder alkylierenden Substanzen wie Mafosfamid detektiert werden. Der beobachtete NFκB aktivierende Effekt war zudem Zelltyp abhängig.

Der letzte Teil dieser Arbeit bestand in der Analyse von Histondeacetylase Inhibitoren (HDI) und deren Einfluss auf die NFκB Aktivität in menschlichen NSCLC Zelllinien. Es konnte gezeigt werden, dass HDI die NFκB Aktivität nach TNF-α Stimulation drastisch reduzierten. Als Ursache wurde eine Reduktion des TNF-R1 auf RNA Ebene auf etwa 10 % innerhalb von 24 Stunden Behandlung der Zellen mit HDI nachgewiesen. Die Proteinexpression sowie die Expression des Rezeptors an der Zelloberfläche wurden ebenfalls stark herabgesetzt. Dies hatte ein verringertes Ansprechen von NFκB auf TNF-α zur Folge, das sich äußerte in: verringerte Phosphorylierung der aktivierenden Kinasen IKK-α und IKK-β, Reduktion der Inhibitor Phosphorylierung sowie des Abbaus, verringerte Translokation von NFκB in den Zellkern verbunden mit einer Reduktion der DNA-Bindung und verminderte Expression NFκB abhängiger Gene. Diese Herabregulation des TNF-R1 konnte nicht nur im NSCLC nachgewiesen werden, sondern auch in anderen Tumor- und Normalzelllinien. Die Reduktion der TNF-R1 Expression wurde von einer Aktivierung der TRAIL-R2 Expression begleitet. Diese Ergebnisse belegen, dass HDI in den NFκB Signalweg nicht direkt eingreifen, sondern durch eine Veränderung der Genexpression Zelloberflächenrezeptoren beeinflussen.

8 REFERENCES

1. World Health Organization. The World Health Report 2002: Reducing Risks, Promoting Healthy Life. 2002.

2. Olsen,J.H. *et al.* Summary of avoidable cancers in the Nordic countries. *APMIS Suppl* **76**, 141-146 (1997).

3. Ozlu,T. & Bulbul,Y. Smoking and lung cancer. *Tuberk. Toraks.* **53**, 200-209 (2005).

4. Baylin,S.B. & Ohm,J.E. Epigenetic gene silencing in cancer - a mechanism for early oncogenic pathway addiction? *Nat. Rev. Cancer* **6**, 107-116 (2006).

5. Balmain,A. Cancer genetics: from Boveri and Mendel to microarrays. *Nat. Rev. Cancer* **1**, 77-82 (2001).

6. de Klein,A. *et al.* A cellular oncogene is translocated to the Philadelphia chromosome in chronic myelocytic leukaemia. *Nature* **300**, 765-767 (1982).

7. Hanahan,D. & Weinberg,R.A. The hallmarks of cancer. *Cell* **100**, 57-70 (2000).

8. Jordan,A., Hadfield,J.A., Lawrence,N.J. & McGown,A.T. Tubulin as a target for anticancer drugs: agents which interact with the mitotic spindle. *Med. Res. Rev.* **18**, 259-296 (1998).

9. Chatelut,E., Delord,J.P. & Canal,P. Toxicity patterns of cytotoxic drugs. *Invest New Drugs* **21**, 141-148 (2003).

10. Heinlein,C.A. & Chang,C. Androgen receptor in prostate cancer. *Endocr. Rev.* **25**, 276-308 (2004).

11. Ropero,S. *et al.* Trastuzumab plus tamoxifen: anti-proliferative and molecular interactions in breast carcinoma. *Breast Cancer Res. Treat.* **86**, 125-137 (2004).

12. Johnston,S.R. & Dowsett,M. Aromatase inhibitors for breast cancer: lessons from the laboratory. *Nat. Rev. Cancer* **3**, 821-831 (2003).

13. Booy,E.P. *et al.* Monoclonal and bispecific antibodies as novel therapeutics. *Arch. Immunol. Ther. Exp. (Warsz.)* **54**, 85-101 (2006).

14. Kumar,C.C. & Madison,V. Drugs targeted against protein kinases. *Expert. Opin. Emerg. Drugs* **6**, 303-315 (2001).

15. Manley,P.W., Cowan-Jacob,S.W. & Mestan,J. Advances in the structural biology, design and clinical development of Bcr-Abl kinase inhibitors for the treatment of chronic myeloid leukaemia. *Biochim. Biophys. Acta* **1754**, 3-13 (2005).

16. Pandya,N.M., Dhalla,N.S. & Santani,D.D. Angiogenesis-a new target for future therapy. *Vascul. Pharmacol.* **44**, 265-274 (2006).

17. Pinkas,J. & Teicher,B.A. TGF-beta in cancer and as a therapeutic target. *Biochem. Pharmacol.* (2006).

18. Folgueras,A.R., Pendas,A.M., Sanchez,L.M. & Lopez-Otin,C. Matrix metalloproteinases in cancer: from new functions to improved inhibition strategies. *Int. J. Dev. Biol.* **48**, 411-424 (2004).

19. Mizejewski,G.J. Role of integrins in cancer: survey of expression patterns. *Proc. Soc. Exp. Biol. Med.* **222**, 124-138 (1999).

20. Milas,L. *et al.* CpG oligodeoxynucleotide enhances tumor response to radiation. *Cancer Res.* **64**, 5074-5077 (2004).

21. Schetter,C. & Vollmer,J. Toll-like receptors involved in the response to microbial pathogens: development of agonists for toll-like receptor 9. *Curr. Opin. Drug Discov. Devel.* **7**, 204-210 (2004).

22. Vose,J. Personalized immunotherapy for the treatment of non-Hodgkin lymphoma: a promising approach. *Clin. Adv. Hematol. Oncol.* **3**, 923-932 (2005).

23. Dean,M., Rzhetsky,A. & Allikmets,R. The human ATP-binding cassette (ABC) transporter superfamily. *Genome Res.* **11**, 1156-1166 (2001).

24. Baker,E.K., Johnstone,R.W., Zalcberg,J.R. & El Osta,A. Epigenetic changes to the MDR1 locus in response to chemotherapeutic drugs. *Oncogene* **24**, 8061-8075 (2005).

25. Ambudkar,S.V. *et al.* Biochemical, cellular, and pharmacological aspects of the multidrug transporter. *Annu. Rev. Pharmacol. Toxicol.* **39**, 361-398 (1999).

26. Shen,D.W., Goldenberg,S., Pastan,I. & Gottesman,M.M. Decreased accumulation of [14C]carboplatin in human cisplatin-resistant cells results from reduced energy-dependent uptake. *J. Cell Physiol* **183**, 108-116 (2000).

27. Liang,X.J., Mukherjee,S., Shen,D.W., Maxfield,F.R. & Gottesman,M.M. Endocytic recycling compartments altered in cisplatin-resistant cancer cells. *Cancer Res.* **66**, 2346-2353 (2006).

28. Schuetz,E.G., Beck,W.T. & Schuetz,J.D. Modulators and substrates of P-glycoprotein and cytochrome P4503A coordinately up-regulate these proteins in human colon carcinoma cells. *Mol. Pharmacol.* **49**, 311-318 (1996).

29. Schuetz,E.G. Induction of cytochromes P450. *Curr. Drug Metab* **2**, 139-147 (2001).

30. Rochat,B. Role of cytochrome P450 activity in the fate of anticancer agents and in drug resistance: focus on tamoxifen, paclitaxel and imatinib metabolism. *Clin. Pharmacokinet.* **44**, 349-366 (2005).

31. Liu,Y.Y., Han,T.Y., Giuliano,A.E. & Cabot,M.C. Ceramide glycosylation potentiates cellular multidrug resistance. *FASEB J.* **15**, 719-730 (2001).

32. Zhou,Y., Eppenberger-Castori,S., Eppenberger,U. & Benz,C.C. The NFkappaB pathway and endocrine-resistant breast cancer. *Endocr. Relat Cancer* **12 Suppl 1**, S37-S46 (2005).

33. Wilhelmsen,K.C., Eggleton,K. & Temin,H.M. Nucleic acid sequences of the oncogene v-rel in reticuloendotheliosis virus strain T and its cellular homolog, the proto-oncogene c-rel. *J. Virol.* **52**, 172-182 (1984).

34. Bose,H.R., Jr. The Rel family: models for transcriptional regulation and oncogenic transformation. *Biochim. Biophys. Acta* **1114**, 1-17 (1992).

35. Barth,C.F., Ewert,D.L., Olson,W.C. & Humphries,E.H. Reticuloendotheliosis virus REV-T(REV-A)-induced neoplasia: development of tumors within the T-lymphoid and myeloid lineages. *J. Virol.* **64**, 6054-6062 (1990).

36. Nakshatri,H., Bhat-Nakshatri,P., Martin,D.A., Goulet,R.J., Jr. & Sledge,G.W., Jr. Constitutive activation of NF-kappaB during progression of breast cancer to hormone-independent growth. *Mol. Cell Biol.* **17**, 3629-3639 (1997).

37. Palayoor,S.T., Youmell,M.Y., Calderwood,S.K., Coleman,C.N. & Price,B.D. Constitutive activation of IkappaB kinase alpha and NF-kappaB in prostate cancer cells is inhibited by ibuprofen. *Oncogene* **18**, 7389-7394 (1999).

38. Wang,W. *et al.* The nuclear factor-kappa B RelA transcription factor is constitutively activated in human pancreatic adenocarcinoma cells. *Clin. Cancer Res.* **5**, 119-127 (1999).

39. Lind,D.S. *et al.* Nuclear factor-kappa B is upregulated in colorectal cancer. *Surgery* **130**, 363-369 (2001).

40. Ni,H. *et al.* Analysis of expression of nuclear factor kappa B (NF-kappa B) in multiple myeloma: downregulation of NF-kappa B induces apoptosis. *Br. J. Haematol.* **115**, 279-286 (2001).

41. Wood,K.M., Roff,M. & Hay,R.T. Defective IkappaBalpha in Hodgkin cell lines with constitutively active NF-kappaB. *Oncogene* **16**, 2131-2139 (1998).

42. Rayet,B. & Gelinas,C. Aberrant rel/nfkb genes and activity in human cancer. *Oncogene* **18**, 6938-6947 (1999).

43. Houldsworth,J. *et al.* REL proto-oncogene is frequently amplified in extranodal diffuse large cell lymphoma. *Blood* **87**, 25-29 (1996).

44. Thakur,S. *et al.* Rearrangement and altered expression of the NFKB-2 gene in human cutaneous T-lymphoma cells. *Oncogene* **9**, 2335-2344 (1994).

45. Neri,A. *et al.* B cell lymphoma-associated chromosomal translocation involves candidate oncogene lyt-10, homologous to NF-kappa B p50. *Cell* **67**, 1075-1087 (1991).

46. Migliazza,A. *et al.* Heterogeneous chromosomal aberrations generate 3' truncations of the NFKB2/lyt-10 gene in lymphoid malignancies. *Blood* **84**, 3850-3860 (1994).

47. Chang,C.C., Zhang,J., Lombardi,L., Neri,A. & Dalla-Favera,R. Rearranged NFKB-2 genes in lymphoid neoplasms code for constitutively active nuclear transactivators. *Mol. Cell Biol.* **15**, 5180-5187 (1995).

48. Krappmann,D. *et al.* Molecular mechanisms of constitutive NF-kappaB/Rel activation in Hodgkin/Reed-Sternberg cells. *Oncogene* **18**, 943-953 (1999).

49. O'Connell,M.A., Cleere,R., Long,A., O'Neill,L.A. & Kelleher,D. Cellular proliferation and activation of NF kappa B are induced by autocrine production of tumor necrosis factor alpha in the human T lymphoma line HuT 78. *J. Biol. Chem.* **270**, 7399-7404 (1995).

50. Skinnider,B.F. & Mak,T.W. The role of cytokines in classical Hodgkin lymphoma. *Blood* **99**, 4283-4297 (2002).

51. Lu,T., Sathe,S.S., Swiatkowski,S.M., Hampole,C.V. & Stark,G.R. Secretion of cytokines and growth factors as a general cause of constitutive NFkappaB activation in cancer. *Oncogene* **23**, 2138-2145 (2004).

52. Kordes,U., Krappmann,D., Heissmeyer,V., Ludwig,W.D. & Scheidereit,C. Transcription factor NF-kappaB is constitutively activated in acute lymphoblastic leukemia cells. *Leukemia* **14**, 399-402 (2000).

53. Brach,M.A. *et al.* Ionizing radiation induces expression and binding activity of the nuclear factor kappa B. *J. Clin. Invest* **88**, 691-695 (1991).

54. Mohan,N. & Meltz,M.L. Induction of nuclear factor kappa B after low-dose ionizing radiation involves a reactive oxygen intermediate signaling pathway. *Radiat. Res.* **140**, 97-104 (1994).

55. Rithidech,K.N., Tungjai,M., Arbab,E. & Simon,S.R. Activation of NF-kappaB in bone marrow cells of BALB/cJ mice following exposure in vivo to low doses of (137)Cs gamma-rays. *Radiat. Environ. Biophys.* **44**, 139-143 (2005).

56. Piret,B. & Piette,J. Topoisomerase poisons activate the transcription factor NF-kappaB in ACH-2 and CEM cells. *Nucleic Acids Res.* **24**, 4242-4248 (1996).

57. Sen,R. & Baltimore,D. Inducibility of kappa immunoglobulin enhancer-binding protein Nf-kappa B by a posttranslational mechanism. *Cell* **47**, 921-928 (1986).

58. Guttridge,D.C., Albanese,C., Reuther,J.Y., Pestell,R.G. & Baldwin,A.S., Jr. NF-kappaB controls cell growth and differentiation through transcriptional regulation of cyclin D1. *Mol. Cell Biol.* **19**, 5785-5799 (1999).

59. Gerondakis,S. *et al.* Rel-deficient T cells exhibit defects in production of interleukin 3 and granulocyte-macrophage colony-stimulating factor. *Proc. Natl. Acad. Sci. U. S. A* **93**, 3405-3409 (1996).

60. Van Antwerp,D.J., Martin,S.J., Kafri,T., Green,D.R. & Verma,I.M. Suppression of TNF-alpha-induced apoptosis by NF-kappaB. *Science* **274**, 787-789 (1996).

61. Fan,C.M. & Maniatis,T. Generation of p50 subunit of NF-kappa B by processing of p105 through an ATP-dependent pathway. *Nature* **354**, 395-398 (1991).

62. Ghosh,S., May,M.J. & Kopp,E.B. NF-kappa B and Rel proteins: evolutionarily conserved mediators of immune responses. *Annu. Rev. Immunol.* **16**, 225-260 (1998).

63. Baeuerle,P.A. & Baltimore,D. I kappa B: a specific inhibitor of the NF-kappa B transcription factor. *Science* **242**, 540-546 (1988).

64. Whiteside,S.T. & Israel,A. I kappa B proteins: structure, function and regulation. *Semin. Cancer Biol.* **8**, 75-82 (1997).

65. DiDonato,J.A., Hayakawa,M., Rothwarf,D.M., Zandi,E. & Karin,M. A cytokine-responsive IkappaB kinase that activates the transcription factor NF-kappaB. *Nature* **388**, 548-554 (1997).

66. Mercurio,F. *et al.* IKK-1 and IKK-2: cytokine-activated IkappaB kinases essential for NF-kappaB activation. *Science* **278**, 860-866 (1997).

67. Rothwarf,D.M., Zandi,E., Natoli,G. & Karin,M. IKK-gamma is an essential regulatory subunit of the IkappaB kinase complex. *Nature* **395**, 297-300 (1998).

68. Delhase,M., Hayakawa,M., Chen,Y. & Karin,M. Positive and negative regulation of IkappaB kinase activity through IKKbeta subunit phosphorylation. *Science* **284**, 309-313 (1999).

69. Traenckner,E.B. *et al.* Phosphorylation of human I kappa B-alpha on serines 32 and 36 controls I kappa B-alpha proteolysis and NF-kappa B activation in response to diverse stimuli. *EMBO J.* **14**, 2876-2883 (1995).

70. Karin,M. & Ben Neriah,Y. Phosphorylation meets ubiquitination: the control of NF-[kappa]B activity. *Annu. Rev. Immunol.* **18**, 621-663 (2000).

71. Yaron,A. *et al.* Identification of the receptor component of the IkappaBalpha-ubiquitin ligase. *Nature* **396**, 590-594 (1998).

72. Siebenlist,U., Franzoso,G. & Brown,K. Structure, regulation and function of NF-kappa B. *Annu. Rev. Cell Biol.* **10**, 405-455 (1994).

73. Baeuerle,P.A. & Henkel,T. Function and activation of NF-kappa B in the immune system. *Annu. Rev. Immunol.* **12**, 141-179 (1994).

74. Baldwin,A.S. Control of oncogenesis and cancer therapy resistance by the transcription factor NF-kappaB. *J. Clin. Invest* **107**, 241-246 (2001).

75. Senftleben,U. *et al.* Activation by IKKalpha of a second, evolutionary conserved, NF-kappa B signaling pathway. *Science* **293**, 1495-1499 (2001).

76. Carswell,E.A. *et al.* An endotoxin-induced serum factor that causes necrosis of tumors. *Proc. Natl. Acad. Sci. U. S. A* **72**, 3666-3670 (1975).

77. Kull,F.C., Jr., Jacobs,S. & Cuatrecasas,P. Cellular receptor for 125I-labeled tumor necrosis factor: specific binding, affinity labeling, and relationship to sensitivity. *Proc. Natl. Acad. Sci. U. S. A* **82**, 5756-5760 (1985).

78. Ryffel,B. & Mihatsch,M.J. TNF receptor distribution in human tissues. *Int. Rev. Exp. Pathol.* **34 Pt B**, 149-156 (1993).

79. Chen,G. & Goeddel,D.V. TNF-R1 signaling: a beautiful pathway. *Science* **296**, 1634-1635 (2002).

80. Micheau,O. & Tschopp,J. Induction of TNF receptor I-mediated apoptosis via two sequential signaling complexes. *Cell* **114**, 181-190 (2003).

81. Kucharczak,J., Simmons,M.J., Fan,Y. & Gelinas,C. To be, or not to be: NF-kappaB is the answer--role of Rel/NF-kappaB in the regulation of apoptosis. *Oncogene* **22**, 8961-8982 (2003).

82. Takeda,K. *et al.* Limb and skin abnormalities in mice lacking IKKalpha. *Science* **284**, 313-316 (1999).

83. Tanaka,M. *et al.* Embryonic lethality, liver degeneration, and impaired NF-kappa B activation in IKK-beta-deficient mice. *Immunity.* **10**, 421-429 (1999).

84. Li,Q., Van Antwerp,D., Mercurio,F., Lee,K.F. & Verma,I.M. Severe liver degeneration in mice lacking the IkappaB kinase 2 gene. *Science* **284**, 321-325 (1999).

85. Li,Z.W. *et al.* The IKKbeta subunit of IkappaB kinase (IKK) is essential for nuclear factor kappaB activation and prevention of apoptosis. *J. Exp. Med.* **189**, 1839-1845 (1999).

86. Beg,A.A., Sha,W.C., Bronson,R.T., Ghosh,S. & Baltimore,D. Embryonic lethality and liver degeneration in mice lacking the RelA component of NF-kappa B. *Nature* **376**, 167-170 (1995).

87. Horwitz,B.H., Scott,M.L., Cherry,S.R., Bronson,R.T. & Baltimore,D. Failure of lymphopoiesis after adoptive transfer of NF-kappaB-deficient fetal liver cells. *Immunity.* **6**, 765-772 (1997).

88. Hu,Y. *et al.* Abnormal morphogenesis but intact IKK activation in mice lacking the IKKalpha subunit of IkappaB kinase. *Science* **284**, 316-320 (1999).

89. Luger,K., Mader,A.W., Richmond,R.K., Sargent,D.F. & Richmond,T.J. Crystal structure of the nucleosome core particle at 2.8 A resolution. *Nature* **389**, 251-260 (1997).

90. Shiio,Y. & Eisenman,R.N. Histone sumoylation is associated with transcriptional repression. *Proc. Natl. Acad. Sci. U. S. A* **100**, 13225-13230 (2003).

91. Hansen,J.C., Tse,C. & Wolffe,A.P. Structure and function of the core histone N-termini: more than meets the eye. *Biochemistry* **37**, 17637-17641 (1998).

92. Cheung,P., Allis,C.D. & Sassone-Corsi,P. Signaling to chromatin through histone modifications. *Cell* **103**, 263-271 (2000).

93. Thorne,A.W., Kmiciek,D., Mitchelson,K., Sautiere,P. & Crane-Robinson,C. Patterns of histone acetylation. *Eur. J. Biochem.* **193**, 701-713 (1990).

94. ALLFREY,V.G., FAULKNER,R. & MIRSKY,A.E. ACETYLATION AND METHYLATION OF HISTONES AND THEIR POSSIBLE ROLE IN THE REGULATION OF RNA SYNTHESIS. *Proc. Natl. Acad. Sci. U. S. A* **51**, 786-794 (1964).

95. Sobulo,O.M. *et al.* MLL is fused to CBP, a histone acetyltransferase, in therapy-related acute myeloid leukemia with a t(11;16)(q23;p13.3). *Proc. Natl. Acad. Sci. U. S. A* **94**, 8732-8737 (1997).

96. Muraoka,M. *et al.* p300 gene alterations in colorectal and gastric carcinomas. *Oncogene* **12**, 1565-1569 (1996).

97. Magnaghi-Jaulin,L. *et al.* Retinoblastoma protein represses transcription by recruiting a histone deacetylase. *Nature* **391**, 601-605 (1998).

98. Mitsiades,C.S. *et al.* Transcriptional signature of histone deacetylase inhibition in multiple myeloma: biological and clinical implications. *Proc. Natl. Acad. Sci. U. S. A* **101**, 540-545 (2004).

99. Gray,S.G. & Ekstrom,T.J. The human histone deacetylase family. *Exp. Cell Res.* **262**, 75-83 (2001).

100. de Ruijter,A.J., van Gennip,A.H., Caron,H.N., Kemp,S. & van Kuilenburg,A.B. Histone deacetylases (HDACs): characterization of the classical HDAC family. *Biochem. J.* **370**, 737-749 (2003).

101. Gregoretti,I.V., Lee,Y.M. & Goodson,H.V. Molecular evolution of the histone deacetylase family: functional implications of phylogenetic analysis. *J. Mol. Biol.* **338**, 17-31 (2004).

102. Finnin,M.S. *et al.* Structures of a histone deacetylase homologue bound to the TSA and SAHA inhibitors. *Nature* **401**, 188-193 (1999).

103. Imai,S., Armstrong,C.M., Kaeberlein,M. & Guarente,L. Transcriptional silencing and longevity protein Sir2 is an NAD-dependent histone deacetylase. *Nature* **403**, 795-800 (2000).

104. Johnstone,R.W. Histone-deacetylase inhibitors: novel drugs for the treatment of cancer. *Nat. Rev. Drug Discov.* **1**, 287-299 (2002).

105. Van Lint,C., Emiliani,S. & Verdin,E. The expression of a small fraction of cellular genes is changed in response to histone hyperacetylation. *Gene Expr.* **5**, 245-253 (1996).

106. Glaser,K.B. *et al.* Gene expression profiling of multiple histone deacetylase (HDAC) inhibitors: defining a common gene set produced by HDAC inhibition in T24 and MDA carcinoma cell lines. *Mol. Cancer Ther.* **2**, 151-163 (2003).

107. Minucci,S. & Pelicci,P.G. Histone deacetylase inhibitors and the promise of epigenetic (and more) treatments for cancer. *Nat. Rev. Cancer. 2006. Jan. ;6. (1):38. -51.* **6**, 38-51 (2006).

108. Chen,L., Fischle,W., Verdin,E. & Greene,W.C. Duration of nuclear NF-kappaB action regulated by reversible acetylation. *Science* **293**, 1653-1657 (2001).

109. Kiernan,R. *et al.* Post-activation turn-off of NF-kappa B-dependent transcription is regulated by acetylation of p65. *J. Biol. Chem.* **278**, 2758-2766 (2003).

110. Hu,J. & Colburn,N.H. Histone deacetylase inhibition down-regulates cyclin D1 transcription by inhibiting nuclear factor-kappaB/p65 DNA binding. *Mol. Cancer Res.* **3**, 100-109 (2005).

111. Drummond,D.C. *et al.* Clinical development of histone deacetylase inhibitors as anticancer agents. *Annu. Rev. Pharmacol. Toxicol.* **45**, 495-528 (2005).

112. Rosato,R.R., Wang,Z., Gopalkrishnan,R.V., Fisher,P.B. & Grant,S. Evidence of a functional role for the cyclin-dependent kinase-inhibitor p21WAF1/CIP1/MDA6 in promoting differentiation and preventing mitochondrial dysfunction and apoptosis induced by sodium butyrate in human myelomonocytic leukemia cells (U937). *Int. J. Oncol.* **19**, 181-191 (2001).

113. Ruefli,A.A. *et al.* The histone deacetylase inhibitor and chemotherapeutic agent suberoylanilide hydroxamic acid (SAHA) induces a cell-death pathway characterized by cleavage of Bid and production of reactive oxygen species. *Proc. Natl. Acad. Sci. U. S. A* **98**, 10833-10838 (2001).

114. Strait,K.A. *et al.* Histone deacetylase inhibitors induce G2-checkpoint arrest and apoptosis in cisplatinum-resistant ovarian cancer cells associated with overexpression of the Bcl-2-related protein Bad. *Mol. Cancer Ther.* **4**, 603-611 (2005).

115. Peart,M.J. *et al.* Novel mechanisms of apoptosis induced by histone deacetylase inhibitors. *Cancer Res.* **63**, 4460-4471 (2003).

116. Magner,W.J. *et al.* Activation of MHC class I, II, and CD40 gene expression by histone deacetylase inhibitors. *J. Immunol.* **165**, 7017-7024 (2000).

117. Maeda,T., Towatari,M., Kosugi,H. & Saito,H. Up-regulation of costimulatory/adhesion molecules by histone deacetylase inhibitors in acute myeloid leukemia cells. *Blood* **96**, 3847-3856 (2000).

118. Kim,M.S. *et al.* Histone deacetylases induce angiogenesis by negative regulation of tumor suppressor genes. *Nat. Med.* **7**, 437-443 (2001).

119. Gore,S.D. & Carducci,M.A. Modifying histones to tame cancer: clinical development of sodium phenylbutyrate and other histone deacetylase inhibitors. *Expert. Opin. Investig. Drugs* **9**, 2923-2934 (2000).

120. Richon,V.M. *et al.* Second generation hybrid polar compounds are potent inducers of transformed cell differentiation. *Proc. Natl. Acad. Sci. U. S. A* **93**, 5705-5708 (1996).

121. Izzo,J.G. *et al.* Association of activated transcription factor nuclear factor kappab with chemoradiation resistance and poor outcome in esophageal carcinoma. *J. Clin. Oncol.* **24**, 748-754 (2006).

122. Zhang,P.L. *et al.* Overexpression of phosphorylated nuclear factor-kappa B in tonsillar squamous cell carcinoma and high-grade dysplasia is associated with poor prognosis. *Mod. Pathol.* **18**, 924-932 (2005).

123. Kunsch,C. & Rosen,C.A. NF-kappa B subunit-specific regulation of the interleukin-8 promoter. *Mol. Cell Biol.* **13**, 6137-6146 (1993).

124. de Martin,R. *et al.* Cytokine-inducible expression in endothelial cells of an I kappa B alpha-like gene is regulated by NF kappa B. *EMBO J.* **12**, 2773-2779 (1993).

125. Sun,S.C., Ganchi,P.A., Ballard,D.W. & Greene,W.C. NF-kappa B controls expression of inhibitor I kappa B alpha: evidence for an inducible autoregulatory pathway. *Science* **259**, 1912-1915 (1993).

126. Kreuz,S., Siegmund,D., Scheurich,P. & Wajant,H. NF-kappaB inducers upregulate cFLIP, a cycloheximide-sensitive inhibitor of death receptor signaling. *Mol. Cell Biol.* **21**, 3964-3973 (2001).

127. Lee,H.H., Dadgostar,H., Cheng,Q., Shu,J. & Cheng,G. NF-kappaB-mediated up-regulation of Bcl-x and Bfl-1/A1 is required for CD40 survival signaling in B lymphocytes. *Proc. Natl. Acad. Sci. U. S. A* **96**, 9136-9141 (1999).

128. Chen,F. *et al.* Involvement of 5'-flanking kappaB-like sites within bcl-x gene in silica-induced Bcl-x expression. *J. Biol. Chem.* **274**, 35591-35595 (1999).

129. Chilov,D. *et al.* Genomic organization of human and mouse genes for vascular endothelial growth factor C. *J. Biol. Chem.* **272**, 25176-25183 (1997).

130. van der Heijden,M.S. *et al.* In vivo therapeutic responses contingent on Fanconi anemia/BRCA2 status of the tumor. *Clin. Cancer Res.* **11**, 7508-7515 (2005).

131. Jimeno,A. & Hidalgo,M. Molecular biomarkers: their increasing role in the diagnosis, characterization, and therapy guidance in pancreatic cancer. *Mol. Cancer Ther.* **5**, 787-796 (2006).

132. Fujioka,S. *et al.* Function of nuclear factor kappaB in pancreatic cancer metastasis. *Clin. Cancer Res.* **9**, 346-354 (2003).

133. Fujioka,S. *et al.* Inhibition of constitutive NF-kappa B activity by I kappa B alpha M suppresses tumorigenesis. *Oncogene* **22**, 1365-1370 (2003).

134. Dewan,M.Z. *et al.* Hodgkin's lymphoma cells are efficiently engrafted and tumor marker CD30 is expressed with constitutive nuclear factor-kappaB activity in unconditioned NOD/SCID/gammac(null) mice. *Cancer Sci.* **96**, 466-473 (2005).

135. Davis,R.E., Brown,K.D., Siebenlist,U. & Staudt,L.M. Constitutive nuclear factor kappaB activity is required for survival of activated B cell-like diffuse large B cell lymphoma cells. *J. Exp. Med.* **194**, 1861-1874 (2001).

136. Karin,M., Yamamoto,Y. & Wang,Q.M. The IKK NF-kappa B system: a treasure trove for drug development. *Nat. Rev. Drug Discov.* **3**, 17-26 (2004).

137. Pierce,J.W. *et al.* Novel inhibitors of cytokine-induced IkappaBalpha phosphorylation and endothelial cell adhesion molecule expression show anti-inflammatory effects in vivo. *J. Biol. Chem.* **272**, 21096-21103 (1997).

138. Bromberg,K.D., Burgin,A.B. & Osheroff,N. A two-drug model for etoposide action against human topoisomerase IIalpha. *J. Biol. Chem.* **278**, 7406-7412 (2003).

139. Liu,L.F. *et al.* Mechanism of action of camptothecin. *Ann. N. Y. Acad. Sci.* **922**, 1-10 (2000).

140. Thomas,C.J., Rahier,N.J. & Hecht,S.M. Camptothecin: current perspectives. *Bioorg. Med. Chem.* **12**, 1585-1604 (2004).

141. Gewirtz,D.A. A critical evaluation of the mechanisms of action proposed for the antitumor effects of the anthracycline antibiotics adriamycin and daunorubicin. *Biochem. Pharmacol.* **57**, 727-741 (1999).

142. Fichtinger-Schepman,A.M., van der Veer,J.L., den Hartog,J.H., Lohman,P.H. & Reedijk,J. Adducts of the antitumor drug cis-diamminedichloroplatinum(II) with DNA: formation, identification, and quantitation. *Biochemistry* **24**, 707-713 (1985).

143. Jung,M., Zhang,Y., Lee,S. & Dritschilo,A. Correction of radiation sensitivity in ataxia telangiectasia cells by a truncated I kappa B-alpha. *Science* **268**, 1619-1621 (1995).

144. Lee,S.J., Dimtchev,A., Lavin,M.F., Dritschilo,A. & Jung,M. A novel ionizing radiation-induced signaling pathway that activates the transcription factor NF-kappaB. *Oncogene* **17**, 1821-1826 (1998).

145. Piret,B., Schoonbroodt,S. & Piette,J. The ATM protein is required for sustained activation of NF-kappaB following DNA damage. *Oncogene* **18**, 2261-2271 (1999).

146. Li,N. *et al.* ATM is required for IkappaB kinase (IKKk) activation in response to DNA double strand breaks. *J. Biol. Chem.* **276**, 8898-8903 (2001).

147. Huang,T.T., Wuerzberger-Davis,S.M., Wu,Z.H. & Miyamoto,S. Sequential modification of NEMO/IKKgamma by SUMO-1 and ubiquitin mediates NF-kappaB activation by genotoxic stress. *Cell* **115**, 565-576 (2003).

148. Wu,Z.H., Shi,Y., Tibbetts,R.S. & Miyamoto,S. Molecular linkage between the kinase ATM and NF-kappaB signaling in response to genotoxic stimuli. *Science* **311**, 1141-1146 (2006).

149. Kozlov,S.V. *et al.* Involvement of novel autophosphorylation sites in ATM activation. *EMBO J.* (2006).

150. Yin,L., Laevsky,G. & Giardina,C. Butyrate suppression of colonocyte NF-kappa B activation and cellular proteasome activity. *J. Biol. Chem.* **276**, 44641-44646 (2001).

151. Kramer,O.H. *et al.* Acetylation of Stat1 modulates NF-kappaB activity. *Genes Dev.* **20**, 473-485 (2006).

152. Kudo,N. *et al.* Leptomycin B inhibition of signal-mediated nuclear export by direct binding to CRM1. *Exp. Cell Res.* **242**, 540-547 (1998).

153. Sun,S.C., Ganchi,P.A., Beraud,C., Ballard,D.W. & Greene,W.C. Autoregulation of the NF-kappa B transactivator RelA (p65) by multiple cytoplasmic inhibitors containing ankyrin motifs. *Proc. Natl. Acad. Sci. U. S. A* **91**, 1346-1350 (1994).

154. Broemer,M., Krappmann,D. & Scheidereit,C. Requirement of Hsp90 activity for IkappaB kinase (IKK) biosynthesis and for constitutive and inducible IKK and NF-kappaB activation. *Oncogene* **23**, 5378-5386 (2004).

155. Aoyagi,S. & Archer,T.K. Modulating molecular chaperone Hsp90 functions through reversible acetylation. *Trends Cell Biol.* **15**, 565-567 (2005).

156. Chen,L. *et al.* Chemical ablation of androgen receptor in prostate cancer cells by the histone deacetylase inhibitor LAQ824. *Mol. Cancer Ther.* **4**, 1311-1319 (2005).

157. Kim,Y.H., Park,J.W., Lee,J.Y. & Kwon,T.K. Sodium butyrate sensitizes TRAIL-mediated apoptosis by induction of transcription from the DR5 gene promoter through Sp1 sites in colon cancer cells. *Carcinogenesis 2004. Oct. ;25. (10):1813. -20. Epub. 2004. May. 13.* **25**, 1813-1820 (2004).

158. Nakata,S. *et al.* Histone deacetylase inhibitors upregulate death receptor 5/TRAIL-R2 and sensitize apoptosis induced by TRAIL/APO2-L in human malignant tumor cells. *Oncogene 2004. Aug.* **23**, 6261-6271 (2004).

159. Vanoosten,R.L., Moore,J.M., Karacay,B. & Griffith,T.S. Histone Deacetylase Inhibitors Modulate Renal Cell Carcinoma Sensitivity to TRAIL/Apo-2L-induced Apoptosis by Enhancing TRAIL-R2 Expression. *Cancer Biol. Ther. 2005. Oct. 13;4(10).* **4**, (2005).

160. Kovacs,J.J. *et al.* HDAC6 Regulates Hsp90 Acetylation and Chaperone-Dependent Activation of Glucocorticoid Receptor. *Mol. Cell* **18**, 601-607 (2005).

161. Wertz,I.E. *et al.* De-ubiquitination and ubiquitin ligase domains of A20 downregulate NF-kappaB signalling. *Nature* **430**, 694-699 (2004).

162. Jones,D.R., Broad,R.M., Madrid,L.V., Baldwin,A.S., Jr. & Mayo,M.W. Inhibition of NF-kappaB sensitizes non-small cell lung cancer cells to chemotherapy-induced apoptosis. *Ann. Thorac. Surg.* **70**, 930-936 (2000).

163. Bargou,R.C. *et al.* High-level nuclear NF-kappa B and Oct-2 is a common feature of cultured Hodgkin/Reed-Sternberg cells. *Blood* **87**, 4340-4347 (1996).

164. Alizadeh,A.A. *et al.* Distinct types of diffuse large B-cell lymphoma identified by gene expression profiling. *Nature* **403**, 503-511 (2000).

165. Gasparian,A.V. *et al.* The role of IKK in constitutive activation of NF-kappaB transcription factor in prostate carcinoma cells. *J. Cell Sci.* **115**, 141-151 (2002).

166. Chuang,S.E. *et al.* Basal levels and patterns of anticancer drug-induced activation of nuclear factor-kappaB (NF-kappaB), and its attenuation by tamoxifen, dexamethasone, and curcumin in carcinoma cells. *Biochem. Pharmacol.* **63**, 1709-1716 (2002).

167. Cuni,S. *et al.* A sustained activation of PI3K/NF-kappaB pathway is critical for the survival of chronic lymphocytic leukemia B cells. *Leukemia* **18**, 1391-1400 (2004).

168. Ho,W.C., Dickson,K.M. & Barker,P.A. Nuclear factor-kappaB induced by doxorubicin is deficient in phosphorylation and acetylation and represses nuclear factor-kappaB-dependent transcription in cancer cells. *Cancer Res.* **65**, 4273-4281 (2005).

169. Zhong,H., SuYang,H., Erdjument-Bromage,H., Tempst,P. & Ghosh,S. The transcriptional activity of NF-kappaB is regulated by the IkappaB-associated PKAc subunit through a cyclic AMP-independent mechanism. *Cell* **89**, 413-424 (1997).

170. Visaria,R.K. *et al.* Enhancement of tumor thermal therapy using gold nanoparticle-assisted tumor necrosis factor-alpha delivery. *Mol. Cancer Ther.* **5**, 1014-1020 (2006).

171. Han,S.Y. *et al.* Activation of NF-kappaB determines the sensitivity of human colon cancer cells to TNFalpha-induced apoptosis. *Biol. Pharm. Bull.* **23**, 420-426 (2000).

172. Yasui,H., Adachi,M. & Imai,K. Combination of tumor necrosis factor-alpha with sulindac in human carcinoma cells in vivo. *Ann. N. Y. Acad. Sci.* **1010**, 273-277 (2003).

173. Lee,F.S., Hagler,J., Chen,Z.J. & Maniatis,T. Activation of the IkappaB alpha kinase complex by MEKK1, a kinase of the JNK pathway. *Cell* **88**, 213-222 (1997).

174. Zhao,Q. & Lee,F.S. Mitogen-activated protein kinase/ERK kinase kinases 2 and 3 activate nuclear factor-kappaB through IkappaB kinase-alpha and IkappaB kinase-beta. *J. Biol. Chem.* **274**, 8355-8358 (1999).

175. Ninomiya-Tsuji,J. *et al.* The kinase TAK1 can activate the NIK-I kappaB as well as the MAP kinase cascade in the IL-1 signalling pathway. *Nature* **398**, 252-256 (1999).

176. Woronicz,J.D., Gao,X., Cao,Z., Rothe,M. & Goeddel,D.V. IkappaB kinase-beta: NF-kappaB activation and complex formation with IkappaB kinase-alpha and NIK. *Science* **278**, 866-869 (1997).

177. Tojima,Y. *et al.* NAK is an IkappaB kinase-activating kinase. *Nature* **404**, 778-782 (2000).

178. Yang,J. *et al.* The essential role of MEKK3 in TNF-induced NF-kappaB activation. *Nat. Immunol. 2001. Jul. ;2(7.):620. -4.* **2**, 620-624 (2001).

179. Blonska,M. *et al.* TAK1 is recruited to the tumor necrosis factor-alpha (TNF-alpha) receptor 1 complex in a receptor-interacting protein (RIP)-dependent manner and cooperates with MEKK3 leading to NF-kappaB activation. *J. Biol. Chem.* **280**, 43056-43063 (2005).

180. Hopkins-Donaldson,S. *et al.* Silencing of death receptor and caspase-8 expression in small cell lung carcinoma cell lines and tumors by DNA methylation. *Cell Death. Differ.* **10**, 356-364 (2003).

181. Munker,M., Munker,R., Saxton,R.E. & Koeffler,H.P. Effect of recombinant monokines, lymphokines, and other agents on clonal proliferation of human lung cancer cell lines. *Cancer Res.* **47**, 4081-4085 (1987).

182. Das,K.C. & White,C.W. Activation of NF-kappaB by antineoplastic agents. Role of protein kinase C. *J. Biol. Chem.* **272**, 14914-14920 (1997).

183. Huang,T.T. *et al.* NF-kappaB activation by camptothecin. A linkage between nuclear DNA damage and cytoplasmic signaling events. *J. Biol. Chem.* **275**, 9501-9509 (2000).

184. Hwang,S. & Ding,A. Activation of NF-kappa B in murine macrophages by taxol. *Cancer Biochem. Biophys.* **14**, 265-272 (1995).

185. Venkatraman,M., Anto,R.J., Nair,A., Varghese,M. & Karunagaran,D. Biological and chemical inhibitors of NF-kappaB sensitize SiHa cells to cisplatin-induced apoptosis. *Mol. Carcinog.* **44**, 51-59 (2005).

186. Arlt,A. *et al.* Inhibition of NF-kappaB sensitizes human pancreatic carcinoma cells to apoptosis induced by etoposide (VP16) or doxorubicin. *Oncogene* **20**, 859-868 (2001).

187. Cutts,S.M., Parsons,P.G., Sturm,R.A. & Phillips,D.R. Adriamycin-induced DNA adducts inhibit the DNA interactions of transcription factors and RNA polymerase. *J. Biol. Chem.* **271**, 5422-5429 (1996).

188. Bottero,V. *et al.* Activation of nuclear factor kappaB through the IKK complex by the topoisomerase poisons SN38 and doxorubicin: a brake to apoptosis in HeLa human carcinoma cells. *Cancer Res.* **61**, 7785-7791 (2001).

189. Andriollo,M., Favier,A. & Guiraud,P. Adriamycin activates NF-kappaB in human lung carcinoma cells by IkappaBalpha degradation. *Arch. Biochem. Biophys.* **413**, 75-82 (2003).

190. Campbell,K.J., O'Shea,J.M. & Perkins,N.D. Differential regulation of NF-kappaB activation and function by topoisomerase II inhibitors. *BMC. Cancer* **6**, 101 (2006).

191. Manna,S.K., Manna,P. & Sarkar,A. Inhibition of RelA phosphorylation sensitizes apoptosis in constitutive NF-kappaB-expressing and chemoresistant cells. *Cell Death. Differ.* (2006).

192. Miller,B.S. & Zandi,E. Complete reconstitution of human IkappaB kinase (IKK) complex in yeast. Assessment of its stoichiometry and the role of IKKgamma on the complex activity in the absence of stimulation. *J. Biol. Chem.* **276**, 36320-36326 (2001).

193. Tegethoff,S., Behlke,J. & Scheidereit,C. Tetrameric oligomerization of IkappaB kinase gamma (IKKgamma) is obligatory for IKK complex activity and NF-kappaB activation. *Mol. Cell Biol.* **23**, 2029-2041 (2003).

194. Lee,J.H. & Paull,T.T. ATM activation by DNA double-strand breaks through the Mre11-Rad50-Nbs1 complex. *Science* **308**, 551-554 (2005).

195. Farrow,B. *et al.* Inflammatory mechanisms contributing to pancreatic cancer development. *Ann. Surg.* **239**, 763-769 (2004).

196. Greten,F.R. *et al.* IKKbeta links inflammation and tumorigenesis in a mouse model of colitis-associated cancer. *Cell* **118**, 285-296 (2004).

197. Sanda,T. *et al.* Growth inhibition of multiple myeloma cells by a novel IkappaB kinase inhibitor. *Clin. Cancer Res.* **11**, 1974-1982 (2005).

198. Pham,L.V. *et al.* A CD40 Signalosome anchored in lipid rafts leads to constitutive activation of NF-kappaB and autonomous cell growth in B cell lymphomas. *Immunity.* **16**, 37-50 (2002).

199. Naumann,M. & Scheidereit,C. Activation of NF-kappa B in vivo is regulated by multiple phosphorylations. *EMBO J.* **13**, 4597-4607 (1994).

200. Goldman-Leikin,R.E. *et al.* Characterization of a novel myeloma cell line, MM.1. *J. Lab Clin. Med.* **113**, 335-345 (1989).

201. Moalli,P.A., Pillay,S., Weiner,D., Leikin,R. & Rosen,S.T. A mechanism of resistance to glucocorticoids in multiple myeloma: transient expression of a truncated glucocorticoid receptor mRNA. *Blood* **79**, 213-222 (1992).

202. Ma,M.H. *et al.* The proteasome inhibitor PS-341 markedly enhances sensitivity of multiple myeloma tumor cells to chemotherapeutic agents. *Clin. Cancer Res.* **9**, 1136-1144 (2003).

203. Burke,J.R. *et al.* BMS-345541 is a highly selective inhibitor of I kappa B kinase that binds at an allosteric site of the enzyme and blocks NF-kappa B-dependent transcription in mice. *J. Biol. Chem.* **278**, 1450-1456 (2003).

204. Mabuchi,S. *et al.* Inhibition of inhibitor of nuclear factor-kappaB phosphorylation increases the efficacy of paclitaxel in in vitro and in vivo ovarian cancer models. *Clin. Cancer Res.* **10**, 7645-7654 (2004).

205. Relic,B. *et al.* 15-deoxy-delta12,14-prostaglandin J2 inhibits Bay 11-7085-induced sustained extracellular signal-regulated kinase phosphorylation and apoptosis in human articular chondrocytes and synovial fibroblasts. *J. Biol. Chem.* **279**, 22399-22403 (2004).

206. Hu,X. *et al.* An IkappaBalpha inhibitor causes leukemia cell death through a p38 MAP kinase-dependent, NF-kappaB-independent mechanism. *Cancer Res.* **61**, 6290-6296 (2001).

207. Mayo,M.W. *et al.* Ineffectiveness of histone deacetylase inhibitors to induce apoptosis involves the transcriptional activation of NF-kappa B through the Akt pathway. *J. Biol. Chem.* **278**, 18980-18989 (2003).

208. Rundall,B.K., Denlinger,C.E. & Jones,D.R. Combined histone deacetylase and NF-kappaB inhibition sensitizes non-small cell lung cancer to cell death. *Surgery* **136**, 416-425 (2004).

209. Chen,L.F., Mu,Y. & Greene,W.C. Acetylation of RelA at discrete sites regulates distinct nuclear functions of NF-kappaB. *EMBO J.* **21**, 6539-6548 (2002).

210. Adam,E. *et al.* Potentiation of tumor necrosis factor-induced NF-kappa B activation by deacetylase inhibitors is associated with a delayed cytoplasmic reappearance of I kappa B alpha. *Mol. Cell Biol.* **23**, 6200-6209 (2003).

211. Catley,L. *et al.* NVP-LAQ824 is a potent novel histone deacetylase inhibitor with significant activity against multiple myeloma. *Blood* **102**, 2615-2622 (2003).

212. Choi,J.H. *et al.* Trichostatin A attenuates airway inflammation in mouse asthma model. *Clin. Exp. Allergy* **35**, 89-96 (2005).

213. Reddy,P. *et al.* Histone deacetylase inhibitor suberoylanilide hydroxamic acid reduces acute graft-versus-host disease and preserves graft-versus-leukemia effect. *Proc. Natl. Acad. Sci. U. S. A* **101**, 3921-3926 (2004).

214. Leoni,F. *et al.* The antitumor histone deacetylase inhibitor suberoylanilide hydroxamic acid exhibits antiinflammatory properties via suppression of cytokines. *Proc. Natl. Acad. Sci. U. S. A* **99**, 2995-3000 (2002).

215. Ashburner,B.P., Westerheide,S.D. & Baldwin,A.S., Jr. The p65 (RelA) subunit of NF-kappaB interacts with the histone deacetylase (HDAC) corepressors HDAC1 and HDAC2 to negatively regulate gene expression. *Mol. Cell Biol.* **21**, 7065-7077 (2001).

216. Dejardin,E. *et al.* Regulation of NF-kappaB activity by I kappaB-related proteins in adenocarcinoma cells. *Oncogene* **18**, 2567-2577 (1999).

217. Birbach,A. *et al.* Signaling molecules of the NF-kappa B pathway shuttle constitutively between cytoplasm and nucleus. *J. Biol. Chem.* **277**, 10842-10851 (2002).

218. Carlotti,F., Dower,S.K. & Qwarnstrom,E.E. Dynamic shuttling of nuclear factor kappa B between the nucleus and cytoplasm as a consequence of inhibitor dissociation. *J. Biol. Chem.* **275**, 41028-41034 (2000).

219. Huang,T.T., Kudo,N., Yoshida,M. & Miyamoto,S. A nuclear export signal in the N-terminal regulatory domain of IkappaBalpha controls cytoplasmic localization of inactive NF-kappaB/IkappaBalpha complexes. *Proc. Natl. Acad. Sci. U. S. A* **97**, 1014-1019 (2000).